Assessment of the inter-individual variation observed between patients receiving HIV antiretroviral therapy

Thesis submitted in accordance with the requirements of the University of Liverpool for the degree of Doctor in Philosophy by Megan Neary.

08/05/2018

DISCLAIMER

This thesis is the result of my own work. The material contained within the thesis has not been presented, either wholly or in part for any other degree or qualification.

Megan Neary

ACKNOWLEDGEMENTS

Firstly I would like to thank Professor Andrew Owen and Dr Marco Siccardi for all your help and guidance throughout my PhD. The opportunities you have given me have changed my life and broadened my ambitions and for that I am truly grateful. Also thank you to Professor Saye Khoo for seeing potential in a naïve student and offering me this opportunity. I would also like to thank and acknowledge the contribution of all the patients who took part in the studies within this thesis.

I'd like to thank everyone in the Infection Pharmacology Group, both at H block and the MIF, who have provided scientific knowledge as well as hilarious and sometimes horrifying stories. Your friendship and advice has been more helpful then you can realise. A huge thank you to Darren Moss for providing prospective, encouragement and apt PhD comics throughout. A massive thank you to Jo Sharp for providing a master class in time management, for taking me under your wing and including me in all the morning meetings. Also to Helen Box for all the laughs, reigning me in when I get over ambitious and for reducing my daily step count to zero. A big thanks to Paul Curley and Neill Liptrott for all your lunchtime encouragement and words of wisdom. Thanks to Chris David, for consistently providing your unique outlook on life throughout the PhD and to Hannah Kinvig, for being an all-round brilliant work colleague (but never a friend).

I would like to thank mum, dad and Dan for your endless love and support. I guess that summer job in McDonalds must have taught me something after all. I'd also like to thank my Nana and Grandad for their encouragement, and for always asking about my PhD and managing to not look bored whilst I answer. I couldn't ask for a more loving and supportive family and it's a privilege to make you all proud.

Finally, I'd like to thank Sam, for getting out of bed early, leaving work super late, eating burnt dinners and not telling me what was in the TripAdvisor reviews when I went away! Doing our PhDs has been a journey that I am so grateful for and I look forward to whatever comes next for us together.

PUBLICATIONS

Peer reviewed publications:

- **Neary M**, Owen A. Pharmacogenetic considerations for HIV treatment in different ethnicities: an update. *Expert Opinion on Drug Metabolism & Toxicology* 2017.
- **Neary M**, Lamorde M, Olagunju A, Darin KM, Merry C, Byakika-Kibwika P, Back DJ, Siccardi M, Owen A, Scarsi KK. The Effect of Gene Variants on Levonorgestrel Pharmacokinetics when Combined with Antiretroviral Therapy containing Efavirenz or Nevirapine. *Clinical Pharmacology and Therapeutics* 2017.
- Cerrone M, Wang X, **Neary M**, Weaver C, Fedele S, Day-Weber I, Owen A, Hill A, McClure M, Boffito M. Pharmacokinetics of efavirenz 400 mg once daily coadministered with Isoniazid and rifampicin in Human Immunodeficiency Virus-infected individuals. *Clinical Infectious Diseases* 2018.
- Lamorde M, Wang X, **Neary M**, Bisdomini E, Nakalema A, Byakika-Kibwika P, Mukonzo J, Khan W, Owen A, McClure M, Boffito M. Pharmacokinetics, pharmacodynamics and pharmacogenetics of efavirenz 400mg once daily dosing during pregnancy and post-partum. *Clinical Infectious Diseases* 2018.
- Olagunju A, Bolaji O, **Neary M**, Back D, Khoo S, Owen A. Pregnancy Effects Nevirapine Pharmacokinetics: Evidence from a CYP2B6 Genotype Guided Observational Study. *Pharmacogenetics and Genomics* 2016.
- Moss DM, **Neary M**, Owen A. The Role of Drug Transporters in the Kidney: Lessons from Tenofovir. *Frontiers in Pharmacology* 2014.

Conference presentations:

- **Neary M**, Chappell C, Scarsi K, Nakalema S, Matovu J, Achilles S, Chen B, Siccardi M, Owen A, Lamorde M. *CYP2B6 variants alter etonogestrel pharmacokinetics when*

combined with efavirenz. Poster presented at the Conference on Retroviruses and Opportunistic Infections (CROI) 2018, Boston USA.

- **Neary M**, Lamorde M, Olagunju A, Darin KM, Merry C, Byakika-Kibwika P, Back DJ, Siccardi M, Owen A, Scarsi KK. *Effect of CYP2B6 variants on levonorgestrel pharmacokinetics when combined with efavirenz based antiretroviral therapy.* Poster presented at the Conference on Retroviruses and Opportunistic Infections (CROI) 2016, Boston USA.
- Box H, Sharp J, **Neary M**, Moss D, Tatham L, Savage A, Ashcroft S, Rannard S, Owen A. *Preclinical evaluation of reduced dose darunavir/ritonavir nanoparticle formulation.* Poster presented at the Conference on Retroviruses and Opportunistic Infections (CROI) 2018, Boston USA.
- Elliot E, **Neary M**, Else L, Khoo S, Moyle G, Carr D, Owen A, Boffito M. *ABCG2 rs2231142 and NR1I2 rs2472677 influence dolutegravir concentrations in plasma.* Poster presented at the Conference on Retroviruses and Opportunistic Infections (CROI) 2018, Boston USA.
- Cerrone M, Wang X, **Neary M**, Weaver C, Fedele S, Day-Weber I, Owen A, Hill A, McClure M, Boffito M. *Pharmacokinetics of efavirenz 400mg with isoniazid/rifampicin in people with HIV.* Poster presented at the Conference on Retroviruses and Opportunistic Infections (CROI) 2018, Boston USA.
- Cerrone M, Alfarisi O, **Neary M**, Marzinke M, Parsons T, Owen A, Maartens G, Pozniak A, Flexner C, Boffito M. *Rifampin effect on tenofovir alafenamide (TAF) plasma/intracellular pharmacokinetics.* Poster presented at the Conference on Retroviruses and Opportunistic Infections (CROI) 2018, Boston USA.
- Bracchi M, **Neary M**, Pagani N, Else L, Khoo S, Abbas Z, Hawkins D, Moyle G, Back D, Owen A, Boffito M. *ABCG2 rs2231142 influences tenofovir concentrations in plasma*

and urine. Poster presented at the Conference on Retroviruses and Opportunistic Infections (CROI) 2017, Seattle USA.

- Lamorde M, Wang X, **Neary M**, Bisdomini E, Nakalema S, Byakika P, Mukonzo J, Khan W, Owen A, McClure M, Boffito M. *Pharmacokinetics, pharmacodynamics and pharmacogenomics of efavirenz 400mg once-daily during pregnancy and postpartum.* 9th IAS Conference on HIV Science 2017, Paris France.

TABLE OF CONTENTS

FIGURES

TABLES

ABBREVIATIONS

Absorbency units	AU
Antiretroviral therapy	ART
Area under the curve	AUC
Atazanavir	ATV
Bicinchoninic acid	BCA
Breast cancer resistance protein	BCRP
Calcium chloride	$CaCl_2$
Central nervous system	CNS
Chi squared value	X^2
Chronic kidney disease	CKD
Cobicistat	COBI
Constitutive androstane receptor	CAR
Cytochrome P450	CYP
Darunavir	DRV
Deoxyribonucleic acid	DNA
Dolutegravir	DTG
Dulbecco's modified eagles medium	DMEM
Efavirenz	EFV
Elvitegravir	EVG
Emtricitabine	FTC
Escherichia coli	E.coli
Estimated glomerular filtration rate	eGFR
Fetal bovine serum	FBS
Green fluorescent protein	GFP
Hanks balanced salt solution	HBSS

High performance liquid chromatography	HPLC
Horse radish peroxidase	HRP
Human embryonic kidney 293	HEK293
Human Immunodeficiency virus	HIV
$_5$-hydroxytryptamine	$_5$-HT
Integrase inhibitor	INSTI
Interquartile range	IQR
Kidney tubular dysfunction	KTD
Lamivudine	3TC
Levonorgestrel	LNG
Liquid chromatography tandem mass spectrometry	LCMS/MS
Lopinavir	LPV
Lysogeny broth	LB
Magnesium chloride	$MgCl_2$
Maximum concentration	C_{max}
Minimum concentration	C_{min}
Messenger ribonucleic acid	mRNA
Multidrug and toxin extrusion protein	MATE
Multidrug resistance protein	MRP
N-methylnicotimide	NMN
Nevirapine	NVP
Non-nucleoside reverse transcriptase inhibitor	NNRTI
Nucleoside reverse transcriptase inhibitor	NRTI
Organic anion transporter	OAT
Organic cation transporter	OCT
P-glycoprotein	P-gp

Phosphate buffered saline	PBS
Polymerase chain reaction	PCR
Post-exposure prophylaxis	PEP
Pre-exposure prophylaxis	PrEP
Potassium chloride	KCl
Pregnane X receptor	PXR
Protease inhibitors	PI
Proximal tubule cells	PTCs
Raltegravir	RAL
Ribonucleic acid	RNA
Ritonavir	RTV
Single nucleotide polymorphism	SNP
Sodium chloride	NaCl
Sodium hydroxide	NaOH
Solute carrier	SLC
Super optimal culture	S.O.C
Tenofovir	TFV
Tenofovir alafenamide	TAF
Tenofovir disoproxil fumarate	TDF
Time to C_{max}	T_{max}
Tris-Borate-EDTA	TBA
Urinary albumin-creatinine ratio	uACR
Urinary albumin-protein ratio	uAPR
Urine protein-creatinine ratio	uPCR
Volts	V
World Health Organisation	WHO

ABSTRACT

The WHO currently recommends tenofovir (TFV) disoproxil fumarate (TDF) or TFV alafenamide (TAF) as a preferred first-line antiretroviral therapy (ART) for the treatment and prevention of HIV. However, mild to moderate TFV-related renal toxicity is an uncommon but significant complication for TDF therapy. Efavirenz (EFV) is also approved for first line treatment, with the approval of a lower dose treatment, 600mg to 400mg, offering an opportunity for a greater number of patients to receive ART for the same amount of current public health expenditure, whilst enabling the maintenance of viral load suppression and partial mitigation of adverse events. However, EFV displays broad inter-patient and inter-population variability in its pharmacokinetics and displays a range of dose dependent adverse effects. In order to gain further understanding of the impact patient genetics has on response to ART, studies investigating the effect of single nucleotide polymorphisms (SNPs) within multi ethnic populations receiving either TFV or EFV were completed. Additional work was conducted to investigate potential drug-substrate interactions at the transporter level within proximal tubule cells (PTCs), and the ramifications this may have for diagnosis of renal impairment.

This work was conducted through assessing the relationship between SNPs found within genes encoding transporters on the apical membrane of PTCs and a diagnosis of renal dysfunction, defined as kidney tubular dysfunction or chronic kidney disease within a Ghanaian population (Chapter 2). Additionally the association between pharmacogenetic variants linked to TDF metabolism or TFV excretion and TFV plasma and urine concentrations, in a majority Caucasian patient population, receiving TFV as part of their ART was investigated (Chapter 3). This thesis sought to assess whether SNPs in genes involved in EFV and nevirapine metabolism were linked to previously observed changes in the contraceptive subdermal implant levonorgestrels (LNG) pharmacokinetics, when prescribed alongside EFV,

within a Ugandan population (Chapter 6). In order to study the effect of transporter interactions at the site of TFV toxicity, the proximal tubule, a transiently transfected Human Embryonic Kidney 293 cell line overexpressing either multidrug and toxin extrusion protein (MATE) 1 or MATE2K was developed and assessed for correct functionality (Chapter 4). This cell line was then utilised for drug-substrate interaction studies between TAF and TFV and either the endogenous biomarker creatinine or the type 2 diabetes drug metformin (Chapter 5).

These studies provided a greater understanding of the contribution pharmacogenetics provides to the interaction observed between EFV and LNG, and outlined a genetic association between TFV transporter SNPs and TFV plasma and urine concentrations. Utilisation of these findings in future pharmacogenetics studies would aid in the understanding of the impact of genetic variants in different populations, and the consequences this has for achieving sustained virological response to ART. The study of the effect of TAF and TFV on MATE1 and MATE2K transport of metformin and creatinine produced novel data on these interactions. Overall, the studies included within this thesis have clinical impact through further elucidating the potential mechanisms of toxicity or treatment failure within patients receiving ART.

Chapter 1. General Introduction

1.1 CURRENT POSITION ON HIV TREATMENT

The past two decades have yielded a revolution in the treatment of human immunodeficiency virus (HIV). Huge reductions in patient mortality have been observed, with the World Health Organisation (WHO) estimating the avoidance of 7.8 million deaths between the years 2000 and 2014. Scale-up of HIV response has reduced new infections from 3.1 million in 2000 to 2.0 million in 2014 (WHO 2016). Success has been made possible in part through the development of highly active antiretroviral therapy (ART) and the licensing of generic drugs, which has resulted in greater accessibility of treatments for patients in low-income countries.

As of 2016, an estimated 36.7 million people lived with HIV worldwide. According to the WHO, in 2015 an estimated 19.7 million of those infected did not receive treatment (WHO 2016). More work is still needed in order to achieve the UNAIDS 2020 90:90:90 target, an ambitious global treatment target to have 90% of HIV-positive people know their status, 90% receive sustained ART and to have 90% of patients being treated achieve viral suppression. If this target can be achieved it is predicted that 73% of people living with HIV will be virally suppressed (UnitedNations 2014).

1.1.1 *HIV antiretroviral drug regimen recommendations*

HIV drugs can be classified into six categories according to their mechanism of action. These are: nucleoside reverse transcriptase inhibitors (NRTIs), non-nucleoside reverse transcriptase inhibitors (NNRTIs), protease inhibitors (PIs), integrase inhibitors (INSTI), entry inhibitors and fusion inhibitors. Antiretroviral drug regimens are now used in a multitude of combinations and settings, from therapy for HIV positive individuals to pre-exposure prophylaxis (PrEP) and post-exposure prophylaxis (PEP) for prevention. For PreP, the PROUD study demonstrated higher protection against HIV within participants receiving ART compared to that seen in

placebo-controlled trials, and no evidence of an increase in other sexually transmitted infections within the PrEP receiving participants (McCormack 2016). Current WHO recommendations for first line HIV therapy for adults and adolescents, is a combination of two NRTIs, tenofovir disoproxil fumarate (TDF) or tenofovir alafenamide (TAF) and emtricitabine (FTC) or lamivudine (3TC), combined with a third active antiretroviral drug (WHO 2016, AntiretroviralGuidelinesforAdults&Adolescents 2017). The third active agent can be an INSTI such as dolutegravir (DTG), or an NNRTI such as efavirenz (EFV) (400 mg or 600 mg) or nevirapine (NVP). (WHO 2016, AntiretroviralGuidelinesforAdults&Adolescents 2017)

1.2 TENOFOVIR

Tenofovir (TFV) is the active compound of the prodrugs TDF and TAF. TFV is not a cytochrome P450 (CYP) substrate and is excreted through a combination of glomerular filtration and proximal tubule secretion. TFV enters proximal tubule cells (PTCs) through organic anion transporter (OAT) 1 and 3 (*SLC22A6* and *SLC22A8*) located on the basolateral membrane of PTCs and exits through multidrug resistance protein (MRP) 4 and MRP7 (*ABCC4* and *ABCC10*) located on the apical cell membrane (Figure 1.1) (Pushpakom 2011, Moss 2014).

Due to TFV's hydrophilic nature, the drug has permeability-limited oral absorption. Therefore, highly lipophilic pro-drugs TDF or TAF are prescribed (Shaw 1997, Van Gelder 2002). TDF is degraded by carboxylesterases into the active metabolite TFV after intestinal absorption (Van Gelder 2002). ABC transporters within the small intestine are considered as the rate-limiting barrier to oral drug absorption. Within the small intestine TDF and TAF passively diffuse into intestinal epithelial cells before being transported into the intestinal lumen by P-glycoprotein (P-gp) (encoded by *ABCB1*) and breast cancer resistance protein

(BCRP) (encoded by *ABCG2*), which are expressed at the apical membrane. TAF is not metabolised to TFV within the small intestine, but through intracellular metabolism by lysosomal serine protease cathepsin A in peripheral blood mononuclear cells and carboxylesterase 1 in the liver (Birkus 2016). Because of this, the systemic delivery of active drug differs between TAF and TDF, with higher systemic circulation of TFV for TDF compared to TAF. The enhanced systemic exposure of TAF, compared to TFV, is of benefit given that enhanced drug loading of TAF can occur within peripheral blood mononuclear cells before conversion to the active metabolite TFV, enabling a lower dose to prescribed that provides greater antiretroviral activity.

Alterations in the transport of TAF or TDF within the small intestine has potential ramifications for overall TFV exposure, with inhibition of efflux intestinal transporters being recognised as a secondary mechanism for pharmacoenhancers to increase systemic exposure. Tong *et al.* previously observed increased TFV plasma pharmacokinetics within patients receiving PIs, which they demonstrated to occur through inhibition of intestinal efflux of TDF by P-gp (Tong 2007). Furthermore, COBI has been shown to inhibit P-gp and BCRP transport of TAF *in vitro* (Lepist 2012). Inhibition of TFV prodrug transport at the intestinal lumen results in increased TFV systemic exposure through reducing prodrug excretion, resulting in elevated prodrug absorption and subsequently increased breakdown to active TFV.

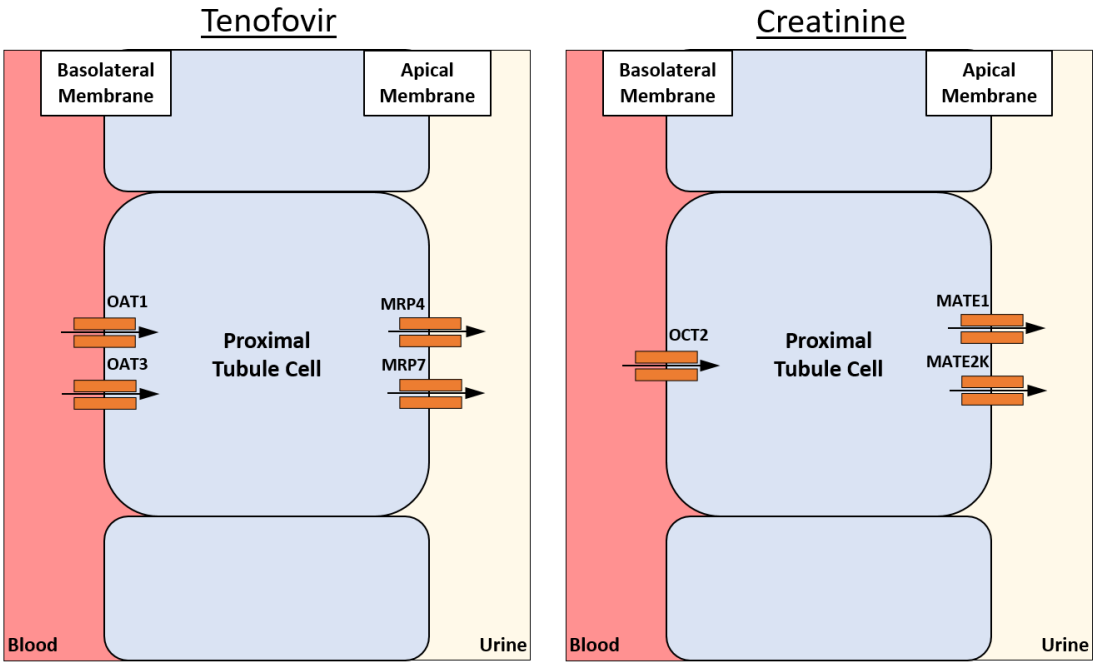

Figure 1.1: Tenofovir and creatinine transporter profiles within the proximal tubule.

TFV enters the proximal tubule from the blood via basolaterally expressed OAT 1 and 3 and is removed into the urine via MRP 4 and 7. Creatinine is transported into proximal tubule cells via organic cation transporter (OCT) 2 (*SLC22A2*) and is excreted by the multidrug and toxin extrusion protein (MATE) 1 and 2K.

1.2.1 *Tenofovir-associated renal toxicity*

The mild to moderate renal toxicity observed within patients taking TFV is an uncommon but significant complication for first line HIV therapy (Rifkin 2004, Jülg 2005, Cooper 2010, Scherzer 2012, Quesada 2015). However incidence of kidney toxicity within patients receiving TAF has been reported to be significantly lower than for patients receiving TDF, most likely due to the reduced dose prescribed for TAF in comparison to TDF (Moss 2014, Sax 2015). In light of the predicted increase in use of TDF post-patent, its anticipated long-term use in an ageing patient population, and its inclusion within PrEP, it is essential that TFV-associated renal toxicity is further investigated.

TFV-associated renal toxicity is a result of the accumulation of TFV in PTCs, resulting in cell death (Herlitz 2010). TFV toxicity also presents less commonly as Fanconi Syndrome, acute kidney injury and kidney tubular dysfunction (KTD) (Karras 2003, Lee 2003, Malik 2005, Gupta 2008, Scherzer 2012). In one clinic, TFV-associated nephrotoxicity accounted for more than 20% of consultations and was the most common single reason for HIV-related referral to specialist renal services (Hall 2011). A time-dependent relationship is observed between TDF use and incidence of renal toxicity, with increased time on therapy resulting in higher incidence. In addition to this, advancing age has been associated with increased risk of renal toxicity (Goicoechea 2008, Hall 2011, Quesada 2015).

Diagnosis of TFV-associated renal toxicity is commonly ascertained through the measurement of estimated glomerular filtration rate (eGFR). eGFR can be calculated through several predictive equations, the most clinically relevant being the Cockcroft–Gault equation and the Modification of Diet in Renal Disease equation (Estrella 2010, Hall 2011). Both equations use creatinine clearance, calculated from serum and urine creatinine

concentrations to predict eGFR. Creatinine is an endogenous waste product of skeletal muscle metabolism and is widely used as a biomarker for renal health (Hall 2011). Excretion of creatinine occurs predominantly through glomerular filtration, with proximal tubular secretion accounting for 15% of total renal clearance. Creatinine enters PTCs via OCT2 and is excreted by MATE transporters 1 and 2K (Figure 1.1) (Motohashi 2013).

An increase in the serum concentration of creatinine is regarded as an indicator of declining renal health, although it has been suggested to poorly represent actual filtration rate in patients with renal disease (Bennett 1971, Carrie 1980). When glomerular filtration rate is low, the serum creatinine concentration and creatinine clearance rate are higher than the actual glomerular filtration rate, due to the additional secretion of creatinine by PTCs (Urakami 2004, Estrella 2010). As TFVs site of toxicity is the PTCs and creatinine excretion by PTCs is modest, a small decline in eGFR would be expected in TFV-associated renal toxicity. In the case of TFV-associated renal toxicity, tests of renal function that utilise changes in creatinine concentration are unlikely to be an adequate indicator of renal toxicity. This is because changes in serum creatinine concentration observed in patients diagnosed with TFV-associated renal toxicity may be caused by TFV inhibiting creatinine excretion in PTCs rather than an actual change to eGFR.

The site of TFV excretion and toxicity, the proximal tubule, is a site of potential drug-transporter-mediated drug interactions that can contribute to TFV-associated renal toxicity. The combination of raltegravir (RAL) with TDF has been shown to result in increased area under the curve (AUC) of TFV, although not to a clinically relevant degree (Wenning 2008). This alteration in AUC may be due to inhibition of OAT1 by RAL, as previously shown *in vitro* (Moss 2011). In addition, co-administration of TDF with didanosine is no longer

recommended due to severe side effects. Both drugs are nephrotoxic and previous studies have shown that co-administration with TDF results in an increase in AUC of didanosine. This alteration in AUC may be attributed to inhibition of didanosine transport via OAT1 (Fulco 2003).

Incidence of TFV toxicity has been shown to increase when TDF is prescribed with concomitant PIs, and increases further with a ritonavir (RTV)-boosted PI (Gupta 2008, Calza 2013). The use of lopinavir (LPV)/RTV in combination with TDF has previously been shown to increase plasma exposure of TFV and has been linked with a reduction in TFV renal clearance (Kearney 2006, Kiser 2008). The same relationship was observed between darunavir (DRV)/RTV and TDF with an increase in TFV plasma concentration and AUC, though not to a clinically relevant degree (Hoetelmans 2007). Given that RTV is a substrate of MRP2, which is situated on the apical membrane of PTCs, and is a known inhibitor of MRP4 and OAT3, it is likely that the observed interaction between RTV and TFV is a result of transporter inhibition (Huisman 2002, Cihlar 2007).

1.3 EFAVIRENZ

EFV is an NNRTI recommended by the WHO as part of first line ART and is traditionally prescribed as a 600 mg daily dose (WHO 2016). The ENCORE1 study found that 400 mg daily dosing of EFV is non-inferior to 600 mg in a diverse patient cohort, with equal representation of African, Asian and Caucasian ethnic-origin patients (ENCORE1 2014). The use of 400 mg EFV daily dosing offers opportunities for a greater number of patients to receive ART for the same amount of current public health expenditure, and enables the maintenance of viral load suppression whilst partially mitigating the risk of adverse events. Accordingly, 400 mg EFV is now a recommended alternative first line therapy in the WHO treatment guidelines

(Boffito 2017). However, it should be recognised that EFV use is widely expected to fall dramatically over the coming years due to the introduction of DTG, which has a better safety profile and higher barrier to resistance.

Although generally well tolerated EFV displays a range of dose-dependent adverse events, the majority of which are mild to moderate in severity and subside within a few weeks of therapy initiation (Marzolini 2001, Apostolova 2017). The most frequently observed adverse events include central nervous system (CNS) symptoms and neuropsychiatric symptoms, including but not limited to dizziness, sleep disturbance and headaches (Apostolova 2015, Apostolova 2017). More severe neurological side effects such as severe depression, depersonalisation and mania have been shown to effect <2% of patients receiving EFV (Scourfield 2012). Nevertheless, EFV-related neuropsychiatric effects have been reported to interrupt therapy in 2-24% of patients receiving EFV (Apostolova 2017). The mechanism of these adverse events are yet to be fully clarified, however Gatch *et al.* and Dalwadi *et al.* demonstrated through *in vivo* and *in vitro* study that EFV interacts with the serotonin receptors $_5$-hydroxytryptamine ($_5$-HT) $_{2A}$, $_5$-HT$_{2B,}$ $_5$-HT$_{2C}$ and $_5$-HT$_6$ which may in part explain reported neuropsychiatric side effects such as night terrors (Gatch 2013). Furthermore *in vitro* study of chronic exposure to EFV demonstrated an antagonistic effect of EFV on serotonin transport by $_5$-HT$_{2A}$ and $_5$-HT$_{2C}$, with an 81% reduction in $_5$-HT$_{2A}$'s responsiveness to serotonin after 3 days of treatment with EFV (Dalwadi 2016). Incidence of EFV CNS toxicity have been shown to be exacerbated by elevated EFV plasma levels (Marzolini 2001, van Luin 2009). Given that EFV displays broad inter-patient and inter-population variability in its pharmacokinetics, the relevance of the influence of genetics on EFV pharmacokinetics must be considered within the context of toxicity as well as virological response.

Studies indicate that EFV plasma clearance is lower in patients of African ancestry than those of European ancestry, due to the difference in frequency of *CYP2B6* alleles (Barrett 2002, Csajka 2003, Haas 2004, Solus 2004, Holzinger 2012, Zanger 2013). EFV is primarily metabolised by CYP2B6, and more moderately by CYP2A6, CYP3A4 and UGT2B7 (Bélanger 2009, Ogburn 2010). Additionally, EFV is an inducer of CYP3A4 and CYP2B6. This high level of CYP enzyme interaction contributes to a multitude of drug-drug interactions. This includes interactions with other antiretroviral drugs such as PIs, and with drugs prescribed concomitantly such as the anti-tuberculosis drug rifampicin (Barry 1999, López-Cortés 2002). Other factors have been shown to contribute to variability in EFV pharmacokinetics, including pregnancy and body weight (Haas 2004, Cressey 2012, Cho 2016). These factors are important in light of the findings of the ENCORE1 study, and to the broad application of low dose 400mg EFV (Orrell 2011). A study within a HIV positive tuberculosis co-infected population has demonstrated comparable viral loads between patients receiving 400mg or 600mg EFV in combination with TDF and FTC alongside rifampicin and isoniazid, regardless of *CYP2B6* 516G>T (rs3745274) or *CYP2B6* 983T>C (rs28399499) genotype (Maddalena Cerrone 2018). Furthermore, a study of pregnant and post-partum women demonstrated non-inferiority of 400mg EFV compared to 600mg regardless of *CYP2B6* 516G>T (rs3745274) or *CYP2B6* 983T>C (rs28399499) genotype (Lamorde 2017). These studies suggest the applicability of 400mg EFV to a wider range of patient demographics, with further study in larger patient populations needed to confirm these promising findings.

1.4 GENETIC VARIANTS AND PHARMACOKINETICS

Variation in the human genome sequence sometimes plays an important role in the pharmacokinetics and pharmacodynamics of drugs and has the potential to be used to predict a patient's clinical outcome so that therapy can be tailored to genetically defined sub-populations. However, a robust understanding of the molecular basis for differences in drug

response also require contextual understanding of other factors such as ethnicity, environment and culture. Single nucleotide polymorphisms (SNPs) can be classed as the deletion, insertion or substitution of a single nucleotide in a gene (Borges 2010). These changes can be found in the protein coding (exonic) or non-protein-coding (regulatory or intronic) regions of genes, or in intergenic regions. A SNP that results in the same amino acid sequence being produced is known as a synonymous SNP, whereas a SNP that results in either a different amino acid or a premature stop codon is classified as nonsynonymous. SNPs in introns may still be of pharmacological relevance due to the regulatory functions that are conducted by these regions, such as transcriptional regulation or messenger ribonucleic acid (mRNA) splicing (Elgar 2008, Heyn 2015). SNPs are usually associated via haplotype groups, which occur due to multiple SNPs being inherited together (Borges 2010). These SNPs can be said to be in linkage disequilibrium, the non-random association of alleles on the same chromosome within a particular population (Slatkin 2008).

The study of SNPs in relation to their effect on the pharmacology of a drug focuses primarily on SNPs in genes relevant to the pharmacokinetics of the drug of interest. These include SNPs in genes involved in the production, through transcriptional regulation or direct coding, of transporters, enzymes and transcription factors. In the case of ART, the use of pharmacogenetic studies to identify SNPs that influence pharmacokinetics, efficacy or toxicity, has yielded clinically and/or mechanistically important information (Table 1.1).

Table 1.1: Clinical application of SNPs associated with changes in patient response to/pharmacokinetics of drug therapy.

Gene	Protein	SNP	Physiological effect	Drug interaction	Alteration in protein function	Clinical recommendation
HLA-B (Ma 2010)	MHCII	*5701	Hypersensitivity reaction	Abacavir	Increased	Test for *HLA-B*5701* allele before initiation of therapy in adults, adolescents and children. If positive for *HLA-B*5701* do not treat with abacavir.
CYP2C19 (Scott 2013)	CYP2C19	*2 and *3	Reduction in metabolism	Clopidogrel	Inactivation	If patient is heterozygous *2/*3 or homozygous for *2 or *3 significantly reduced platelet expression is expected, increasing risk of adverse cardiovascular events. Alternative antiplatelet therapy should be prescribed.
DPYD (Caudle 2013)	DPD	*2A	Inactivation of catalytic activity	Fluoropyrimidines	Inactivation	If patient is heterozygous for *2A dose is reduced by a minimum of 50%, if patient is homozygous an alternative drug should be prescribed.
TPMT (McLeod 2000, Nguyen 2011)	TPMT	*1, *2, *3A and/or *3C	Severe myelosuppression	Thiopurines	Reduced or Inactive	For patients who possess a single functional allele (*1) and a non-functional allele (*2, *3A or *3C) reduce azathioprine or 6-mercaptopurine dose by 30-70%, reduce thioguanine dose by 30-50%. Patients homozygous for non-functional alleles have initial dose of all drugs reduced by 10% and dosing frequency is extended, or an alternative drug is prescribed.
CYP3A5 (Birdwell 2015)	CYP3A5	*3	Reduction in metabolism	Tacrolimus	No expression	Patients who are homozygous for *3 should initiate therapy with standard recommended dose. Patients who are heterozygous *3 or do not possess the variant allele should start dose 1.5 to 2 times higher than the recommended starting dose.
UGT1A1 (Marques 2010, Dean 2015)	UGT1A1	*28	Increased risk of neutropenia	Irinotecan	Reduced	Patients homozygous for *28 receiving a dose <250 mg/m^2 require a dose reduction of 30%.

1.4.1 *Influence of genetic diversity*

Variation between different ethnicities in modern humans has occurred due to migration, through colonisation events and rapid variations in population numbers over thousands of years (Marth 2003). An example of this is the colonisation of Europe around 40,000 years ago, which led to a reduction of genetic diversity within this population. This produced a bottleneck caused by a reduction in genetic diversity being followed by a gradual increase in human population size. Because of this, fewer recombination events occurred in European populations compared to those of ancient African ancestry. Therefore, people of European ancestry possess gene variants that remain coinherited as a result of fewer recombination events and those of ancient African ancestry have a greater diversity of gene variation due to a greater number of recombination events (Marth 2003, Ortega 2014). Large scale increases in human population size over the last 400 generations has skewed previous patterns of genetic variation and has resulted in greater incidence of rare variants, due to recent mutations, which may contribute to disease risk and alterations in pharmacological outcome (Keinan 2012, Ortega 2014).

1.4.2 *Population stratification*

The availability of high-throughput sequencing has enhanced the study of the development of human genetic diversity and the identification of low-frequency variants. Exome and whole genome sequencing has enabled the characterisation of huge numbers of common (>5% frequency) variants and the incidence of low-frequency variants, in ethnically diverse populations. The 1000 Genomes Project aimed to identify over 95% of SNPs at 1% frequency or above in a broad range of populations and found that people from populations of substantial African ancestry had up to three-times more low-frequency variants than those of European or East Asian origin. Additionally, for some common variants strong differentiation was observed between populations within ancestry-based groups, with a

difference in frequency of at least 0.25 between pairs of populations within an ancestry group (GenomesProjectConsortium 2012). These findings highlight the importance of studying SNPs within a wide range of ethnically diverse populations to ascertain the overall effect of a SNP for patients of different ethnicities. Furthermore, the extent of diversity between ethnic groups, that has been previously reported, means that study populations should be separated by ethnicity during statistical analysis, or appropriate steps must be taken (e.g. use of microsatellites) to ensure that a SNP association is not wrongfully attributed as statistically significant, due to population stratification.

Population stratification occurs because of the collinearity between factors that influence a particular phenotype. To exemplify this with a non-genetic paradigm, it is difficult to dissociate the impact of body weight and gender on a particular phenotype (e.g. pharmacokinetics of a specific drug) when assessing their impact within a mixed gender cohort. Because women generally have a lower body weight than men, it may appear that there are gender differences, which are driven by the body weight. This collinearity is even more challenging when considering genetic associations within mixed ethnicity cohorts because there are likely to be many variants that differ in frequency between populations, and not all are usually considered. Thus, a polymorphism that is highly prevalent in one population compared to another may be statistically associated with the phenotype within a mixed-ethnicity population, because it is a marker of ethnicity (and therefore other unknown variants or groups of variants) rather than having a direct effect on the phenotype. For this reason, it is important to consider potential population stratification when conducting pharmacogenetic studies, particularly when trying to attribute a phenotype to a specific marker. Several approaches have been developed to account for population stratification in genetic association studies including the use of microsatellites (Wilson 2001, Lewis 2002, Apolinário 2017, Iacovacci 2017).

1.5 PHARMACOGENETICS STUDIES IN HIV

In broad terms, pharmacogenetic studies in HIV have focused upon defining the importance of variants for either the efficacy or safety of antiretroviral drugs, with the aim of informing drug selection or dose optimisation within genetically predefined sub-populations. The combination of multiple antiretroviral drugs, as part of the WHO recommended three-drug antiretroviral treatment, adds further complexity to these studies. Co-administration of antiretroviral drugs alongside drugs to treat comorbidities must also be considered within pharmacogenetic studies. Drug-drug interactions between the antiretroviral drugs in isolation and with other drug regimens, and the potential side effects that this can elicit, may be exacerbated by genetic variations with the patient. Furthermore, the prescription of a suitable drug regimen may be hampered by a patient's genetics resulting in alterations in outcome for one drug within the regimen. Pharmacokinetic boosters such as RTV, further complicate the picture, making the determination of a relationship between a patient's genetics and the relevant drug more difficult to decipher.

Since efficacy and safety are both underpinned by pharmacokinetics and biodistribution, most pharmacogenetic studies to date have focused on genes involved in drug metabolism enzymes, drug transporters, or nuclear receptor type transcription factors. Notwithstanding, probably one of the best examples of a clinically implemented genetic test is presented by the influence of the *HLA-B*57-01* allele on abacavir hypersensitivity reactions. A list of key pharmacogenetic markers that have been shown to be important in the context of HIV therapy is given in Table 1.2, and these observations are also discussed in the sections below.

Table 1.2: Population frequencies of SNPs previously associated with toxicity and/or pharmacokinetics of HIV antiretroviral drugs.

Gene	Protein	SNP	Drug interaction	Allele frequencies (%)											
				All		AFR		AMR		EAS		EUR		SAS	
CYP2B6	CYP2B6	516G>T	Efavirenz Nevirapine	G	T	G	T	G	T	G	T	G	T	G	T
				68.4	31.6	62.6	37.4	62.7	37.3	78.5	21.5	76.4	23.6	61.9	38.1
		983T>C		T	C	T	C	T	C	T	C	T	C	T	C
				97.7	2.3	91.8	8.2	99.0	1.0	100	0.0	100	0.0	100	0.0
		15582C>T		C	T	C	T	C	T	C	T	C	T	C	T
				71.1	28.9	91.8	8.2	64.8	35.2	56.4	43.6	68.0	32.0	65.8	34.2
ABCB1	P-gp	1236C>T	Efavirenz Raltegravir	C	T	C	T	C	T	C	T	C	T	C	T
				58.4	41.6	86.4	13.6	59.7	40.3	37.3	62.7	58.4	41.6	41.3	58.7
		4036A>G		A	G	A	G	A	G	A	G	A	G	A	G
				81.2	18.8	83.6	16.4	84.0	16.0	70.4	29.6	86.1	13.9	82.1	17.9
		3435C>T		C	T	C	T	C	T	C	T	C	T	C	T
				60.5	39.5	85.0	15.0	57.2	42.8	60.2	39.8	48.2	51.8	42.5	57.5
ABCC2	MRP2	-24C>T	Tenofovir	C	T	C	T	C	T	C	T	C	T	C	T
				86.5	13.5	96.9	3.1	83.4	16.6	78.3	21.7	79.3	20.7	90.5	9.5
		1249G>A		G	A	G	A	G	A	G	A	G	A	G	A
				81.3	18.7	81.1	18.9	84.1	15.9	90.4	9.6	79.6	20.4	72.2	27.8
		3563T>A		T	A	T	A	T	A	T	A	T	A	T	A
				96.3	3.7	94.4	5.6	96.3	3.7	100	0.0	93.0	7.0	98.3	1.7
		3972C>T		C	T	C	T	C	T	C	T	C	T	C	T
				71.2	28.8	78.4	21.6	65.9	34.1	75.3	24.7	62.9	37.1	69.5	30.5
ABCC10	MRP7	526G>A	Tenofovir Nevirapine	G	A	G	A	G	A	G	A	G	A	G	A
				63.5	36.5	97.0	3.0	55.9	44.1	41.4	58.6	54.0	46.0	56.4	43.6
		2843T>C		T	C	T	C	T	C	T	C	T	C	T	C
				80.0	20.0	69.2	30.8	81.4	18.6	92.0	8.0	76.8	23.2	84.5	15.5
ABCG2	BCRP	421C>A	Tenofovir Raltegravir	C	A	C	A	C	A	C	A	C	A	C	A
				88.1	11.9	98.7	1.3	85.9	14.1	70.9	29.1	90.6	9.4	90.3	9.7
NR1I2	PXR	63396C>T	Atazanavir	C	T	C	T	C	T	C	T	C	T	C	T
				46.6	53.4	63.5	36.5	51.6	48.5	37.7	62.3	34.0	66.0	42.6	57.4
NR1I3	CAR	540C>T	Efavirenz	C	T	C	T	C	T	C	T	C	T	C	T
				66.4	33.6	89.3	10.7	67.4	32.6	48.1	51.9	65.1	34.9	54.7	45.3
		1089C>T		C	T	C	T	C	T	C	T	C	T	C	T
				49.8	50.2	47.0	53.0	53.6	46.4	42.6	57.4	56.4	43.6	51.6	48.4

Data derived from Phase 3 of the 1000 Genome Project Ensembl datatbase (GenomesProjectConsortium 2015).

All = total population studied (n = 2504). AFR = African (n = 661), AMR = American (n = 347), EAS = East Asian (n = 504), EUR = European (n = 503), SAS = South Asian (n = 489).

African subpopulations: African Caribbean Barbados, African ancestry Southwest US, Esan Nigeria, Gambian in Western Division, Luhya Webuye Kenya, Mende Sierra Leone, Yoruba Ibadan Nigeria.

American subpopulations: Colombian Medellin Colombia, Mexican ancestry Los Angeles California, Peruvian Lima Peru, Puerto Rican Puerto Rico.

East Asian subpopulations: Chinese Dai Xishuangbanna China, Han Chinese Beijing China, Southern Han Chinese China, Japanese Tokyo Japan, Kinh Ho Chi Minh City Vietnam.

European subpopulations: Northern and Western European ancestry Utah USA, Finnish Finland, British England and Scotland, Iberian Spain, Toscani Italy.

South Asian subpopulations: Benglai Bangladesh, Gujarati Indian Houston USA, Indian Telugu UK, Punjabi Lahore Pakistan, Sri Lankan Tamil UK.

1.6 DRUG METABOLISM ENZYMES

Drug metabolising enzymes have taken a central role in pharmacogenetics studies to date with a major focus on the CYP family, for which many antiretroviral drugs are substrates, including NRTIs, PIs, and entry inhibitors.

1.6.1 *CYP2B6*

Variations in *CYP2B6* have been linked to alterations in protein activity via several mechanisms. The most common haplotype for *CYP2B6* is *CYP2B6*6* which is comprised of *CYP2B6* 516G>T (rs3745274) and 785A>G (rs2279343). As shown in Table 1.2, *CYP2B6* 516G>T is found most commonly in South Asian populations and least frequently in East Asian populations. The variant is also very common in African populations. *CYP2B6* 516G>T is used as a marker for the effect of *CYP2B6*6* and has been linked to alterations in EFV and NVP metabolism, pharmacokinetics and toxicity in a variety of populations (Haas 2004, Rotger 2005, Wyen 2008, Schipani 2011, Hui 2016, Nightingale 2016). The link between *CYP2B6*6* and alterations in EFV and NVP pharmacokinetics is due to a 50-75% reduction in CYP2B6 expression occurring through aberrant liver mRNA splicing (Hofmann 2008).

CYP2B6 516G>T screening alone is not adequate as an identifier for potential EFV toxicity (Pinillos 2016), and pharmacogenetics studies have identified other *CYP2B6* SNPs that also contribute to inter-individual response to EFV and NVP. The *CYP2B6*18* haplotype made up of 183G>A (rs2279344), 62G>A (rs12721649), 983T>C (rs28399499) and 17897C>T, is of interest as it results in the expression of a non-functional protein and is found predominantly in African populations (Table 1.2). *CYP2B6* 983T>C is the defining SNP of *CYP2B6*18* and was first identified through genetic screening of the exon and flanking intronic regions of 11 CYP enzymes (Solus 2004, Wang 2006). Since its discovery it has been associated with increased

NVP steady state plasma exposure and increased EFV exposure, however associations with NVP have been conflicting, which may be due in part to the low frequency of *CYP2B6* 983T>C (Rotger 2005, Wyen 2008, Haas 2009).

Overall it can be said that *CYP2B6* polymorphisms have a huge impact on EFV and NVP pharmacokinetics and that incidence of occurrence of key SNPs within this enzyme are more predominant in African and South East Asian ethnicity groups. Although *CYP2B6* polymorphisms have proven to be of limited value in terms of personalisation of therapy, they have provided the genetic basis for differences in drug exposure between different populations.

1.7 TRANSPORTERS

Transporters are key to the absorption, distribution, metabolism and excretion of all drugs and so SNPs that alter transporter function and expression can result in variability in drug pharmacokinetics between individuals. Drug transporter variants have previously been associated with alterations in the pharmacokinetics and disposition of antiretroviral drugs, in some cases influencing the incidence of toxicity.

1.7.1 *ABC transporters*

ABC gene-encoded transporters are found within multiple locations in the body including the brain, liver and kidney. Because of this, alterations in the frequency of production or morphology of these transporters have potential ramifications for the transport of multiple endogenous substrates and xenobiotics. The most widely studied ABC transporter has been P-gp. *ABCB1* pharmacogenetic studies to date have yielded highly conflicting data (Yen-Revollo 2009, Swart 2012, Coelho 2013, Ngaimisi 2013, Dalal 2015, Russo 2016).

In the case of TFV, SNPs within *ABCC* genes have been established as risk factors for increased likelihood of developing TFV-associated KTD within multiple studies. This is due to some of the encoded MRP transporters transporting TFV across the apical membrane of PTCs within the kidney, into the lumen and out into the urine. Loss of function of these transporters results in a reduction in TFV transport, resulting in greater TFV accumulation in PTCs. This accumulation leads to mitochondrial toxicity and subsequent cell death (Lewis 1995, Kohler 2009).

ABCC2 encodes the MRP2 transporter, an efflux transporter located on the apical membrane of polarised cells. MRP2 is present in multiple locations including on hepatocytes, renal PTCs and intestinal epithelia (Pratt 2015). The *ABCC2* 'CATC' haplotype is a combination of the polymorphisms –24C>T (rs717620), 1249G>A (rs2273697), 3563T>A (rs17222723) and 3972C>T (rs3740066) and has been significantly associated with TFV-induced renal proximal tubulopathy (Rodríguez-Nóvoa 2009). The CGAC haplotype was found to safeguard against toxicity in a majority Caucasian population (Izzedine 2006). A study of Japanese patients found *ABCC2* –24C>T allele T and 1249G>A allele G to be protective against TFV-induced KTD (Nishijima 2012). These results are surprising given that TFV has not been reported as a substrate of MRP2 as discussed previously (Moss 2014). Variation in allele frequencies between ethnicities is observed within each SNP of the haplotype group, with a 17.6% difference in variant allele frequency between African ancestry and East Asian ethnicity for *ABCC2* –24C>T. Given that this SNP has been linked as both a protective and contributory SNP to TFV-induced renal dysfunction, differences in its frequency may affect the way this SNP can be used as a potential marker for kidney toxicity.

The efflux transporter MRP7 is expressed ubiquitously throughout the body and is encoded for by the *ABCC10* gene. MRP7 was previously demonstrated to transport TFV (Pushpakom 2011). *ABCC10* 526G>A (rs9349256) and 2843T>C (rs2125739) have previously been associated with TFV-induced KTD within a majority Caucasian study group (Pushpakom 2011). *ABCC10* 526G>A was among the top 20 of 30 SNPs studied within a Genome Wide Association Study looking at Caucasian and Black participants, and was among the top 20 of 594 SNPs studied within the Caucasian participants in the study to be linked with alterations in TFV clearance, however not to a statistically significant degree (P = 0.100) (Wanga 2015). An association of genetic polymorphisms with TFV-induced KTD was further established within two patients, both of whom were heterozygous for *ABCC10* 2843T>C (rs2125739) and *ABCC2* –24C>T (rs717620) (Giacomet 2013).

In addition to the observed interactions with TFV toxicity, *ABCC10* 2843T>C (rs2125739) has been associated with lower NVP plasma concentrations within a cohort of Caucasian and Black patients, and within the Caucasian patients in isolation, but not to a statistically significant degree within the Black participants (Liptrott 2012). This result is surprising given comparable frequency of the variant allele within both ethnicities in the study. This study provides further evidence for a direct functional effect of *ABCC10* 2843T>C that warrants further investigation within larger diverse study populations.

SNPs within the *ABCG2* gene, which encodes BCRP, have been associated with elevated plasma and urine TFV concentrations. *ABCG2* 421C>A (rs2231142) was associated with elevated TFV AUC in a study of majority African American participants. Patients possessing the variant allele had a 1.5-fold increase in TFV AUC compared to homozygous wild-type patients (Baxi 2017). *ABCG2* 421C>A has also been linked to higher peak RAL plasma concentrations (Tsuchiya 2016). This relationship between *ABCG2* 421C>A and elevated drug

pharmacokinetics was attributed within both studies to a hypothesised loss of function of BCRP caused by *ABCG2* 421C>A, resulting in a reduction in drug transport. This mechanism has been demonstrated *in vitro* for other BCRP substrates (Polgar 2008, Neumanova 2014).

Within phase 3 of the 1000 Genomes project it was shown that the variant allele for *ABCG2* 421C>A occurs at the lowest frequency within African participants (1.3%) and at highest frequency in East Asian populations (29.1%). The variation in frequency observed for this SNP highlights its potential clinical impact within particular populations (Table 1.2) and demonstrates the need for population-specific pharmacogenetic studies.

1.8 TRANSCRIPTIONAL REGULATORS

Alterations in transcriptional regulator expression through SNPs that reduce or increase function have the potential to produce wide-ranging effects, due to the intricate network of interactions that are associated with enzyme and transporter regulation. While nuclear receptors are classically involved in induction of drug metabolism, they also correlate with enzyme and transporter expression in patients not receiving enzyme inducers (Owen 2004, Albermann 2005, Vyhlidal 2006, Betts 2015).

1.8.1 *NR1I2*

NR1I2 encodes the pregnane X receptor (PXR), an important transcription factor in regard to the regulation of expression of CYP enzymes and transporters (Svärd 2010). P-gp expression has been directly correlated with CYP3A5 expression in the intestine, through co-regulation of expression of the two proteins by PXR (Burk 2004, Ufer 2008, Cascorbi 2011). The antiretroviral drug RTV has previously been confirmed as an activator of PXR (Luo 2002). This effect is not observed for the pharmacokinetic booster cobicistat (COBI) (Marzolini 2016).

Additionally, EFV has been demonstrated to induce *CYP3A4* promoter activity through PXR activation (Hariparsad 2004). Significant differences in *NR1I2* SNP frequencies have been observed between ethnicities (Table 1.2) (Swart 2012).

NR1I2 63396C>T (rs2472677), has been significantly associated with below minimum effective concentrations of unboosted atazanavir (ATV) in a population of 43% Caucasian patients, the ethnicity of the remainder of the cohort was unspecified however the association was observed within the total population (Siccardi 2008). This observation was further confirmed through pharmacokinetic modelling, which demonstrated an association between *NR1I2* 63396C>T and variation in unboosted ATV clearance in a majority Caucasian population (Schipani 2010). The proposed mechanism of this interaction is that the presence of *NR1I2* 63396C>T results in increased expression and activity of PXR, resulting in increased expression of proteins transcriptionally regulated by PXR and thus increased metabolism of ATV by its PXR regulated metaboliser enzymes (Schipani 2010). These observations for ATV were partially validated in another predominantly Caucasian population (Kile 2012), but a Malawian cohort study showed no association between *NR1I2* 63396C>T and NVP pharmacokinetics (Brown 2012). However, frequency of the *NR1I2* 63396C>T variant allele T varies between European (66%) and African (36.5%) populations according to phase 3 of the 1000 Genomes Project (Table 1.2).

1.8.2 *NR1I3*

NR1I3 encodes the constitutive androstane receptor (CAR) a transcription factor that functions to regulate the expression of a complex network of phase I and II metabolising enzymes. Being homozygous CC for the SNP *NR1I3* 453C>T (rs2307424) has been associated with early discontinuation of EFV therapy in a majority Caucasian study group (Wyen 2011). Furthermore, incidence of discontinuation was seen more frequently in Caucasian patients

compared to Black patients in the study. The variant allele was also seen more frequently in the Caucasian participants (32%) compared to the Black participants (15%) (Wyen 2011), suggesting that this effect may have more impact in Caucasian populations. Additionally, two separate studies have observed *NR1I3* 453C>T to be associated with early discontinuation of EFV in a Chilean population and a Bantu South African population (Swart 2012, Cortes 2013). Furthermore, within the Chilean population *NR1I3* 453C>T was also significantly associated with lower EFV plasma concentration (Cortes 2013).

NR1I3 1089C>T (rs3003596) CC and CT genotypes have been significantly associated with a reduction in plasma EFV concentration in Bantu South Africans, suggesting that the presence of a C allele may result in increased *NR1I3* expression, and therefore increased expression of proteins that metabolise EFV (Swart 2012). Statistically significant inter- and intra-ethnic variation has been observed for the frequency of both the *NR1I2* and *NR1I3* SNPs (Table 1.2) (Swart 2012).

1.9 THESIS OBJECTIVES

The primary aim of this thesis was to analyse the impact patient genetics has on adverse HIV drug response and drug-drug interactions, through studying multi-ethnic populations receiving one of two key antiretroviral drugs, TFV or EFV. Furthermore, we investigated potential interactions between TFV or its prodrug TAF with transporters at the site of TFV-associated renal toxicity, with the goal of understanding how these interactions may influence the way in which TFV-associated renal toxicity is diagnosed. These aims were completed through the studies outlined below.

A HIV positive mixed gender population of Ghanaian adults was studied in order to determine the contribution of SNPs in transporters found within PTCs to the presentation of TFV-associated renal dysfunction, defined as KTD or chronic kidney disease (CKD). The SNPs included in the study were found within *ABCC10*, *ABCC2* and *ABCC4*, these genes were selected based on their protein expression on the apical membrane of PTCs.

In order to further investigate the contribution of PTC transporter SNPs to the disposition of TFV, the effect of SNPs in genes linked to TFV excretion and TDF metabolism (*ABCC2, ABCC4, ABCC10* and *ABCG2*) were studied in a HIV positive majority male Caucasian population. Additionally, the contribution of these SNPs to variability in TFV plasma and urine concentrations was investigated.

A transiently transfected Human Embryonic Kidney 293 (HEK293) cell line expressing either MATE1 or MATE2K transporter was developed through utilisation of lipid-based transfection of plasmid deoyribonucleic acid (DNA), obtained from vectors encoding either MATE1 or MATE2K. These cell lines were then used to study potential interactions between TAF and TFV with the renal biomarker creatinine or the type 2 diabetes drug metformin. These drug interactions are of interest given the use of creatinine to calculate renal function and metformin's classification of being unsuitable for use in patients with CKD (Munar 2007, Estrella 2010).

The effect of gene variants on levonorgestrel (LNG) pharmacokinetics was assessed in patients receiving either EFV or NVP based antiretroviral drug regimens. SNPs in *CYP2B6, CYP2A6, NR1I3* and *NR1I2* were selected based on the role of their expressed protein in EFV or NVP metabolism. A cohort of Ugandan HIV-positive women participating in a drug-drug interaction pharmacokinetic study were selected (Scarsi 2016). Within this study an

interaction between EFV and LNG which resulted in suboptimal LNG pharmacokinetics had been observed (Scarsi 2016).

These studies have relevance in light of the growing number of patients receiving ART through efforts to achieve the UNAIDS 2020 90:90:90 targets. A greater understanding of the mechanisms behind drug-drug interactions, adverse events and treatment failure in patients receiving ART is required to achieve these targets. Through analysing the contribution a patient's genetics has to their response to ART, it is possible to determine the clinical relevance of these interactions, and thus determine the relevance of personalised medicine to global HIV treatment strategies. Furthermore, studying the mechanisms by which antiretroviral drugs are metabolised and excreted from the body has utility through enabling the prediction of potential adverse events and drug-drug interactions in patients receiving these drugs in the future, enabling a greater number of patients to achieve the final 90 target of achieving sustained viral suppression.

Chapter 2: Assessment of the Relationship Between Polymorphisms in *ABCC10*, *ABCC2* and *ABCC4* and Tenofovir-Induced Renal Dysfunction

2.1 INTRODUCTION

TFV administered as a once daily dose of the prodrug TDF, has a favourable pharmacological profile of high efficacy and once daily dosing with no CYP enzyme interactions. Despite early reports of a low toxicity profile in the kidney (Barditch-Crovo 2001, Schooley 2002) mild to moderate kidney toxicity is now recognised as a modest but significant risk for patients given TFV-containing regimens (Jülg 2005, Mauss 2005, Scherzer 2012, Quesada 2015). A number of different manifestations of kidney injury have been documented with TDF use, including acute kidney injury, Fanconi syndrome, CKD and KTD (Lee 2003, Barrios 2004, Rifkin 2004, Herlitz 2010). Toxicity has led to concerns over the long-term use of TDF, with a correlation between increasing time on TDF therapy and incidence of kidney damage being identified (Rifkin 2004, Fafin 2012, Quesada 2015).

Host genetic polymorphisms in PTC transporters have previously been associated with TFV-induced KTD. *ABCC10* 526G>A (rs9349256) and 2843T>C (rs2125739) were associated with TFV-induced KTD in patients receiving TDF ART (Pushpakom 2011). *ABCC2* SNPs have been linked with KTD in multiple studies of patients of varied ethnicity (Izzedine 2006, Rodríguez-Nóvoa 2009, Nishijima 2012). The CATC haplotype for *ABCC2* at positions -24C>T (rs717620), 1249G>A (rs2273697), 3563T>A (rs8187694) and 3972C>T (rs3740066) was shown to be a predisposing haplotype for TFV-associated renal dysfunction, with CGAC haplotype being protective against renal proximal tubulopathy (Izzedine 2006). The *ABCC4* SNP, 4131T>C (rs3742106), has been associated with increased TFV-diphosphate in human peripheral mononuclear cells (Kiser 2008). Additionally, older age and low body weight have also been associated as risk factors for KTD (Nelson 2007).

In comparison to Caucasian patients, the risk of renal dysfunction in HIV-1 positive patients of African descent is heightened (Rostand 1982, Kopp 2003). Our study sought to assess the relationship between four SNPs in key genes of interest and markers of KTD and CKD in patients taking TFV-containing ART. With the overarching aim to further elucidate the relationship between host genetics and renal toxicity in HIV-1 positive patients of African descent.

2.2 METHODS

2.2.1 *Ethical approval*

Research ethics approval was obtained from the Committee on Human Research Publications and Ethics at KNUST Kumasi (CHRPE21/11), along with written informed consent from all patients.

2.2.2 *Study design and cohort*

This study was a retrospective cross-sectional study of renal dysfunction in patients from the Komofo Anokye Teaching Hospital in Kumasi Ghana (Chadwick 2015). The study included 66 HIV-1 positive Ghanaian adults receiving TDF. All patients had received treatment for at least 6 months before study entry.

2.2.3 *Parameter definitions*

CKD was defined as either having an eGFR < 60 mL/min or the presence of proteinuria. Positive proteinuria was determined through a urine dipstick (being ≥ 1 plus) then confirmed with a urine protein-creatinine ratio (uPCR) > 30 mg/mmol. eGFR was calculated in house using the Cockcroft-Gault equation. eGFR slopes using baseline (pre-treatment) and current (sampling) values were calculated. KTD was defined as the presence of two or more of the following: fractional phosphate excretion > 18%, fractional urate excretion > 15%, glycosuria (with normoglycaemia), hypophosphataemia < 0.8 mmol/L, presence of proteinuria, a uPCR > 30 mg/mmol, urinary albumin-protein ratio (uAPR) < 0.4 and either a uPCR > 20 or urine albumin-creatinine ratio (uACR) > 3 mg/mmol. Possible KTD was classed as positive if the patient presented with one of any of the above factors, excluding testing positive for the presence of proteinuria.

2.2.4 *Sample and data collection*

Sampling data was collected between 2012 and 2013 from whole blood. Serum creatinine, phosphate, glucose, urate and potassium values were obtained, and urine creatinine, phosphate, urate and protein levels were calculated from urine samples. Patients with known causes of kidney dysfunction or urinary tract infections (identified by positive dipsticks for nitrites and/or leukocytes) were excluded from the study.

2.2.5 *Genotyping*

Genomic DNA was extracted from whole blood using the manufacturers' protocol (E.Z.N.A Blood DNA Mini Kit; Omega bio-tek; Norcross, GA). In brief this consisted of the addition of 25 µL of protease solution and 250 µL of BL buffer to 250 µL of each blood sample before incubation at 65 °C for 10 minutes. 260 µL of ethanol was then added to each sample before the sample was transferred to a HiBind® DNA Mini Column inside a collection tube. The sample was then centrifuged at 10,000 ×*g* for 1 minute. The filtrate was discarded and 500 µL of HBC Buffer was added to the column, the sample was then span at 10,000 ×*g* for 1 minute. The filtrate was discarded, and the sample was then washed twice with 700 µL of Wash Buffer and centrifuged at 10,000 ×*g* for 1 minute. The HiBind® DNA Mini Column was centrifuged at 10,000 ×*g* for 2 minutes to dry the column membrane and remove any residual ethanol before elution. The HiBind® DNA Mini Column was transferred to a fresh collection tube and incubated with 50 µL of Elution Buffer at 65 °C for 5 minutes. The tube was then centrifuged at 10,000 ×*g* for 1 minute before repeating the incubation with elution buffer. The tube was centrifuged again at 10,000 × *g* for 1 minute. The resulting DNA was stored at -20 °C ready for downstream applications. Extracted DNA was quantified using NanoDrop (Thermo Fisher Scientific, Wilmington, DE). Genotyping was completed using real-time allelic discrimination polymerase chain reaction (PCR) assays on a DNA Engine Chromo4 system (Bio-Rad Laboratories, Hercules, CA). The PCR protocol followed denaturation at 95 °C for 10

minutes, followed by 50 cycles of amplification at 92 °C for 15 seconds and annealing at 60 °C for 1 minute 30 seconds. TaqMan Genotyping Master mix and assays *ABCC10* 2843T>C (rs2125739), *ABCC10* 526G>A (rs9349256), *ABCC2* -24C>T (rs717620) *ABCC4* 4131T>C (rs3742106) were purchased from Life Technologies (Paisley, Renfrewshire, UK). Opticon Monitor v.3.1 software (Bio-Rad Laboratories) was used to obtain allelic discrimination plots and identify genotypes.

2.2.6 *Statistical analysis*

Compliance with Hardy-Weinberg equilibrium was tested through previously outlined methods (Rodriguez 2009). Following the equation:

$$p^2 + 2pq + q^2 = 1$$

Where p is the frequency of the common allele and q is the frequency of the variant allele within the study population. Within the equation, p^2 is the frequency of the common homozygous genotype, q^2 is the frequency of the variant homozygous genotype and 2pq is the frequency of the heterozygous genotype. The aim of this equation is to determine if the observed genotype frequencies in the study population differ from the frequencies predicted by the equation. With a chi squared value (X^2) assigned to an associated *P* value range used to determined statistical significance. $P \leq 0.05$ was considered as statistically significant.

Genotypes were coded for regression analyses as 0 = homozygous common allele, 1 = heterozygous and 2 = homozygous variant allele. Categorical variables were described using relative frequencies, whilst continuous variables were described using median and N interquartile range (IQR). The Shapiro-Wilk Test was used to test for normality with $P \leq 0.05$

considered as statistically significant. A univariate analysis through linear and binary logistical regression was carried out to identify independent variables associated with factors for renal toxicity. Variables with $P \leq 0.2$ for the univariate analysis were carried through to a linear or binary logistical backwards multivariate analysis where $P \leq 0.05$ was classed as statistically significant. All statistical analyses were carried out using SPSS Statistics v.22 (IBM Armonk, NY). All charts were produced using GraphPad Prism 6 (GraphPad Software, La Jolla, CA).

2.3 RESULTS

2.3.1 *Patient characteristics*

Sixty-six patients receiving TDF-containing regimens were recruited into the study, patient characteristics are summarised in Table 2.1. The median (IQR) age and weight of all patients was 38 years (34-47 years) and 58 kg (52-65 kg). Patients were predominantly female and more likely to be taking EFV (than NVP or LPV/RTV) alongside TDF and zidovudine or 3TC. All SNPs were in Hardy-Weinberg equilibrium within the study population. Genotype frequencies are shown in Table 2.1.

Table 2.1: Characteristics of the study participants at entry.

Characteristics	Total (n = 66)			Patient number per parameter
Age (years)	38.0 (34.0-47.0)			61
Weight (kg)	58.0 (52.0-65.0)			60
Height (m)	1.6 (1.5-1.6)			52
Male (n [%])	10 (15)			62
Hepatitis B positive (n [%])	6 (11)			17
CD4 count (cells/mm^3)	544.5 (312.3-645.8)			31
eGFR at start of study	93.1 (75.7-133.6)			18
eGFR at time of sampling	105.5 (86.5-120.9)			15
Proteinuria (n [%])	36 (55)			66
ART 3rd drug				
EFV (n [%])	35 (53)			66
NVP (n [%])	11 (17)			
LPV/RTV (n [%])	7 (11)			
N/A (n [%])	13 (19)			
Genotype frequencies				
ABCC10 2843T>C (rs2125739) (n [%])	**TT**	**CT**	**CC**	66
	27 (40)	38 (58)	1 (2)	
ABCC10 526G>A (rs9349256) (n [%])	**GG**	**AG**	**AA**	66
	60 (90)	5 (8)	1 (2)	
ABCC2 -24C>T (rs717620) (n [%])	**CC**	**CT**	**TT**	66
	58 (88)	8 (12)	0 (0)	
ABCC4 4131T>C (rs3742106) (n [%])	**TT**	**TC**	**CC**	66
	26 (39)	40 (61)	0 (0)	

Values shown as median (IQR) and percentage of population.

2.3.2 *Non-significant associations*

After univariate or multivariate regression analysis age was not significantly associated with log_{10} baseline creatinine, log_{10} creatinine at time of sampling, eGFR slope change per year, log_{10} urine creatinine or any incidence of KTD or CKD. No difference in log_{10} baseline creatinine, baseline eGFR, log_{10} creatinine at time of sampling, sampling eGFR, eGFR slope change per year, log_{10} urine creatinine, or any incidence of KTD was observed between male and female participants. Log_{10} height was not associated with log_{10} baseline creatinine, baseline eGFR, sampling eGFR, eGFR slope change per year, log_{10} urine creatinine, or any incidence of KTD or CKD. Variation in weight was not associated with log_{10} baseline creatinine, baseline eGFR, log_{10} creatinine at time of sampling, sampling eGFR, eGFR slope change per year, log_{10} urine creatinine, or any incidence of KTD. Time receiving TDF was not associated with alterations in log_{10} baseline creatinine, baseline eGFR, log_{10} creatinine at time of sampling, log_{10} urine creatinine or incidence of possible KTD or CKD. No relationship was observed between *ABCC10* 2843T>C (rs2125739) and baseline eGFR, eGFR slope change per year, log_{10} urine creatinine or possible KTD. Furthermore, no associations were seen for *ABCC10* 526G>A (rs9349256) and log_{10} baseline creatinine, log_{10} creatinine at time of sampling, sampling eGFR, eGFR slope change per year, log_{10} urine creatinine or any incidence of possible KTD or CKD. No associations were observed between *ABCC2* -24C>T (rs717620) and any parameter other than eGFR at time of sampling. No associations were observed between *ABCC4* 4131T>C (rs3742106) and any parameter other than CKD. Figure 2.1 shows the relationships between the non-significant SNPs and parameters of KTD after univariate linear regression analysis.

2.3.3 *Trends observed from univariate analysis*

Through univariate regression analysis a relationship was observed between *ABCC10* 2843T>C (rs2125739) and incidence of KTD (P = 0.181, OR = 0.4). A trend was seen between

ABCC4 4131T>C (rs3742106) and incidence of CKD (*P* = 0.110, OR = 2.3). A relationship between *ABCC2* -24C>T (rs717620) and higher eGFR at time of sampling (*P* = 0.178, β = 33.9) was also seen, but a low sample size for this association compromises its interpretation (CC; n= 13, CT; n= 1) as shown in Table 2.1. Subsequently these trends were carried through to multivariate analysis where they were seen to not be statistically significant.

A relationship between being female and having a lower $\log_{10}$ creatinine concentration at time of sampling and higher incidence of CKD was seen (*P* = 0.021, β = -0.1; *P* = 0.078, OR = 0.3; respectively), however the low number of male participants within our study compromises this association. Additionally this effect may in fact be due to stratification, given that typically a lower body weight is observed in females compared to males, a factor which has previously been linked with reduced renal function (Nelson 2007). A relationship between length of time on TDF and incidence of KTD was found (*P* = 0.120, OR = 0.1). Furthermore, a trend between age and $\log_{10}$ creatinine at time of sampling was observed (*P* = 0.033, β = 0.0). Log_{10} height was seen to be linked with higher eGFR slope change per year (*P* = 0.158, β = 721.0). However, these trends were not statistically significant within multivariate analysis. Figure 2.2 shows the relationships with parameters of KTD found to be linked through univariate linear regression analysis only.

2.3.4 *Significant associations from multivariate analysis*

As shown in Table 2.2, *ABCC10* 2843T>C (rs2125739) was associated with lower $\log_{10}$ baseline creatinine (*P* = 0.001, β = -0.4), higher baseline eGFR (*P* = 0.005, β = 61.6), higher $\log_{10}$ serum creatinine at time of sampling (*P* = 0.008, β = 0.1), lower eGFR at time of sampling (*P* = 0.040, β = -19.2) and lower eGFR slope change per year (*P* = 0.041, β = -43.4). *ABCC10* 526G>A (rs9349256) was associated with higher baseline eGFR (*P* = 0.045, β = 82.7), however this

result must be interpreted in light of the low sample size for this association (GG; n= 15, AG; n= 1) (Table 2.1). Figure 2.3 provides a visual representation of all significant genetic associations within the TFV group.

Increasing age was significantly associated with lower baseline eGFR (*P* = 0.049, β = -2.2) and lower eGFR at time of sampling (*P* = 0.018, β = -1.1). Log_{10} height was associated with higher log_{10} creatinine at time of sampling (*P* = 0.011, β = 2.0). Log_{10} duration on TFV was associated with higher eGFR slope change per year (*P* = 0.001, β = 155.1). Multivariate binary logistic regression including independent factors such as age and weight found no statistically significant associations between the study SNPs and KTD or CKD (Table 2.3). Low body weight was seen to be significantly associated with higher incidence of CKD (*P* = 0.012, OR = 0.9) (Figure 2.4 and Table 2.3).

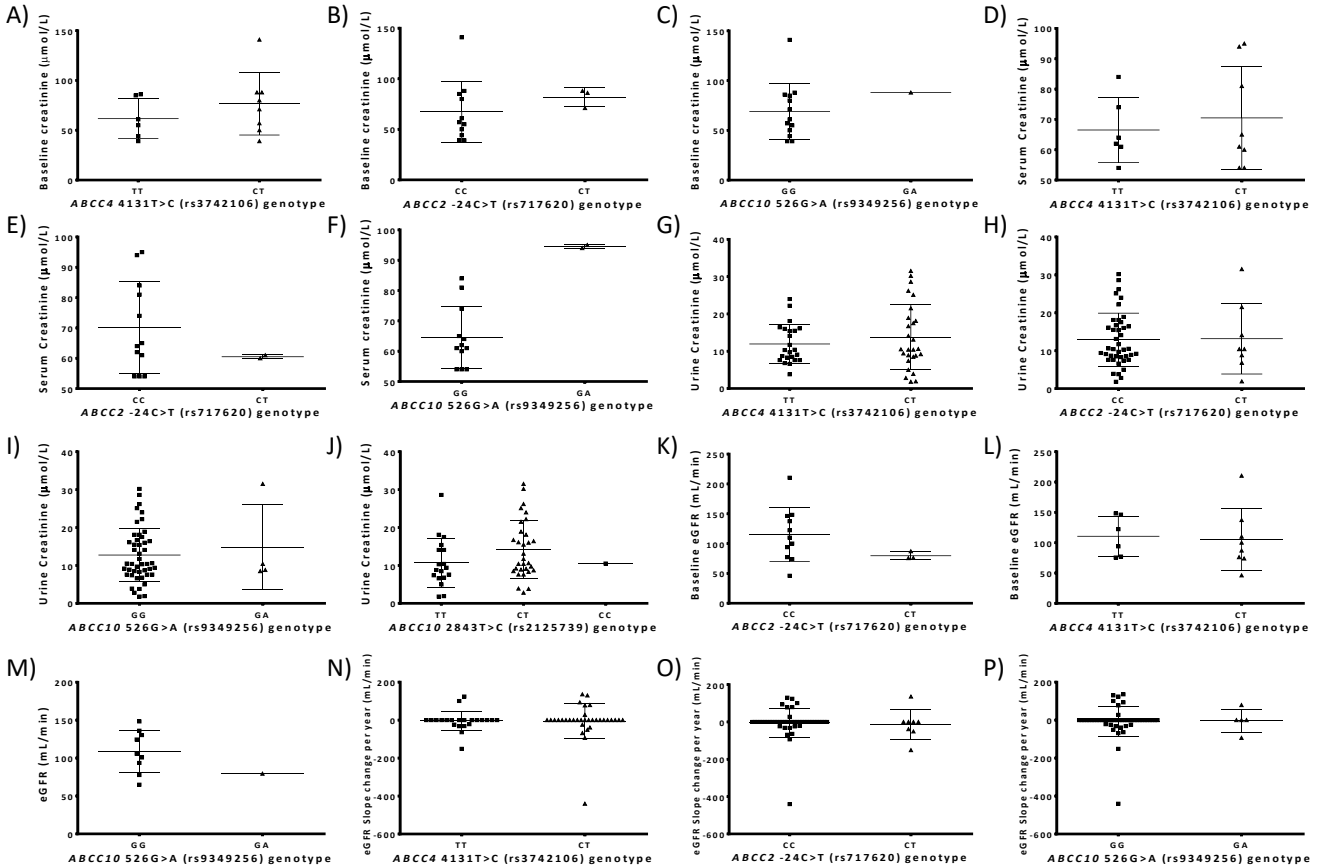

Figure 2.1: Non-significant relationships between parameters of KTD and genetic variants.

Graphs A-C: Non-significant relationships between SNPs and baseline creatinine. Graphs D-F: Non-significant relationships between SNPs and serum creatinine at time of sampling. Graphs G-J: Non-significant relationships between SNPs and urine creatinine at time of sampling. Graphs K-L: Non-significant relationships between SNPs and eGFR at baseline. Graph M: Non-significant relationship between SNP and eGFR at time of sampling. Graphs N-P: Non-significant relationships between SNPs and eGFR slope change. Data points represent the mean ± SD

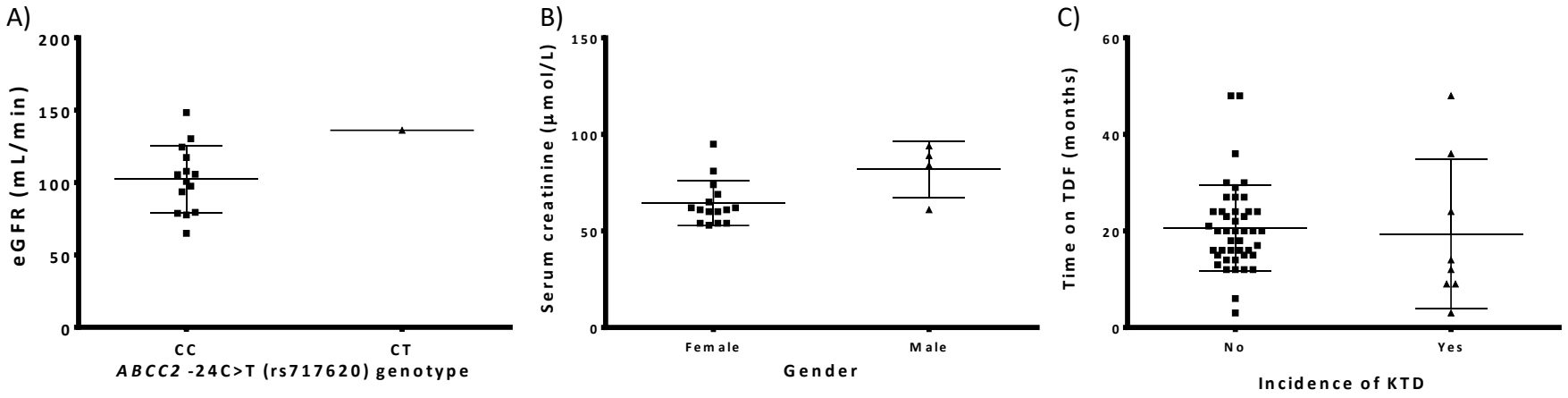

Figure 2.2: Relationships between parameters of KTD and genetic variants or patient characteristics from univariate analysis.

Graph A: Relationship between *ABCC2* -24C>T and eGFR at time of sampling. Graph B: Relationship between gender and serum creatinine at time of sampling. Graph C: Relationship between incidence of KTD and length of time receiving TDF. All relationships found to be significant ($P \leq 0.2$) through univariate regression analysis only. Data points represent the mean ± SD

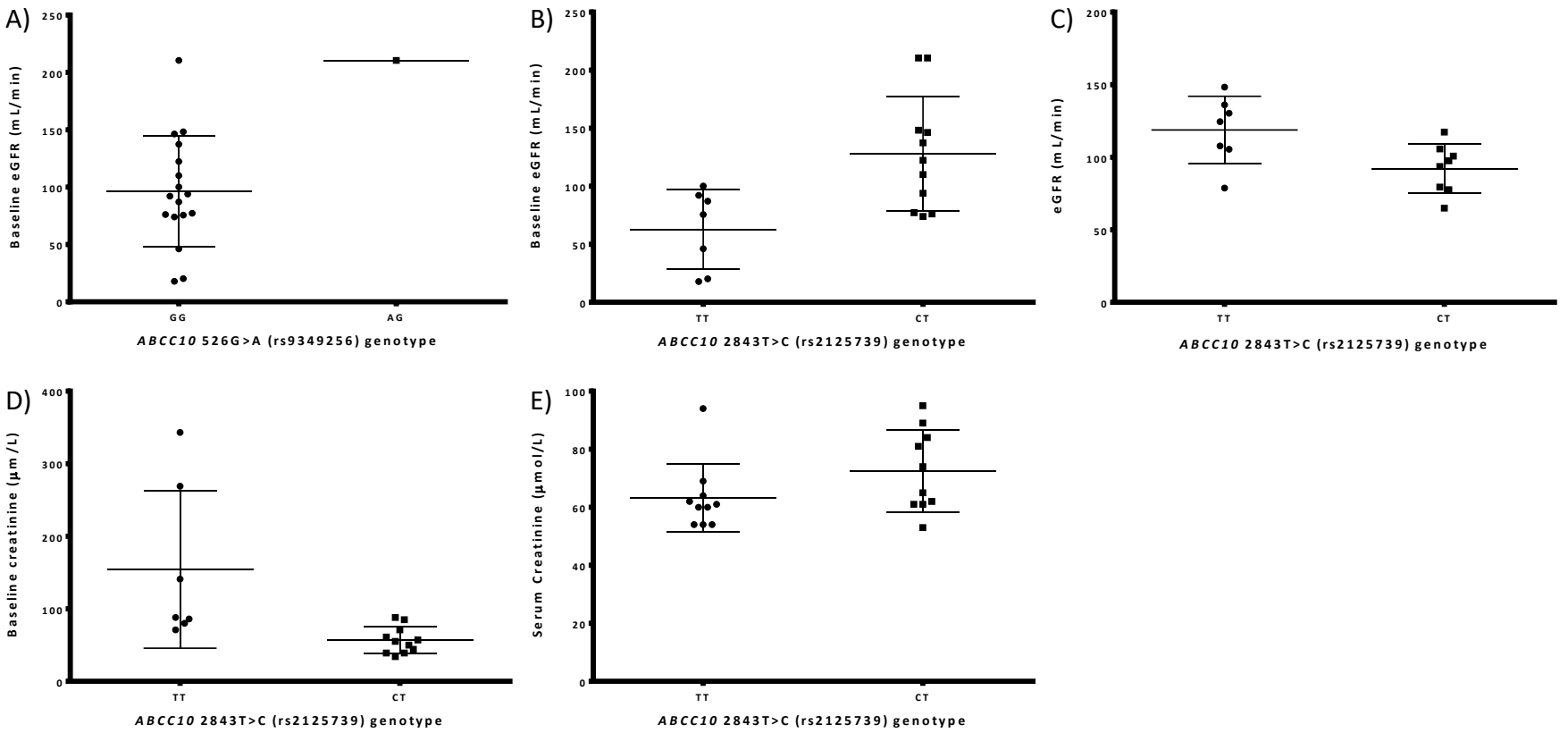

Figure 2.3: Statistically significant associations between parameters of KTD and genetic variants in proximal tubule transporters from multivariate analysis.

Graphs A-B: Significant associations between SNPs and eGFR at baseline. Graph C: Significant association between SNP and eGFR at time of sampling. Graph D: Significant relationship between SNP and serum creatinine at baseline. Graph E: Significant relationship between SNP and serum creatinine at time of sampling. All relationships found to be statistically significant ($P \leq 0.05$) through multivariate regression analysis. Data points represent the mean ± SD

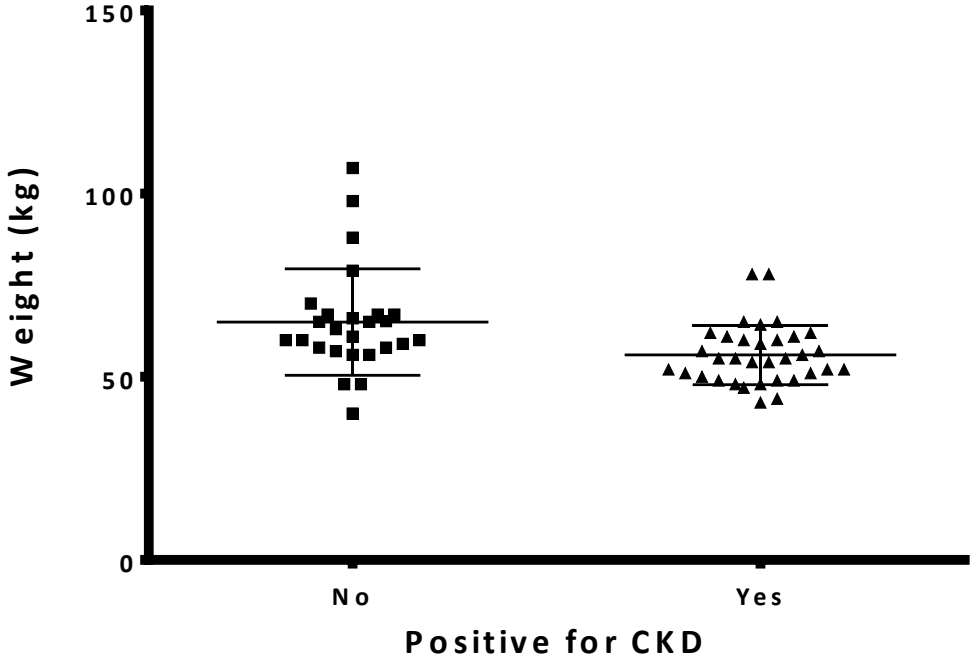

Figure 2.4: Relationship between weight and a positive diagnosis for CKD in patients receiving TDF from multivariate analysis.

Data points represent the mean ± SD

Table 2.2: Statistically significant univariate and multivariate linear regression analysis.

log_{10} Baseline creatinine	Univariate linear regression			Multivariate linear regression		
	P value	β value (95% CI)	r^2	*P* value	β value (95% CI)	r^2
***ABCC10* 2843T>C (rs2125739)**	0.001	-0.4 (-0.6,0.2)	0.5	**0.001**	**-0.4 (-0.6,0.2)**	**0.5**
Baseline eGFR	Univariate linear regression			Multivariate linear regression		
	P value	β value (95% CI)	r^2	*P* value	β value (95% CI)	r^2
Age (years)	0.095	-2.7 (-5.7,0.6)	0.1	**0.049**	**-2.2 (-4.3,0.0)**	**0.7**
***ABCC10* 2843T>C (rs2125739)**	0.008	65.2 (19.8,110.4)	0.4	**0.005**	**61.6 (22.1,101.1)**	**0.7**
***ABCC10* 526G>A (rs9349256)**	0.035	114.3 (9.3,219.3)	0.3	**0.045**	**82.7 (2.1,163,2)**	**0.7**
log_{10} Sampling serum creatinine	Univariate linear regression			Multivariate linear regression		
	P value	β value (95% CI)	r^2	*P* value	β value (95% CI)	r^2
Age (years)	0.033	0.0 (0.0,0.1)	0.3	0.382	0.0 (0.0,0.0)	0.6
Gender	0.021	-0.1 (-0.2,0.2)	0.3	0.378	-0.1 (-0.2,0.1)	0.6
log_{10} height (log_{10} m)	0.094	1.5 (-0.3,3.2)	0.2	**0.011**	**2.0 (0.5,3.4)**	**0.5**
***ABCC10* 2843T>C (rs2125739)**	0.115	0.1 (0.0,0.1)	0.1	**0.008**	**0.1 (0.0,0.2)**	**0.5**
Sampling eGFR	Univariate linear regression			Multivariate linear regression		
	P value	β value (95% CI)	r^2	*P* value	β value (95% CI)	r^2
Age (years)	0.023	-1.2 (-2.2,-2.0)	0.4	**0.018**	**-1.1 (-2.0,-0.2)**	**0.6**
***ABCC10* 2843T>C (rs2125739)**	0.024	-26.6 (-49.2,-4.1)	0.3	**0.040**	**-19.2 (-37.3,-1.1)**	**0.6**
ABCC2 -24C>T (rs717620)	0.178	33.9 (-17.5,85.2)	0.1	0.549	11.4 (-29.5,52.3)	0.6
eGFR slope change per year	Univariate linear regression			Multivariate linear regression		
	P value	β value (95% CI)	r^2	*P* value	β value (95% CI)	r^2
log_{10} height (log_{10}m)	0.158	721.0 (-290.2,1732.1)	0.0			
log_{10} time on TDF (log_{10} months)	0.002	126.0 (48.6,202.3)	0.2	**0.001**	**155.1 (66.9,243.3)**	**0.3**
***ABCC10* 2843T>C (rs2125739)**	0.093	-31.6 (-68.6,5.5)	0.1	**0.041**	**-43.4 (-84.9,-1.8)**	**0.3**

Univariate linear regression ($P \leq 0.2$) was completed, all statistically significant results were then carried through to multivariate linear regression ($P \leq 0.05$). All statistically significant variables from multivariate linear regression are shown in bold type. For linear regression β is the regression coefficient and represents incremental change in the renal toxicity parameter per unit change in a patient characteristic (e.g. per kg body weight or per allele carried). So if β = 0.5 an increase per unit in the patient characteristic results in the renal toxicity parameter increasing by a factor of 0.5. In the case of log transformed variables, the renal toxicity parameter would increase by a factor of $\log_{10} 0.5$.

Table 2.3: Statistically significant univariate and multivariate binary logistical analysis.

KTD	Univariate binary logistical regression		Multivariate binary logistical regression	
	P	Odds ratio (95%CI)	*P*	Odds ratio (95%CI)
$\log_{10}$ time on TDF ($\log_{10}$ months)	0.120	0.1 (0.0,1.7)		
ABCC10 2843T>C (rs2125739)	0.181	0.4 (0.1,1.5)		
CKD	Univariate binary logistical regression		Multivariate binary logistical regression	
	P	Odds ratio (95%CI)	*P*	Odds ratio (95%CI)
Gender	0.078	0.3 (0.1,1.2)		
Weight (kg)	0.012	0.9 (0.9,1.0)	**0.012**	**0.9 (0.9,1.0)**
ABCC10 2843T>C (rs2125739)	0.183	0.5 (0.2,1.4)		
ABCC4 4131T>C (rs3742106)	0.110	2.3 (0.8,6.2)		

Univariate binary logistic regression ($P \leq 0.2$) was completed, all statistically significant results were then carried through to multivariate binary logistical analysis ($P \leq 0.05$). All statistically significant variables from multivariate linear regression are shown in bold type.

2.4 DISCUSSION

To further elucidate the connection between PTC transporter SNPs and TFV-induced KTD, this study investigated the association between *ABCC10* 2843T>C (rs2125739), *ABCC10* 526G>A (rs9349256), *ABCC2* -24C>T (rs717620) and *ABCC4* 4131T>C (rs3742106) with renal function and parameters of KTD.

In our study, no statistically significant associations were observed between the SNPs studied and TFV-induced KTD or CKD. *ABCC10* 2843T>C (rs2125739) was significantly associated with both KTD and CKD as part of univariate analysis. However, these associations did not hold as part of multivariate analysis. *ABCC10* 2843T>C was associated with reduced creatinine at baseline and elevated creatinine at time of sampling. *ABCC10* 2843T>C (rs2125739) was also associated with higher eGFR at baseline and lower eGFR at time of sampling. These associations between *ABCC10* SNPs and baseline eGFR are of clinical relevance given that a low eGFR prior to receiving TDF has been indicated as a risk factor for developing TFV-associated renal toxicity (Antoniou 2005).

ABCC10 2843T>C (rs2125739) was associated with a decline in eGFR slope change per year indicating a net decline in eGFR during the study. *ABCC10* 526G>A (rs9349256) was also associated with lower eGFR at baseline however due to the low sample size conclusions cannot be drawn from this association. The effect of *ABCC10* SNPs on TFV-induced KTD has been observed in two previous studies Pushpakom *et al.* first reported a significant association between the *ABCC10* 526G>A (rs9349256) and KTD and *ABCC10* 2843T>C (rs2125739) and KTD in a predominantly Caucasian population (Pushpakom 2011). Giacomet *et al.* also associated *ABCC10* SNPs with TFV induced KTD using two patient case studies (Giacomet 2013).

The relationship described above may in part be explained by encoded transporter function. The *ABCC10* gene encodes for the MRP7 transporter. TFV has been demonstrated to be a substrate of this transporter (Pushpakom 2011) and it has been suggested that TFV may be transported by MRP7 within PTCs, however substrate specificity of MRP7 within PTCs is yet to be confirmed. Potentially alterations in the frequency of production of MRP7, or its morphology, caused by *ABCC10* 2843T>C could reduce TFV transport, resulting in greater TFV accumulation in PTCs. This accumulation would lead to mitochondrial damage and subsequent cell death (Kohler 2009, Herlitz 2010, Hall 2011). Through inhibition of mitochondrial DNA polymerase γ by TFV, resulting in inhibition of mitochondrial DNA synthesis (Lewis 1995). The consequent reduction in PTCs may result in low serum creatinine transport, leading to an increase in serum creatinine concentration and reduced eGFR over time. Further study is warranted in order to delineate the physiological mechanism by which this SNP may contribute to an accelerated eGFR decline in patients taking TFV, given that in a study of patients on TDF with a decline in eGFR, the decline in function was not reversible in over one-third of patients (Jose 2014).

In this study, lower weight was associated with increased incidence of CKD, a relationship that has previously been observed within a South African and a Tanzanian population (Mpondo 2014, De Waal 2017). Low weight has previously been defined as a risk factor for TFV-associated renal dysfunction in multiple studies of different ethnicities (Antoniou 2005, Nelson 2007, Nishijima 2011).

Future studies would benefit from the inclusion of TFV urine and plasma concentrations alongside kidney toxicity parameters, to better study the effect of kidney toxicity on TFV excretion. Furthermore, the effect of SNPs included within this study on the excretion of TFV

when prescribed alongside co-medications for other comorbidities, such as tuberculosis, would be of interest considering the wide-ranging application of TDF.

2.4.1 *Limitations*

The association of *ABCC10* 2843T>C (rs2125739) with alterations in creatinine concentration and eGFR builds on the findings of previous pharmacogenetic studies, as outlined in Chapter 1 (Section 1.7). However, these results should be interpreted in the context of the limitations of our study. An alternative method of study design could benefit this work, specifically applying a case-control model. This would involve dividing the total population into KTD positive or negative groups and comparing statistically significant associations between the two groups. This would allow us to determine if associations between parameters were found within the general patient cohort or was specific to patients with a positive phenotype.

An additional limitation of our study is the low overall sample size, which resulted in a low frequency of variant alleles for all of the SNPs studied within our patient population and limited the number of parameters which could be included in the analysis. Additionally incomplete population data was available for each parameter, due to patients being absent from clinic, meaning some parameters had significantly reduced patient numbers, compromising the significance of these associations, as shown in Table 2.1. This was seen for the significant association of *ABCC10* 526G>A with higher baseline creatinine which had both limited total patient number and low allele frequency.

Interpretation of these findings within a wider context is made complex through different studies applying different criteria for defining KTD. Our KTD definition was defined based on parameters included within the primary cross-sectional observational study of KTD and CKD incidence within patients receiving ART (Chadwick 2015). A clinical definition of KTD for

research would have utility as it would enable more accurate comparisons of findings between studies, given that different studies may be making comparisons about findings based off incidence of renal dysfunction at different severity levels.

Chapter 3: *ABCG2* 421C>A Influences Tenofovir Concentrations in Plasma and Urine

3.1 INTRODUCTION

TDF is currently used as part of both pre- and post- exposure prophylaxis for HIV and is recommended by the WHO as a preferred first-line ART for the treatment and prevention of HIV, and for the treatment of Hepatitis B (WHO 2016). TFV is generally well tolerated and has a favorable pharmacological profile. However, long-term use of TDF has previously been associated, in a dose-dependent manner, with increased incidence of osteomalacia and renal impairment in the form of Fanconi syndrome and KTD (Woodward 2009, Rodríguez-Nóvoa 2010, Hall 2011, Fafin 2012, Ezinga 2014, Chadwick 2015). TFV is primarily excreted in the urine via glomerular filtration and active tubular secretion via the PTCs of the kidney (Imaoka 2007).

TFV plasma and urine concentrations are of relevance as a measure of drug pharmacokinetics and as potential indicators of TFV-associated renal toxicity. High plasma TFV and TDF concentrations have previously been identified as risk factors for TFV-associated renal toxicity (Rodríguez-Nóvoa 2010, Ezinga 2014, Kunimoto 2016). Furthermore, previous pharmacogenetics studies have linked SNPs in transporters present within PTCs with alterations to TFV pharmacokinetics and incidence of kidney toxicity, within multiple studies of different ethnicities (Moss 2011). In the case of *ABCG2*, the rs2231142 SNP has previously been associated with variation in TFV pharmacokinetics (Baxi 2017).

Our study sought to investigate the relationship between pharmacogenetic variants in genes linked to TFV excretion (*ABCC2, ABCC4, ABCC10*) and TDF metabolism (*ABCG2*), and plasma/ urine TFV concentrations. The primary objectives of this study were to determine a genetic contribution to the inter-patient variation in TFV concentration observed between patients

receiving TDF, and to elucidate if the presence of SNPs previously shown to contribute to TFV-associated renal toxicity were an indicator of variable plasma/urine TFV concentrations.

3.2 METHODS

3.2.1 *Ethical approval*

Research ethics approval was obtained from NRES Committee London- Bloomsbury, along with written informed consent from all patients. Funding was provided by MSD.

3.2.2 *Study design and cohort*

This study was a retrospective sub-study of the clinical trial SSAT066 (ClinicalTrials.gov Identifier: NCT02351908), involving a multi-ethnic treatment naive patient population of 59 HIV positive patients receiving TDF alongside RAL (n = 19), DTG (n = 18) or elvitegravir (EVG) and COBI (EVG/COBI; n = 22). Patients were recruited from the St Stephen's AIDS Trust, London, UK.

3.2.3 *Sample and data collection*

Whole blood, plasma and urine concentrations were taken for pharmacogenetic and pharmacokinetic analysis 21 hours post dose, at study week 4. TFV concentrations in blood and urine at steady state were determined using a validated liquid chromatography tandem mass spectrometry (LCMS/MS) method.

3.2.4 *Genotyping*

Genomic DNA was extracted from whole blood through use of the manufacturers' protocol (E.Z.N.A Blood DNA Mini Kit; Omega bio-tek; Norcross, GA) as outlined in Chapter 2, Section 2.2.5. Extracted DNA was quantified using NanoDrop (Thermo Fisher Scientific, Wilmington, DE). Genotyping was completed using real-time allelic discrimination PCR assays on a DNA Engine Chromo4 system (Bio-Rad Laboratories, Hercules, CA). The PCR protocol followed denaturation at 95 °C for 10 minutes, followed by 50 cycles of amplification at 92 °C for 15

seconds and annealing at 60 °C for 1 minute 30 seconds. Taqman Genotyping Master mix and assays *ABCC4* 4131T>C (rs3742106), *ABCC10* 2843T>C (rs2125739), *ABCC10* 526G>A (rs9349256), *ABCC2* 1249G>A (rs2273697), *ABCC2* -24C>T (rs717620), *ABCC2* 1249G>A (rs2273697), *ABCC2* 3563T>A (rs17222723), *ABCC2* 3972C>T (rs3740066), *ABCG2* 421C>A (rs2231142) were purchased from ThermoFisher Scientific (Wilmington, DE). Opticon Monitor v.3.1 software (Bio-Rad Laboratories) was used to obtain allelic discrimination plots and identify genotypes.

3.2.5 *Statistical analysis*

Compliance with Hardy-Weinberg equilibrium was tested as outlined in Chapter 2 Section 2.2.6. Genotypes were coded for regression analyses as 0 = homozygous common allele, 1 = heterozygous and 2 = homozygous variant allele. Categorical variables were described using relative frequencies, whilst continuous variables were described using median and IQR. The Shapiro-Wilk test was used to test for normality with $P \leq 0.05$ considered as statistically significant. A univariate analysis through linear regression was conducted to identify independent variables associated with TFV plasma and urine concentrations. Variables with $P \leq 0.2$ for the univariate analysis were carried through to a linear backwards multivariate analysis where $P \leq 0.05$ was classed as statistically significant. Statistical analyses were carried out using SPSS Statistics v.22 (IBM Armonk, NY). All charts were produced using GraphPad Prism 6 (GraphPad Software, La Jolla, CA).

3.3 RESULTS

3.3.1 *Patient characteristics*

Fifty-nine patients were recruited for this study from the clinical trial SSAT066, patients were of multiple ethnicities: Caucasian (n = 50), Black (n = 2), Asian (n = 1), Mixed race (n = 2) and unclassified ethnicity defined as 'Other' (n = 4). Patient characteristics and genotype frequencies are summarised in Table 3.1. The median (IQR) age and weight of all patients was 34 years (28-42 years) and 71 kg (64-83 kg). All SNPs were in Hardy-Weinberg equilibrium.

Table 3.1: Characteristics of the study participants at entry.

Characteristics	Total (n = 59)
Age	34.2 (28.5-42.2)
Weight (kg)	71.6 (64.8-83.4)
Height (cm)	176.0 (171.0-181.0)
Gender (Female [%])	4 (7)
Drug regimen with tenofovir (n [%]): • Raltegravir • Dolutegravir • Elvitegravir and cobicistat	 18 (32) 19 (31) 22 (37)
Ethnicity (n [%]): • Caucasian • Black • Asian • Mixed race • Other	 45 (77) 2 (3) 4 (7) 2 (3) 6 (10)
Time post dose plasma sample (hours.minutes)	21.5 (13.4-25.3)
Time post dose urine sample (hours.minutes)	21.6 (14.1-25.4)
Tenofovir urine concentration (ng/mL)	21924.3 (14837.4-47405.6)
Tenofovir plasma concentration (ng/mL)	43.53 (28.1-72.2)
Tenofovir plasma:urine	531.9 (316.5-855.3)

Genotype frequencies			
ABCC4 4131T>C (rs3742106) (n [%])	**TT**	**CT**	**CC**
	27 (46)	27 (46)	5 (8)
ABCC10 2843T>C (rs2125739) (n [%])	**TT**	**CT**	**CC**
	38 (65)	19 (32)	2 (3)
ABCC10 526G>A (rs9349256) (n [%])	**GG**	**AG**	**AA**
	18 (31)	25 (42)	16 (27)
ABCC2 1249G>A (rs2273697) (n [%])	**GG**	**AG**	**AA**
	(39)	(27)	(5)
ABCC2 -24C>T (rs717620) (n [%])	**CC**	**CT**	**TT**
	40 (68)	17 (29)	2 (3)
ABCC2 3563T>A (rs17222723) (n [%])	**TT**	**AT**	**AA**
	18 (31)	41 (69)	0 (0)
ABCC2 3972C>T (rs3740066) (n [%])	**CC**	**CT**	**TT**
	22 (37)	27 (46)	10 (17)
ABCG2 421C>A (rs2231142) (n [%])	**CC**	**AC**	**AA**
	44 (75)	15 (25)	0 (0)

Values shown as median (IQR) and percentage of population.

3.3.2 *Non-significant associations*

Through univariate and multivariate linear regression analysis age was shown not to be associated with TFV urine concentration or TFV plasma:urine ratio. Weight, height, gender and co-medication with DTG where not associated with any alterations in TFV parameters. Co-medication with EVG/COBI was not associated with a change in TFV plasma or urine concentration. Sampling time post dose was not associated with TFV plasma or urine concentration. *ABCC10* 2843T>C (rs2125739), *ABCC10* 526G>A (rs9349256), *ABCC4* 4131T>C (rs3742106), *ABCC2* 3563T>A (rs17222723) and *ABCC2* 1249G>A (rs2273697) where not associated with any TFV parameters. *ABCC2* -24C>T (rs717620) and *ABCC2* 3972C>T (rs3740066) where not associated with alterations in TFV plasma or urine concentration. Figure 3.1 shows all non-significant results for SNPs and TFV plasma concentration and Figure 3.2 shows all non-significant results for SNPs and TFV urine concentration after univariate linear regression analysis.

3.3.3 *Trends observed from univariate analysis*

A trend was observed between *ABCC10* 2843T>C (rs2125739) and higher TFV urine concentration ($P = 0.136$, $\beta = 0.1$) through univariate linear regression analysis. Relationships between *ABCC2* -24C>T (rs717620) and *ABCC2* 3972C>T (rs3740066) with a lower TFV plasma:urine ratio ($P = 0.186$, $\beta = -0.1$; $P = 0.112$, $\beta = -0.1$; respectively) were also seen.. A trend was seen between longer time post dose for urine samples and a higher TFV plasma:urine ratio ($P = 0.036$, $\beta = 0.0$). Figure 3.3 shows all genetic associations found to be linked through univariate linear regression analysis, however these relationships were not seen to be significant within multivariate regression analysis.

3.3.4 *Significant associations from multivariate analysis*

Statistically significant univariate and multivariate regression analysis results for TFV plasma and urine concentrations and plasma to urine ratio are presented in Table 3.2. *ABCG2* 421C>A (rs2231142) was significantly associated with lower $\log_{10}$ TFV plasma (P = 0.030, β = -0.2) and $\log_{10}$ TFV urine (P = 0.010, β = -0.3) concentrations. No other genetic associations were observed. Increasing age was significantly associated with a higher $\log_{10}$ TFV plasma concentration (P = 0.037, β = 0.0). Co-medication of TFV with EVG/COBI was significantly associated with lower TFV plasma to urine ratio (P = 0.005, β = -0.2) when compared to co-medication with RAL. Time post-dose was significantly associated with higher TFV plasma to urine ratio (P = 0.010, β = 0.0).

TFV plasma and urine concentrations are summarised by significantly associated SNP in Table 3.3 and visually represented in Figure 3.4. TFV plasma concentration was 31.9% lower in heterozygous *ABCG2* 421 CA patients compared to those who were homozygous CC. TFV urine concentration was 40.0% lower in *ABCG2* 421 CA patients compared to patients who were homozygous CC.

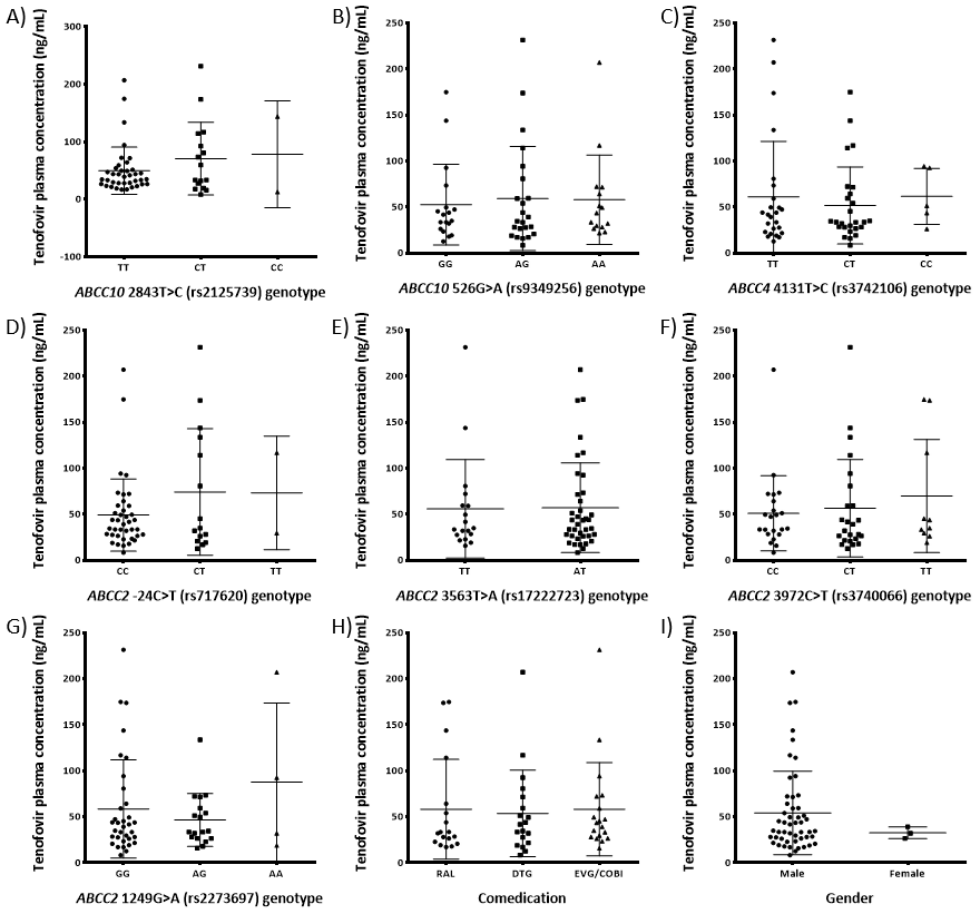

Figure 3.1: Non-significant association for TFV plasma concentration.

Graphs A-G: Non-significant relationships between SNPs and TFV plasma concentration. Graph H: Non-significant relationship between co-medication prescribed with TDF and TFV plasma concentration. Graph I: Non-significant relationship between gender and TFV plasma concentration. Data points represent the mean ± SD

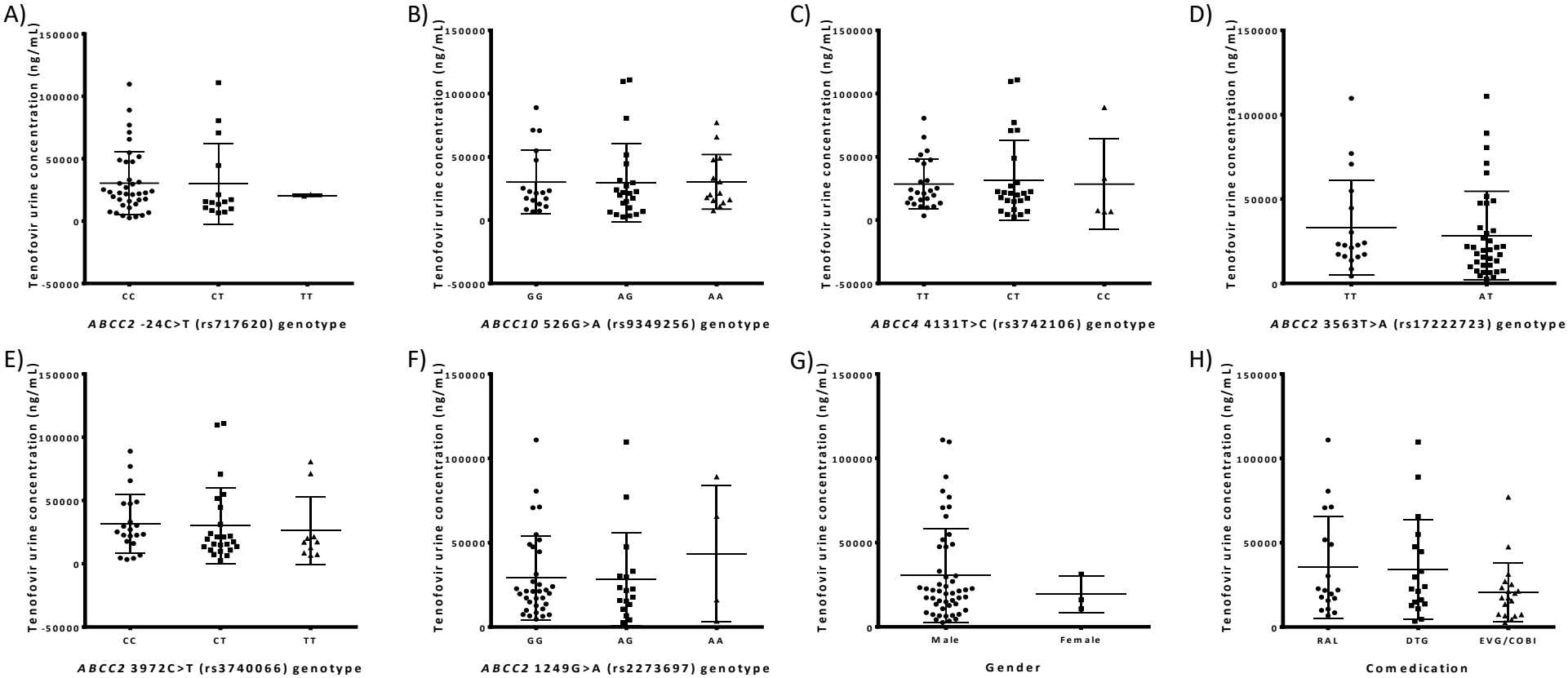

Figure 3.2: Non-significant association for TFV urine concentration.

Graphs A-F: Non-significant relationships between SNPs and TFV urine concentration. Graph G: Non-significant relationship between gender and TFV urine concentration. Graph H: Non-significant relationship between co-medication prescribed with TDF and TFV urine concentration. Data points represent the mean ± SD

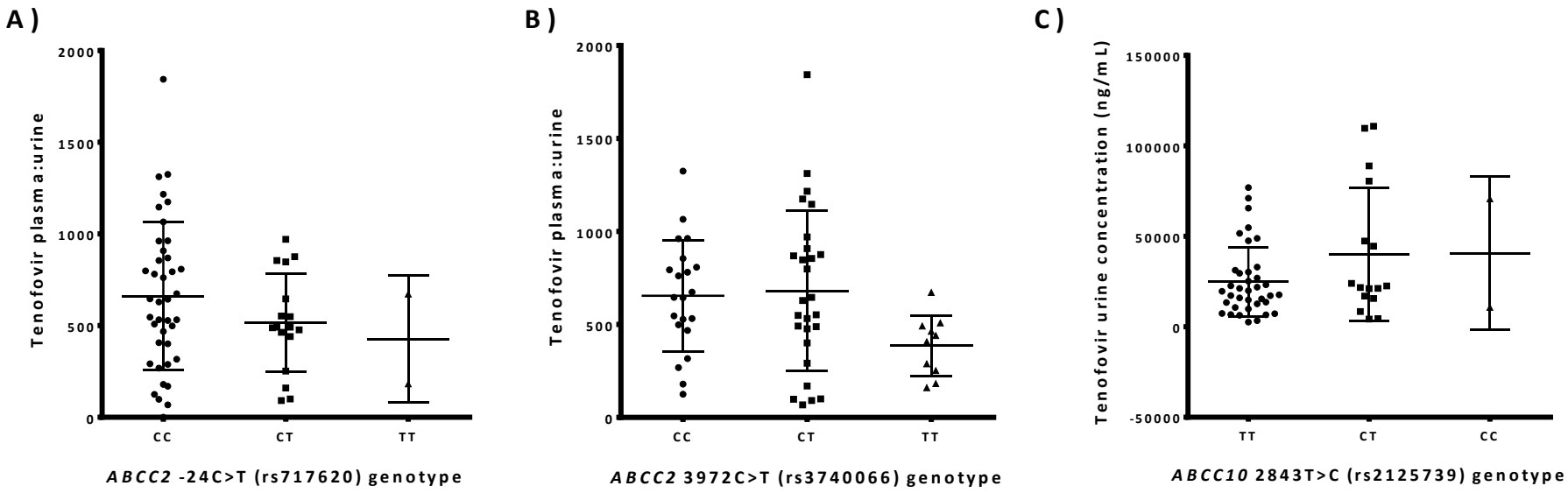

Figure 3.3: Relationships between TFV plasma or urine concentrations and genetic variants or patient characteristics from univariate analysis.

Graphs A-B: Relationship between SNPs and TFV plama:urine ratio. Graph C: Relationship between SNP and TFV urine concentration. All relationships found to be significant ($P \leq 0.2$) through univariate linear regression analysis only. Data points represent the mean ± SD

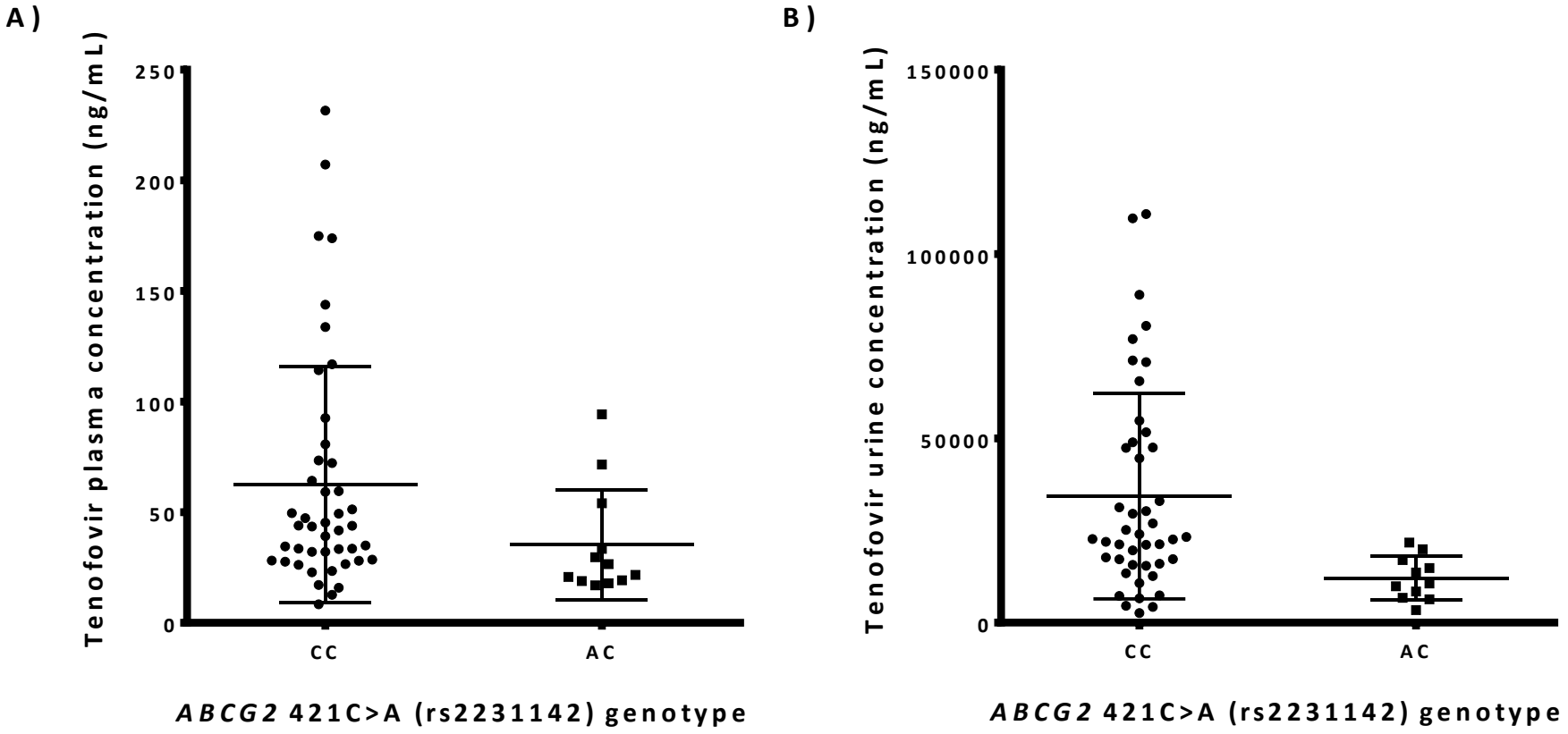

Figure 3.4: Statistically significant associations for tenofovir plasma and urine concentrations through multivariate regression analysis.

Graph A: Significant relationship between SNP and TFV plasma concentration. Graph B: Significant relationship between SNP and TFV urine concentration.

Table 3.2: Statistically significant results through multivariate linear regression.

TFV plasma concentration (log_{10} ng/mL)	Univariate linear regression			Multivariate linear regression		
	P value	β value (95% CI)	r^2	*P* value	β value (95% CI)	r^2
Age (years)	0.146	0.0 (0.0,0.0)	0.0	**0.037**	**0.0 (0.0,0.0)**	**0.2**
Ethnicity compared to white patients:						
• Asian	0.152	0.2 (-0.1,0.5)	0.1			
• Other	0.104	-0.3 (-0.6,0.1)	0.1	**0.037**	**-0.4 (-0.7,0.0)**	**0.2**
***ABCG2* 421C>A (rs2231142)**	0.097	-0.2 (-0.3,0.0)	0.1	**0.030**	**-0.2 (-0.4,0.0)**	**0.2**
TFV urine concentration (log_{10} ng/mL)	Univariate linear regression			Multivariate linear regression		
	P value	β value (95% CI)	r^2	*P* value	β value (95% CI)	r^2
Height (cm)	0.221	0.0 (0.0,0.0)	0.0			
Treatment compared to combination with raltegravir:						
• Elvitegravir and cobicistat	0.135	-0.2 (-0.4,0.1)	0.1			
Ethnicity compared to white patients:						
• Other	0.142	-0.3 (-0.8,0.1)	0.1	**0.024**	**-0.5 (-1.0,0.0)**	**0.2**
Time post dose (hours.minutes)	0.175	0.0 (0.0,0.0)	0.0			
ABCC10 2843T>C (rs2125739)	0.136	0.1 (0.0,0.3)	0.0			
***ABCG2* 421C>A (rs2231142)**	0.025	-0.3 (-0.5,0.0)	0.1	**0.010**	**-0.3 (-0.6,-0.1)**	**0.2**
TFV plasma:urine ratio	Univariate linear regression			Multivariate linear regression		
	P value	β value (95% CI)	r^2	*P* value	β value (95% CI)	r^2
Treatment compared to combination with raltegravir:						
• Elvitegravir and cobicistat	0.024	-0.2 (-0.4,0.0)	0.1	**0.005**	**-0.2 (-0.4,0.1)**	**0.3**
Ethnicity compared to white patients:						
• Black	0.105	0.4 (-0.1,0.9)	0.1			
Time post dose blood (hours.minutes)	0.035	0.0 (0.0,0.0)	0.1	**0.010**	**0.0 (0.0,0.0)**	**0.3**
Time post dose urine (hours.minutes)	0.036	0.0 (0.0,0.0)	0.1			
ABCC2 -24C>T (rs717620)	0.186	-0.1 (-0.3,0.1)	0.0			
ABCC2 3972 C>T (rs3740066)	0.112	-0.1 (-0.2,0.0)	0.0			

Univariate linear regression ($P \leq 0.2$) completed, all statistically significant results then carried through to multivariate linear regression analysis ($P \leq 0.05$). Statistically significant associations from the multivariate analysis are shown in bold type.

Table 3.3: TFV concentrations, summarised by *ABCG2* 421C>A genotype.

	***ABCG2* 421C>A (rs2231142)**			**Percentage difference between genotypes (%)**
	CC	**CA**	**AA**	
TFV plasma concentration (ng/mL)	43.53 (28.1-73.4)	29.65 (19.2-54.1)	-	31.9
TFV urine concentration (ng/mL)	22662.91(15677.5-48910.2)	13601.97 (9890.6-21730.9)	-	40.0

All values shown as median (IQR)

3.4 DISCUSSION

Through this secondary analysis, we studied SNPs previously associated with TFV excretion and TDF metabolism, with the aim of further elucidating the contribution genetics has to inter-patient variability in TFV concentrations and determining if these SNPs were an indicator of variable plasma/urine TFV concentrations.

The primary finding was the association of *ABCG2* 421C>A (rs2231142) with lower $\log_{10}$ TFV plasma (P = 0.030, β = -0.2) and $\log_{10}$ TFV urine (P = 0.010, β = -0.3) concentrations. *ABCG2* 421C>A is a missense variant that has previously been linked with loss of BCRP function. It has been shown that TDF but not TFV is a dual substrate of P-gp and BCRP (Neumanova 2014, Wen 2015, Roberts 2016). As TDF is broken down to TFV by esterases in intestinal tissue, *ABCG2* 421C>A may potentially alter TDF transport in the small intestine resulting in reduced break down to TFV and thus reduced TFV plasma and urine concentrations.

The lack of significant associations between SNPs in transporters and TFV excretion that have previously been associated with TFV-associated renal dysfunction, may suggest that TFV plasma concentrations may be a minor contributor to TFV toxicity compared to other genetic and environmental factors such as age, weight and renal function (Moss 2014). A previous study also found no association between multiple *ABCC2* and *ABCC4* SNPs and TFV AUC, but did observe an association of *ABCG2* 421C>A (rs2231142) with a 1.51 fold increase in TFV AUC for variant allele carriers of *ABCG2* 421C>A (Baxi 2017). The contradictory nature of our findings in relation to this study suggests that the observed *ABCG2* 421C>A (rs2231142) association may in part be due to SNPs not included within either study, which are in linkage disequilibrium with *ABCG2* 421C>A. Differences in patient ethnicity between the two study groups further complicates the picture as our study consisted of a majority Caucasian cohort

whilst Baxi *et al.*'s study contained predominantly African American patients (Baxi 2017). The prevalence of different genotypes for SNPs in linkage disequilibrium with one another would differ between ethnicity populations, making the SNPs contributing to the phenotype difficult to decipher. Further studies are required in different ethnicity populations, looking at a range of pharmacokinetic parameters, in order to understand the impact of *ABCG2* 421C>A (rs2231142) on TFV plasma and urine concentrations.

A second pro-drug of TFV, TAF, has an alternative activation mechanism to TDF (Birkus 2016). Use of TAF is associated with lower plasma TFV concentrations, and therefore reduced incidence of kidney toxicity, in comparison to TDF. This is most likely because efficacy is achieved with a much lower dose (Ray 2016). In light of this, the *ABCG2* 421C>A association observed within this study is not anticipated to significantly alter TFV plasma and urine concentrations within patients receiving TAF. However, given that TAF is a substrate of BCRP (GileadSciences 2016), it would be anticipated that the *ABCG2* 421C>A SNP would alter TAF transport. Further study is required to confirm the mechanism of this interaction and the potential ramifications this may have for TAF pharmacokinetics.

In addition to genetics, other factors including age and weight have previously been associated with alterations in TFV plasma and urine concentrations (Baheti 2013, Baxi 2014, Rungtivasuwan 2015). Age was found to be significantly associated with an elevated $\log_{10}$ TFV plasma concentration (P = 0.037, β = 0.0), and this could be due to the decline in renal function that is linked to increasing age, resulting in reduced excretion of TFV (Coresh 2003).

Co-medication of TFV with EVG/COBI was associated with lower TFV plasma to urine ratio (*P*

= 0.005, β = -0.2) when compared to co-medication with RAL. COBI has previously been shown *in vitro* to inhibit P-gp and BCRP, to a degree suggested to be clinically relevant for the intestine. This resulted in increased absorption of co-administered transporter substrates, (Lepist 2012) further suggesting that a reduction in TFV plasma concentration may be linked to a reduction in function of BCRP, within the small intestine. Furthermore, through *in vitro* study it has been demonstrated that COBI does not significantly inhibit TFV transport by OAT1, OAT3 or MRP4. A combination of COBI with EVG or FTC did not affect the sensitivity of TFV to primary renal PTCs indicating a low potential for a pharmacokinetic renal drug-drug interaction between COBI and TFV (Stray 2013).

Through this study an association with *ABCG2* 421C>A and TFV plasma and urine concentrations was observed, further building knowledge of the contributory effect of SNPs on inter-patient variability in TFV concentrations. Furthermore, a lack of significance of SNPs previously associated with TFV-associated renal toxicity as indicators of plasma or urine TFV concentrations was demonstrated. Further study of the mechanism of interaction between *ABCG2* and TFV, and the subsequent effect on TFV pharmacokinetics, is imperative given the frequency of use of TFV and the potential impact reduced TFV plasma concentrations could have for achieving a sustained virological response in patients.

3.4.1 *Limitations*

A limitation of our study is the low numbers of Black, Asian and mixed-race participants. Population numbers for these ethnicities were not large enough to enable robust statistical associations to be determined for each ethnicity independently. Consideration of ethnicity within the study population is of critical importance given the difference in frequency of SNPs

between ethnicities. The *ABCG2* 421C>A variant allele is found at a frequency of 9.4% in European populations, 1.3% in African populations, 29.1% in East Asian populations and 9.7% in South Asian populations as studied in the 1000 Genome Project (GenomesProjectConsortium 2015). Given that the observed differences in genotype frequencies between the populations included is high, these data require validation in other patient cohorts to ensure the observations are not influenced by stratification. Furthermore our study would benefit from a larger total patient cohort, given that the frequency of variant alleles for some SNPs were low or absent, as shown in Table 3.1. This was seen for *ABCG2* 421C>A were a homozygous variant genotype was not observed within our total population.

Chapter 4: The Development of an Overexpressing MATE1 or MATE2K Transporter Cell Line

4.1 INTRODUCTION

Drug transporters are known to play a significant role in the absorption, distribution, metabolism and elimination of drugs. Any alteration in their ability to transport substrates can result in changes in pharmacokinetics, drug accumulation, loss of efficacy, toxicity or drug-drug interactions. The MATE 1 and 2K transporters are members of the solute carrier (SLC) superfamily and have previously been identified as H^+ coupled organic cation exporters (Otsuka 2005, Masuda 2006). MATE1 is predominantly expressed on the brush border membrane of PTCs within the kidney, and the canalicular membrane of hepatocytes (Otsuka 2005, Damme 2011). MATE2K is expressed almost exclusively on the brush border membrane of PTCs (Otsuka 2005, Tanihara 2007). Within PTCs MATE1 and MATE2K act as proton/cation antiporters transporting cationic endogenous substrates and xenobiotics from the blood into the lumen where they are excreted in the urine (Moss 2014). This transport occurs through utilisation of a proton gradient to enable substrate efflux (Figure 4.1).

In terms of substrate affinity, most substrates have demonstrated comparable affinities for both MATE1 and MATE2K. However, some exceptions are observed, such as in the case of metformin which has a higher affinity for MATE1, and oxaliplatin which has been shown to be preferentially transported by MATE2K (Damme 2011). Metformin is a first line type 2 diabetes drug that is well characterised as a substrate for both MATE1 and MATE2K (Masuda 2006, Tanihara 2007, Elsby 2017, Zhang 2017). Creatinine is a renal biomarker previously shown to be a substrate of both MATE1 and MATE2K within PTCs (Tanihara 2007).

Transfection of immortalised cell lines with foreign nucleic acids can be stable or transient. Transient transfection results in the short term expression of the nucleic acid of interest and does not incorporate the nucleic acid into the host cell genome (Yin 2005). As a result of this,

the nucleic acid is not passed on through generations and so is lost through cell division. Nevertheless transient transfection results in high levels of plasmid nucleic acid within the cell and thus results in high expression of encoded protein (Schlaeger 1998). The key difference between stable transfection and transient transfection is that stable transfection incorporates the plasmid nucleic acid into the host genome and therefore passes the foreign DNA to subsequent generations. This result is obtained by transiently transfecting cells before exposing the cell culture to a suitable antibiotic. Incorporating a gene encoding for antibiotic resistance into the DNA construct to be transfected means that cells that have incorporated the foreign DNA into their genome are resistant to the antibiotic, and so survive within long-term cultures. Advantages of transient transfection over stable transfection are that production of plasmid overexpressing cell lines is quicker, cheaper and more straightforward. However, the production of stably transfected cell lines provides cell lines suitable for large scale and long-term study.

Regardless of whether transfection is to be transient or stable, successful integration of the foreign nucleic acid into the cells is essential. This can be achieved through multiple methods as described by Gao *et al* (Gao 2007). Our chosen method was cationic lipid transfection. Cationic lipid transfection enables high efficiency transfection and is suitable for transfection of DNA and ribonucleic acid (RNA) of all sizes within a wide range of cell lines (Gao 2007). Cationic lipid transfection works through cationic lipids forming a complex with the foreign nucleic acid known as a lipoplex (Chesnoy 2000, Gao 2007). DNA in lipolexes are protected from nuclease degradation. The positive surface charge of the lipids mediates an interaction between the nucleic acid and the cell membrane, enabling the lipoplex to enter the cell by endocytosis (Chesnoy 2000, Gao 2007). The DNA then dissociates from the lipid complex, before entering lysosomal compartments, and enters the nucleus where it is expressed (Chesnoy 2000, Gao 2007). We sought to develop a transiently transfected cell line

overexpressing either the MATE1 or MATE2K transporter with the final aim of studying drug-drug interactions between TAF or TFV and known substrates of MATE1 and MATE2K.

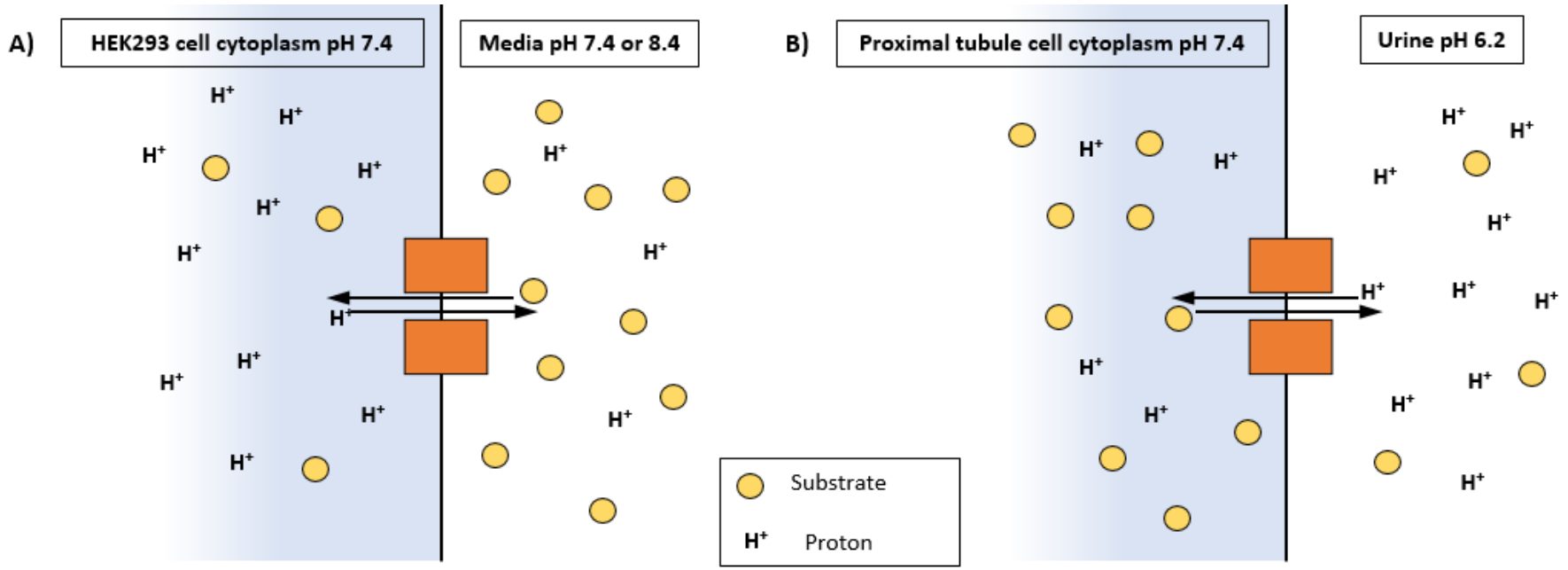

Figure 4.1: Mechanism of substrate transport by MATE transporters *in vitro* and *in vivo*.

Substrate transport through secondary active transport utilising an H^+ pump mechanism via the antiporters MATE1 or MATE2K.
A) Accumulation of substrate in HEK293 cells transfected with the MATE1 or MATE2K transporter. B) Mechanism of substrate efflux via MATE1 or MATE2K in proximal tubule cells within the kidney.

4.2 METHODS

4.2.1 *Materials*

pEZ-M01 vectors containing MATE1 (SLC47A1), MATE2K (SLC47A2), or green fluorescent protein (GFP) encoding DNA were purchased from GeneCopoeia™ (Rockville, MD). *Escherichia coli* (E.coli) DH5α cells, super optimal culture (S.O.C) medium, Gel loading buffer II, Tris-Borate-EDTA (TBE) buffer, Lipofectamine 3000 transfection kit, OptiMEM media, Nunclon Delta Surface 24 well plates, SYTOX Red Dead cell stain, Pierce™ BCA Protein Assay Kit, NuPAGE™ LDS Sample Buffer (4X), NuPAGE™ Sample Reducing agent (10X), NuPAGE™ 4-12% Bis-Tris Protein Gels 1.5mm 10 wells, NuPAGE™ MOPS SDS Running Buffer (20X), Nitrocellulose membranes and ECL western blotting substrate, were obtained from ThermoFisher Scientific (Wilmington, DE). GenElute Plasmid mini-prep kit, Fetal Bovine Serum (FBS), Lysogeny broth (LB) powder, Dulbecco's Modified Eagle's Medium (DMEM), Hanks Balanced Salt Solution (HBSS), Molecular Biology Grade Water, Poly-L-lysine solution, Phosphate Buffered Saline (PBS), RIPA buffer, Triton X-100 and protease inhibitor cocktail were purchased from Sigma Aldrich (Dorset, UK). A 1 kilobase DNA ladder and the restriction enzyme StuI were obtained from New England BioLabs (Beverly, MA). Radiolabeled metformin (^{14}C metformin) and radiolabeled creatinine (^{14}C creatinine) was purchased from American Radiolabeled Chemicals (St Louis, MO). HEK293 cells were purchased from ATCC-LGC (Middlesex, UK). Precision Plus Protein™ Kaleidoscope™ pre-stained protein standard was purchased from BioRad (Watford, UK). Rabbit polyclonal antihuman SLC47A1 antibody, Goat polyclonal antihuman SLC47A2 antibody, Mouse monoclonal antihuman beta actin antibody, Donkey polyclonal anti-goat IgG heavy and light chain horse radish peroxidase (HRP) antibody, goat polyclonal anti-rabbit IgG heavy and light chain HRP antibody and goat polyclonal anti-mouse IgG1 heavy chain HRP antibody were purchased from Abcam (Cambridge, UK).

4.2.2 *Transfection of E. coli DH5α cells and colony isolation*

All plasmids contained a His-tag a region encoding for ampicillin resistance. In order to transfect the E. coli cells with the MATE1 (SLC47A1), MATE2K (SLC47A2) or GFP encoding vectors the following procedure was conducted. 50 µL of E. coli DH5α cells were mixed with 2.5 µL of each plasmid solution and kept at -20 °C for 30 minutes before heat shock at 42 °C for 45 seconds, followed by incubation at -20 °C for 2 minutes. 500 µL of 37 °C S.O.C medium was then added before incubation at 37 °C, 250 rpm, for 45 minutes. The E. coli cells were then plated onto LB agar and ampicillin (100 µg/mL) containing plates and incubated at 37 °C for 14-18 hours.

Individual colony isolation was then conducted through the removal of individual colonies from the plates before incubation in LB and ampicillin (50 µg/mL) at 37 °C, 250 rpm, for 14-18 hours. After this time cells were stored at -80 °C. Cells were prepared for storage at -80 °C through a five times dilution with glycerol and molecular biology grade water prepared in a 50:50 ratio.

4.2.3 *Plasmid DNA extraction and PCR*

To ensure the correct plasmid was transfected into each E. coli cell colony, StuI digestion was completed. Plasmid DNA was isolated from the transfected E. coli cells and a PCR was conducted with the restriction enzyme StuI. This digestive enzyme experiment was conducted to ensure each cell colony was transfected with the correct plasmid and that the MATE DNA localisation and position were as expected, based on the manufacturers information provided in the GeneCopoeia™ SLC47A1, SLC47A2 and GFP plasmid data sheets.

Transfected E. coli DH5α cells were thawed and cultured for 14-18 hours at 37 °C, 250 rpm, in LB and ampicillin (50 µg/mL). Plasmid DNA was then extracted using a GenElute plasmid mini-prep kit following the user guide provided. In brief, this included harvesting cells through centrifugation at 12,000 × *g* for 1 minute and resuspension in 200 µL of Resuspension Solution before lysing cells with 200 µL of Lysis Solution for 5 minutes. Cell lysis was stopped through precipitating the cell debris in 350 µL of Neutralisation/Binding Solution. The solution was then centrifuged at 12,000 × *g* for 10 minutes. The supernatant fraction was removed and carried into a Miniprep Binding Column placed within a collection tube which had been prepped with 500 µL of Column Preparation Solution and spun at 12,000 × *g* for 1 minute with the flow-through discarded. The supernatant fraction and binding column were then centrifuged at 12,000 × *g* for 1 minute, the flow-through was discarded and 500 µL of Optional Wash Solution was added before centrifugation at 12,000 × *g* for 1 minute. The flow-through was discarded and two washes with 750 µL of Wash Solution followed by centrifugation at 2,000 × *g* for 1 minute was completed. The column was then centrifuged at 12,000 × *g* for 2 minutes in isolation to ensure the removal of excess ethanol. The column was transferred to a fresh collection tube and 50 µL of Elution Solution was added to the column followed by centrifugation at 12,000 × *g* for 1 minute. The DNA concentration was then quantified using NanoDrop (ThermoFisher Scientific, Wilmington, DE). The DNA was then stored at -20 °C.

A PCR was completed using the extracted plasmid DNA and the StuI restriction enzyme. 1 µg of plasmid DNA, 5 µL of buffer, 2 µL of enzyme and 3 µL of molecular biology grade water were combined and PCR was conducted. The PCR protocol included 90 minutes at 37 °C followed by 20 minutes at 80 °C and was completed on a GeneAmp PCR9700 machine (Thermo Fisher Scientific, Wilmington, DE). The StuI restriction enzyme cleavage sites for each plasmid are detailed in Figure 4.2. After PCR, gel electrophoresis was conducted using

a 0.75% agarose gel. The gel was produced by dissolving 375 mg of agarose in 50 mL of (1X) TBE buffer in a microwave followed by the addition of 30 µL of ethidium bromide (0.5 µg/mL). The gel was then poured and left to set. 2 µL of gel loading buffer II was added to 8 µL of each DNA sample. 10 µL of each sample was then loaded into the wells of the set gel alongside 2 µL of a 1 kilobase DNA ladder. The gel was then immersed in (1X) TBE buffer and run at a constant voltage of 100 volts (V) for 20 minutes. The gel was then examined using a UV light box attached to a backlight camera.

4.2.4 *Cell culture*

HEK293 cells were stored in liquid nitrogen at -196 °C, before being thawed and grown in 10% FBS DMEM containing media at 37 °C, 5% CO_2 for 72 hours. Once cells achieved 90% confluence, a 1 in 3 dilution was completed. The flask was washed with HBSS solution and incubated with trypsin for 5 minutes at 37 °C, 5% CO_2. DMEM was then added in a 1:1 ratio with the trypsin, the solution was then centrifuged at 600 × *g* for 5 minutes. The supernatant fraction was removed, and the cell pellet was resuspended in DMEM. 1 mL of cell solution was then added to a new flask containing DMEM. Cells were then incubated at 37 °C, 5% CO_2 to 90% confluence. A 100 µL aliquot of cell solution was taken and a cell count completed with a Nucleocounter (Chemometec, Denmark). 200,000 cells in 1 mL of DMEM per well was then plated onto a sterile Nunclon Delta Surface 24 well plate and incubated for 24 hours at 37 °C, 5% CO_2. Prior to the addition of cells, the Nunclon Delta 24 well plate was treated with 250 µL of poly-L-lysine solution per well and incubated at 37 °C, 5% CO_2 for 3 hours. The poly-L-lysine was then aspirated and the plates where left for 1 hour to dry at 37 °C, 5% CO_2.

4.2.5 *Protein lysate preparation and bicinchoninic acid (BCA) protein assay*

Two hundred thousand HEK293 cells per well were plated onto a Nunclon Delta 24 well plate as described in Chapter 4, Section 4.2.4 and incubated at 37 °C, 5% CO_2 for 24 hours. The cells

were transfected with either MATE1 or MATE2K plasmid DNA using a Lipofectamine 3000 reagent kit and OptiMEM media using the manufacture protocol. This briefly consisted of combining per well of the 24 well plate a 1.5% or 3% of total volume Lipofectamine 3000 reagent solution with 25 µL of OptiMEM medium. Alongside this 25 µL of OptiMEM medium, 4% of total volume P3000 reagent and 0.5-5 µg/µL of plasmid DNA were also combined. The two solutions were then combined and incubated for 5 minutes at room temperature before 50 µL of the final solution was added to each well of the plate. Cells were then incubated for 72 hours at 37 °C, 5% CO_2.

After this incubation period, protein lysate preparation was conducted. The cell culture plate was washed with 250 µL per well of ice cold PBS (0.01 M), the PBS was then aspirated and 250 µL of trypsin was added to each well before incubation for 10 minutes at 37 °C, 5% CO_2. 250 µL of PBS was then added to each well and the cell solution was centrifuged for 5 minutes at 600 × *g*. The supernatant was removed, and the cell pellet was resuspended in 2 mL of ice-cold NP-40 lysis buffer and 400 µL of protease inhibitor cocktail. NP-40 buffer was made in house using sodium chloride (NaCl) (150 mM), 20 mL of 1% Triton X-100 and 50 mM Tris base. The cell solution was then incubated at 4 °C for 30 minutes on an oscillating table before centrifugation at 4 °C, 12,000 × *g* for 20 minutes.

A BCA assay was completed to determine the protein concentration from each of the samples using a set of BCA protein standards prepared following the manufactures protocol provided with the Pierce™ BCA protein assay kit. A set of diluted albumin standards was prepared in a range of concentrations from 25-2000 µg/mL. Working reagent was then prepared in a 50:1 ratio of reagent A:B. 100 µL of each standard and protein sample was added to 2 mL of working reagent and vortexed before incubation for 30 minutes at 37 °C. All solutions were then cooled to room temperature and absorbance at 562 nm, for all samples and standards,

before measurement on a spectrophotometer within 10 minutes. Values were normalised through subtraction of the absorbance reading for a blank sample. A standard curve was prepared by plotting the average blank-corrected 562 nm measurement for each BSA standard vs its concentration (µg/mL). This standard curve was then used to calculate the protein concentration of the samples from their corresponding 562 nm absorbance measurement. The total protein concentration for the MATE1, MATE2K, or control samples was determined through use of the TREND function on Microsoft Excel 2010 that utilises the following formula:

$$TREND(Absorbance, [protein\ concentration\ of\ standards], [protein\ concentration\ of\ samples], [const = 0])$$

4.2.6 *Western blot analysis*

384.6 µL of NuPAGE™ sample buffer, 153.84 µL of NuPAGE™ reducing agent and 1 mL of protein lysate was combined and incubated at 95 °C for 10 minutes. Each solution was then sonicated for 10 seconds. A gel electrophoresis tank was assembled containing a NuPAGE™ 4-12% Bis-Tris 1.5 mm protein gel and was filled with a 1:20 dilution of MOPS running buffer in distilled water. 20 µL of protein lysate solution and 10 µL of a pre-stained protein standard ladder with a molecular weight range of 10-250 kD was loaded onto the gel. Gels were run for 3 hours with an electrical current of 100 V. Once gel electrophoresis was complete the gel was removed from the gel cassette and washed in transfer buffer made up of 14.4 g glycine, 3.0 g tris base, 80 mL deionised water and 200 mL methanol.

A gel transfer onto a nitrocellulose membrane was then conducted with a continuous electrical current of 60 V for 1 hour at 4 °C. All components were submerged in transfer buffer throughout the gel transfer. Subsequently, nitrocellulose membrane blocking was completed through incubation of the membrane with 5% no fat milk powder/ 0.1% TBST, for 2 hours at

room temperature on an oscillating table. TBST consisted of 50 mL of TBS (20X) (TBS solution made up of 175.2 g NaCl, 4.4 g potassium chloride (KCl), 60.5 g Tris base, and 1 L of deionised water) 1 mL of TWEEN detergent and 949 mL deionised water. The membrane was then washed 4 times for 5 minutes per wash with TBST before incubation with 100 µL of rabbit polyclonal anti-SLC47A1 antibody or 10 µL of goat polyclonal anti-SLC47A2 antibody in 20 mL 5% no fat milk powder/ 0.1% TBST for 14 hours at 4 °C on an oscillating table.

Once primary antibody incubation was complete the membrane was washed 4 times for 5 minutes per wash with TBST and then incubated for MATE1 with 5 µL of goat anti-Rabbit HRP antibody and for MATE2K with 2 µL of donkey anti-goat HRP antibody in 20 mL 5% no fat milk powder/ 0.1% TBST for 90 minutes at 4 °C on an oscillating table. After secondary antibody incubation, the membrane was washed 3 times for 5 minutes with TBST and once for 5 minutes with TBS. Signal development was conducted using ECL, which was prepared according to the manufactures protocol by mixing reagents 1 and 2 in a 1:1 ratio. The mixture was then added to the membrane and incubated for 1 minute. Excess reagent was drained and the membrane was covered with clear plastic wrap and stored in an x-ray cassette. Under zero light conditions the membrane was exposed to x-ray film in the closed cassette for 2 minutes. The film was washed in developer until protein bands appeared and then submerged in fixer for 1 minute before being rinsed in water.

The nitrocellulose membrane was stripped of bound antibodies through washing with TBST for 5 minutes followed by two 10-minute washes with stripping buffer, all of which were completed on an oscillating table. Stripping buffer was made up of 15 g glycine, 1 g SDS, 10 mL TWEEN detergent, 1 L deionised water, with pH adjusted to 2.2 using hydrochloric acid (1 M) or sodium hydroxide (NaOH) (1 M). The membrane was washed twice with TBS for 10 minutes on an oscillating table followed by two washes with TBST for 10 minutes each.

The membrane was then blocked with 5% no fat milk powder/0.1% TBST for 2 hours at room temperature on an oscillating table. Primary antibody incubation was completed with 0.1 µL of anti-beta actin antibody in 40 mL 5% no fat milk powder/ 0.1% TBST for 2 hours at 4 °C on an oscillating table. The membrane then underwent 4 times 5-minute washes with TBST on an oscillating table. Secondary antibody incubation was completed using 2 µL of goat anti-mouse HRP antibody in 20 mL 5% no fat milk powder/ 0.1% TBST for 90 minutes at 4 °C on an oscillating table. The membrane was washed 3 times for 5 minutes with TBST and once for 5 minutes with TBS. Signal development was completed as described above.

4.2.7 *Viability assay*

Cells were plated at 200,000 cells per well in a 24 well Nunclon Delta plate and transfected 24 hours later with either MATE1 or MATE2K plasmid DNA using the protocol stated previously in Chapter 4 (Section 4.2.4 and Section 4.2.5). The MTT assay was completed after 2, 3, 4 and 6 days of incubation post transfection. 100 µL of thiazolyl blue tetrazolium (12 mM) was added to each well. Cells were incubated for 2 hours at 37 °C, 5% CO_2. After 2 hours 100 µL of lysis buffer (50% v/v dimethylformahyde, 20% v/v sodium dodecyl sulphate) was added to each well and incubated for 14 hours at 37 °C, 5% CO_2. The absorbance from each well was then measured at 570 nm on a GENios microplate reader (TECAN, Austria). Cell viability was calculated as a percentage of the reading of the untreated HEK293 cells, normalised from the absorbance reading of the blank wells on the plate.

4.2.8 *Control cell line transient transfection*

As a control for plasmid transfection of the HEK293 cells, GFP expressing plasmid was transfected into HEK293 cells under varied conditions. A 24 well Nunclon Delta plate containing 200,000 HEK293 cells and 1 mL of DMEM per well, set up as previously described

(Section 4.2.4), was transfected after 24 hours incubation 37 °C, 5% CO_2. Transfection of the GFP expressing plasmid DNA into the plated HEK293 cells was completed using a Lipofectamine 3000 reagent kit as previously outlined (Section 4.2.5). GFP fluorescence was measured at 48 hours post-transfection. Cell viability was measured using a Red Dead Cell Cytotoxicity Stain. This was conducted through incubation with 1 mL of trypsin for 10 minutes followed by 1 mL of 10% FBS/ DMEM media being added to the cell solution before centrifugation at 600 × *g* for 5 minutes. 1 mL of cell suspension was then added to a flow cytometer tube alongside 1 µL of Red Dead Cell Cytotoxicity Cell Stain. The solution was incubated for 15 minutes before measurement on a Macs Quant Analyser (MacQuantify version 2.6). GFP fluorescence was measured in channel B1 using dye FITC-A. Cell viability was measured using the AlexaFluoro 6 dye, which only crosses over dead cell membranes, fluorescence was measured in channel R1 using the APC dye.

4.2.9 *Uptake of ^{14}C metformin in MATE1 or MATE2K expressing cell lines*

To ascertain the correct functionality of the transporters within the transfected cell lines, we studied the accumulation of ^{14}C metformin within the MATE1 and MATE2K transfected cell lines. A 24 well Nunclon Delta plate containing 200,000 HEK293 cells and 1 mL of DMEM per well, was set up as previously described (Section 4.2.4), before being transfected after a 24 hour incubation at 37 °C, 5% CO_2, using a Lipofectamine 3000 reagent kit as previously outlined (Section 4.2.5). All cells were incubated at 37 °C, 5% CO_2 for 72 hours before conducting the ^{14}C metformin accumulation experiment.

For the accumulation experiment, incubation media normalised to pH 7.4 using 1 M NaOH was prepared, containing 145 mM NaCl, 3 mM KCl, 1 mM calcium chloride ($CaCl_2$), 0.5 mM magnesium chloride ($MgCl_2$), 5 mM $_{D}$-Glucose, 5 mM HEPES and distilled water. The transfected HEK293 cells were pre-incubated with 200 µL of incubation medium for 10

minutes at 37 °C, 5% CO_2. Incubation medium was aspirated and for experiments including ammonium chloride incubation, plates were treated with 200 µL of 30 mM ammonium chloride per well before being incubated at 37 °C, 5% CO_2 for 10 minutes. Each well was then incubated with 200 µL of 9.9 µM ^{14}C metformin combined with incubation medium at either a pH of 7.4 or 8.4, at 37 °C, 5% CO_2. Plates were then incubated for either 5, 15 or 30 minutes at 37 °C, 5% CO_2. After this time a 100 µL sample was taken from each well and prepared for analysis with 4 mL of scintillation fluid. The remaining medium was then removed from each well and cells were washed rapidly three times with 1 mL of ice-cold incubation medium at pH 7.4. 500 µL of 0.5 M NaOH was then added to each well. Cells were incubated for 10 minutes at 37 °C, 5% CO_2. A second 100 µL aliquot was then taken from each well of the plate and prepared for analysis through the addition of 4 mL of scintillation fluid. The radioactivity of each sample was then analysed using a Tri-Carb scintillation counter and QuantaSmart™ software (DPM Solutions Ltd, Chesterfield, UK). Total cell volumes were calculated using the following equation:

$$Total\ cell\ volume\ (\mu L) = \frac{(internal\ volume\ of\ HEK293\ cell\ (pL) \times number\ of\ cells\ per\ well)}{1 \times 10^6}$$

The intracellular and extracellular concentration of radiolabeled drug was calculated using the following equation:

$$Intra\ or\ Extra\ cellular\ concentration\ of\ drug = \frac{Intra\ or\ Extra\ cellular\ concentration}{Intra\ or\ extra\ cellular\ volume}$$

The cellular accumulation ratio (CAR) was then calculated using the following equation:

$$CAR = \frac{(intracellular\ concentration)}{(extracellular\ concentration)}$$

4.2.10 *Statistical analysis*

Normality was assessed using The Shapiro-Wilk Test, with $P \leq 0.05$ considered as statistically significant. An unpaired t-test was then used to analyse potential differences in ^{14}C metformin accumulation and percentage cell viability between the control (untreated) and transfected HEK293 cells, with $P \leq 0.05$ classed as significant. All statistical analyses and chart production were carried out using GraphPad Prism 6 (GraphPad Software, La Jolla, CA).

4.3 RESULTS

4.3.1 *StuI restriction enzyme digest*

Figure 4.2 shows the restriction map of the pEZ-M01 vector containing either MATE1, MATE2K or GFP control DNA, and the StuI restriction sites within each of the vectors. Accompanying each is a virtual digest showing the results of a vector-containing insert in the correct orientation. Figure 4.3 is the output of StuI restriction enzyme cleavage for the colonies picked following the transformation of E. coli with the MATE1, MATE2K or GFP containing pEZ-M01 plasmids. As shown in Figure 4.3 for each plasmid type the band patterns matched the predicted digest shown in Figure 4.2 for each of the three colonies. The gel images confirm the correct presence and orientation of the desired transporter within each cell colony, with the exception of colony 2 for MATE1, which was thus excluded from the study.

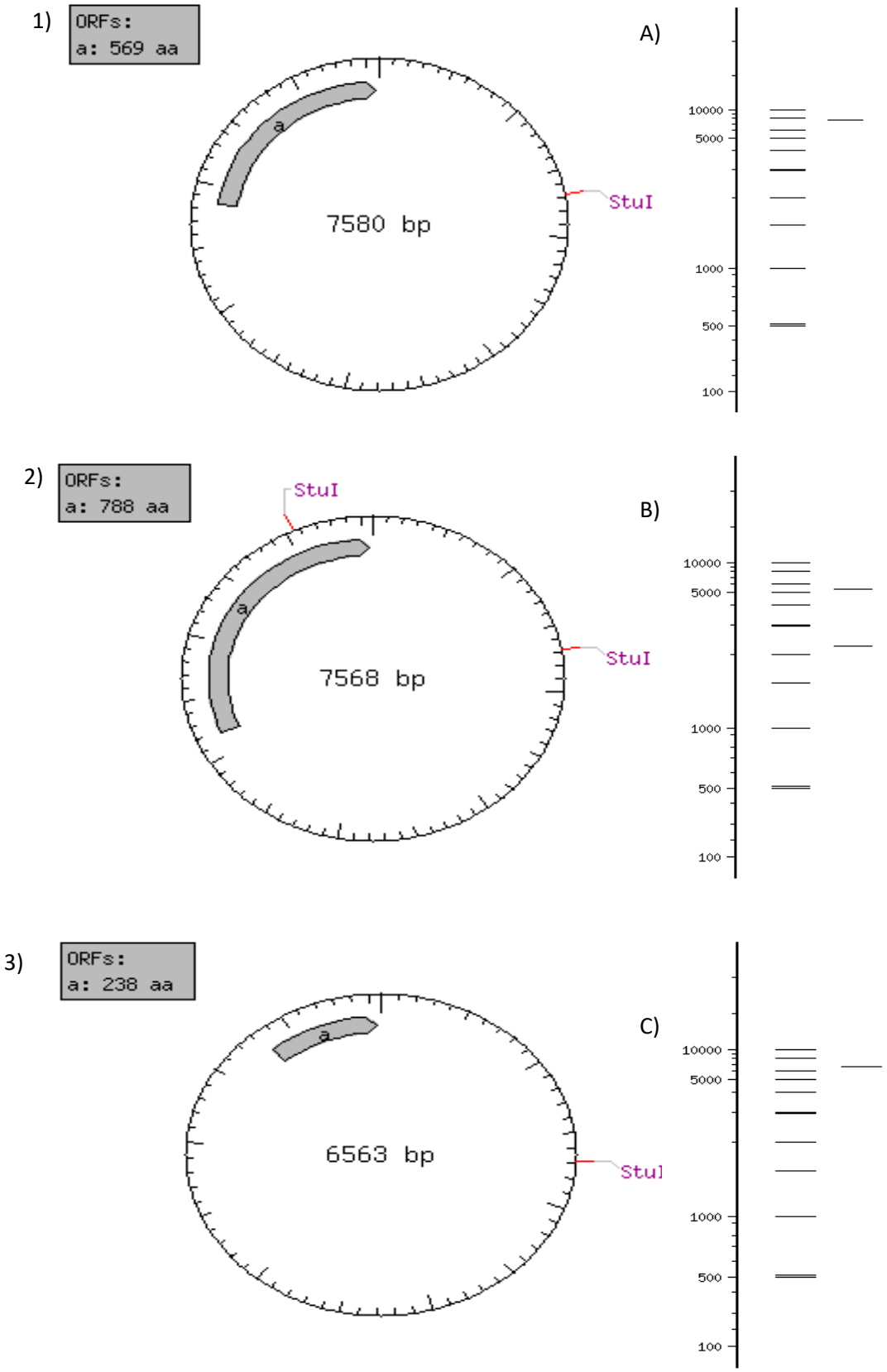

Figure 4.2: Restriction sites within the pEZ-M01 vector.

Restriction site for StuI within the 1) MATE1 2) MATE2K 3) GFP expressing plasmids. Alongside a model gel image for a virtual digest of A) MATE1 B) MATE2K C) GFP by the StuI enzyme.

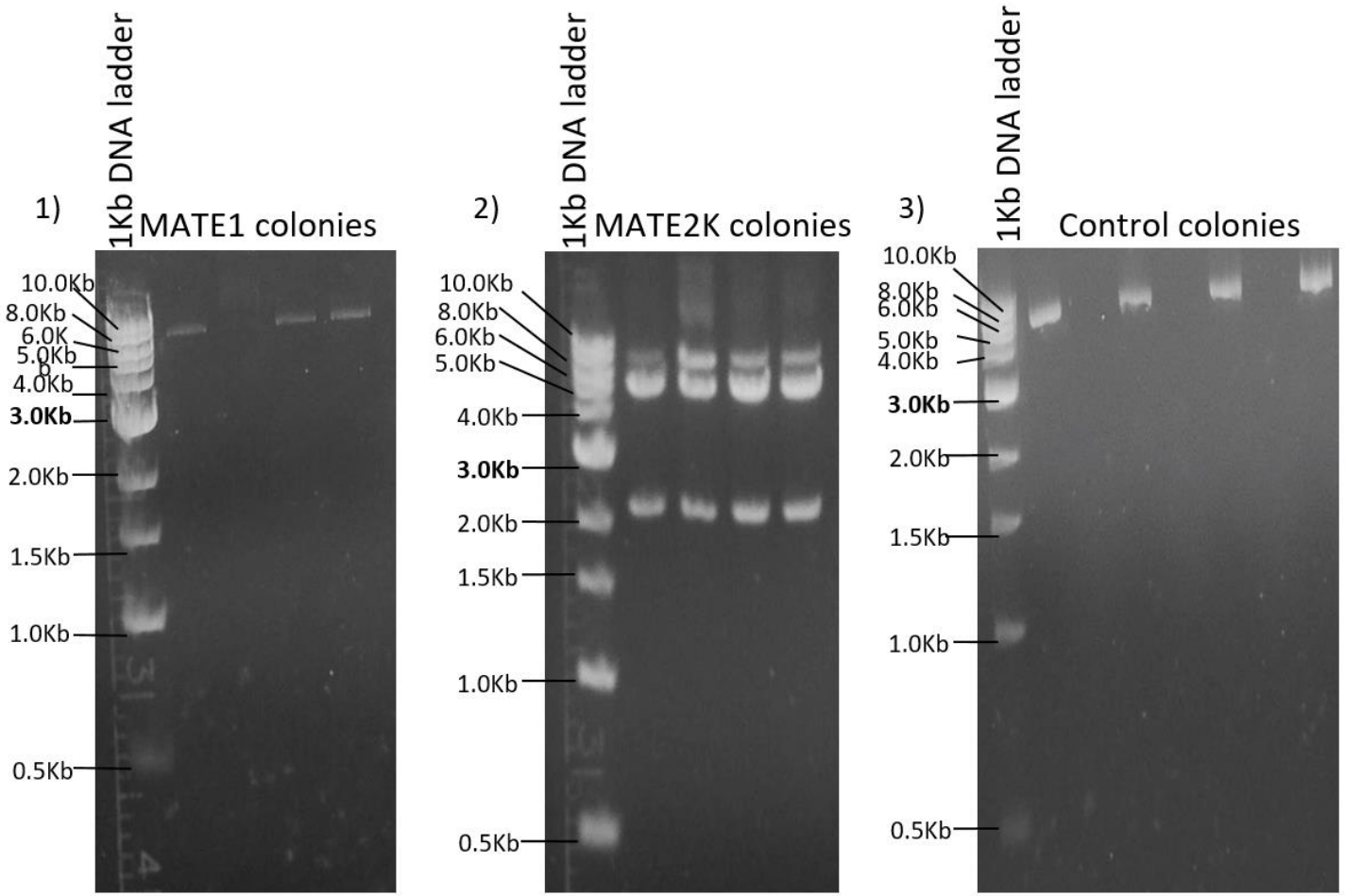

Figure 4.3: Restriction StuI enzyme digest of MATE1, MATE2K or GFP expressing plasmid DNA.

Restriction enzyme digest output for 1) DNA from 4 colonies expressing MATE1 plasmid DNA 2) DNA from 4 colonies expressing MATE2K plasmid DNA 3) DNA from 4 colonies expressing GFP (control) plasmid DNA.

4.3.2 *Cell viability and fluorescence assay*

Figure 4.4 shows the output for flow cytometry of HEK293 treated cells under three conditions:

- Condition 1: HEK293 cells treated with 1.5% of total volume Lipofectamine 3000 reagent solution and viability stained
- Condition 2: HEK293 cells transfected with GFP plasmid DNA, treated with 1.5% of total volume Lipofectamine 3000 reagent solution and viability stained
- Condition 3: HEK293 cells transfected with GFP plasmid DNA, treated with 3% of total volume Lipofectamine 3000 reagent solution and viability stained

As shown in Figure 4.4 cells were initially gated to a population of 10,000 cells. As AlexaFluoro 6 dye accumulates in dead cells the plot was gated to the cell population with a reading less than $1e^1$ absorbency unit (AU) for APC fluorescence. GFP production from this population can be seen in graph C for each condition. Cells expressing GFP less than $3e^1$ AU were excluded. As seen in Table 4.1 both Condition 2 and Condition 3 FITC-A dye fluorescence, measuring GFP fluorescence, was higher in both Condition 2 and 3, 934.8 AU and 919.1 AU respectively, than that seen in Condition 1 the control population, which produced a FITC-A dye fluorescence of 1.5 AU. These results confirm the expression of GFP plasmid DNA in the transfected HEK293 cells.

A higher APC-A dye output, 2.7 AU was recorded for Condition 3, treatment with 3% of total volume Lipofectamine 3000 reagent solution, compared to Condition 1, 0.6 AU and Condition 2 1.8 AU, treatment with a 1.5% of total volume Lipofectamine 3000 reagent solution. This indicated higher cell death in Condition 3. Given that use of 1.5% of total volume Lipofectamine 3000 reagent solution over 3% did not influence transfection success, with a negligible difference in FITC-A dye output of 934.1 AU for Condition 2 and 919.1 AU for

Condition 3, and that cell viability was higher in Condition 2, it was decided that all forward experiments would use a 1.5% of total volume Lipofectamine 3000 reagent.

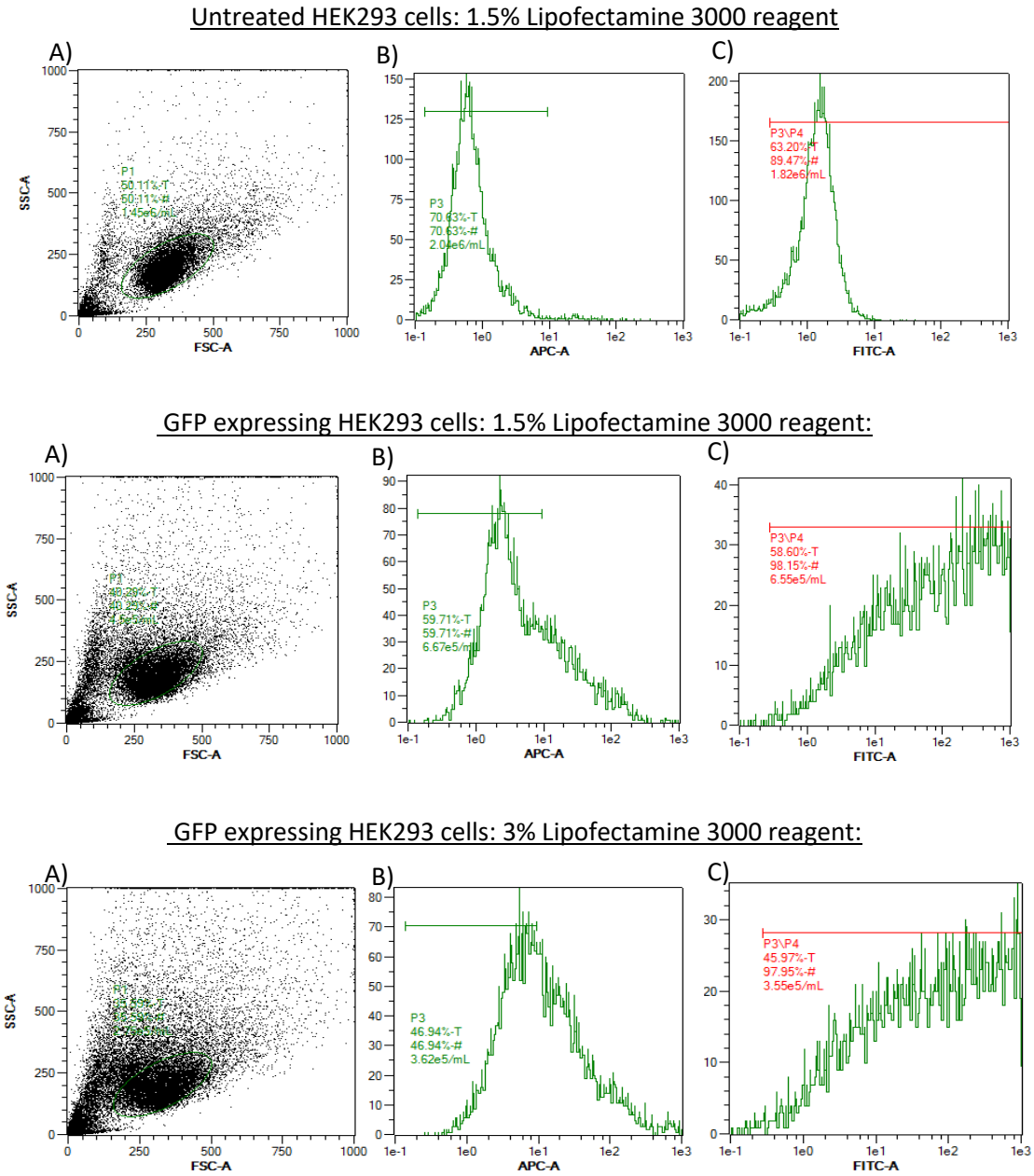

Figure 4.4: Measurement of cell viability and GFP fluorescence from GFP expressing HEK293 cells.

Graph A: Isolation of viable 10,000-cell population taken from total cell population. Graph B: AlexaFluoro 6 dye fluorescence, shown in the APC-A channel, in a gated 10,000-cell population, low fluorescence is indicative of healthy cells. Graph C: FITC-A dye fluorescence from viable cell population gated from graph 2, a high fluorescence is indicative of greater GFP production.

Table 4.1: Dye outputs from flow cytometer for each experimental condition (AU).

Condition	FITC-A dye (AU)	APC-A dye (AU)
Untreated HEK293 cells: 1.5% Lipofectamine solution	1.47	0.64
GFP plasmid transfected HEK293 cells: 1.5% Lipofectamine solution	934.84	1.81
GFP plasmid transfected HEK293 cells: 3% Lipofectamine solution	919.09	2.74

FITC-A dye output is a measure of GFP fluorescence. A higher FITC-A dye output indicates greater GFP production.

APC-A dye represents AlexaFluoro 6 dye fluorescence. A higher APC-A dye output indicates lower cell viability.

4.3.3 *BCA protein assay*

To produce protein lysate for western blot analysis, protein from MATE1 transfected, MATE2K transfected or HEK293 cells treated with Lipofectamine 3000 reagent but not transfected DNA (Control) was extracted and lysed. The concentration of lysed protein was determined through a BCA protein assay. As shown in Figure 4.5 the known concentrations of albumin standard were plotted against each concentrations absorbance at 562 nm, the concentrations of the MATE1 transfected, MATE2K transfected or Control protein samples where then calculated based on the samples absorbance at 562 nm. The concentration for the MATE1, MATE2K or control samples was found to be 1634 µg/mL, 1303 µg/mL, and 531 µg/mL, respectively.

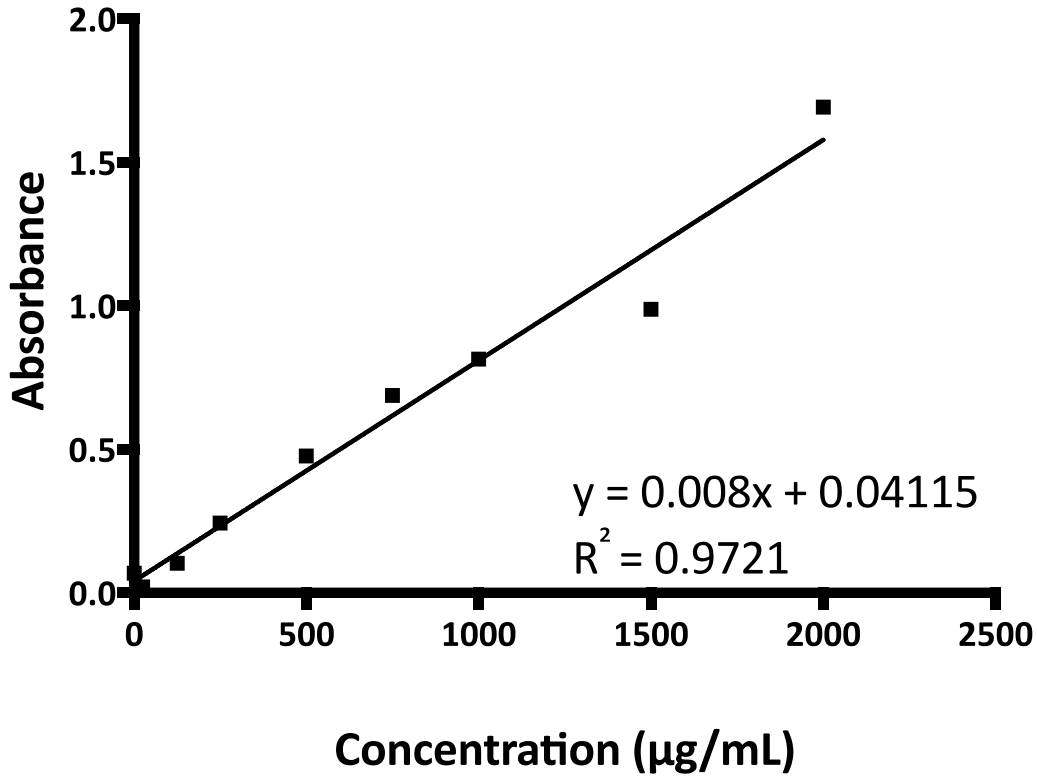

Figure 4.5: A concentration vs absorbance graph for diluted albumin standards of known concentrations.

A set of albumin standards of known concentrations were prepared and plotted against absorbance at 562 nm, the concentration of sample protein was then determined through extrapolating the protein concentration from the absorbance reading at 562 nm for each sample.

4.3.4 *Western blot analysis*

Once the total protein concentration within each of the samples was determined, a western blot analysis was conducted to establish the production of the protein of interest within the transfected HEK293 cells. Figure 4.6 shows the blots developed after staining with beta actin, anti-SLC47A1 (MATE1) or anti-SLC47A2 (MATE2K) antibodies. Beta actin was used as the loading control antibody. As shown in Figure 4.6 protein lysate from untreated HEK293 cells, transfected HEK293 cells overexpressing the MATE1 transporter or HEK293 cells overexpressing the MATE2K transporter produced protein bands for all 3 antibody stains. This confirms the successful production of the transporters of interest, MATE1 and MATE2K, within the transiently transfected HEK293 cell lines.

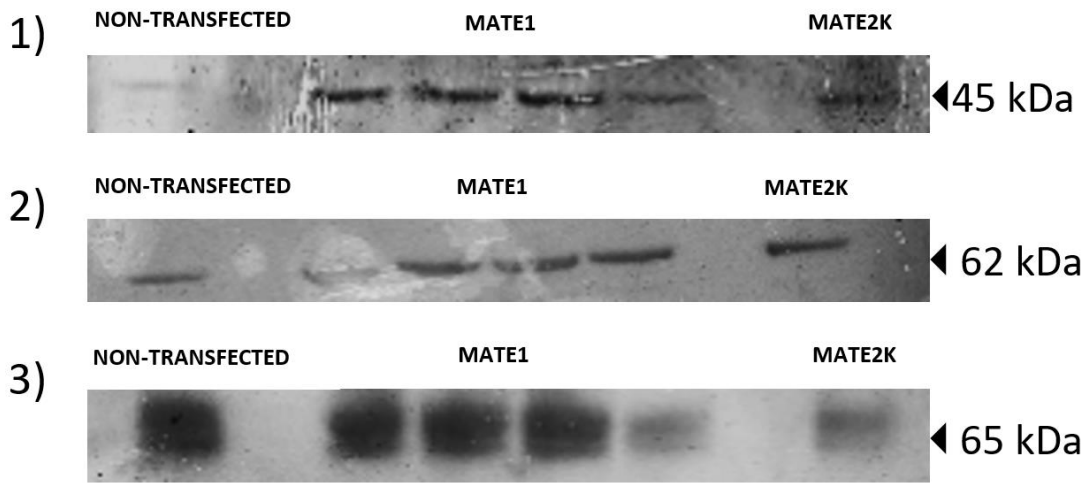

Figure 4.6: Western Blot membrane outputs after staining for MATE1, MATE2K or beta actin protein.

Blots developed after staining with 1) beta actin antibody 2) anti-SLC47A1 (MATE1) antibody 3) anti-SLC47A2 (MATE2K) antibody. Predicted band size for beta actin antibody= 45kDa, MATE1= 62kDa and MATE2K=65kDa

4.3.5 *Accumulation of ^{14}C metformin*

As substrate efflux via MATE1 and MATE2K is pH dependent, within the ^{14}C metformin accumulation experiment the transport of substrates is reversed from that observed *in vivo* (Figure 4.1). This is completed through manipulation of extracellular and intracellular pH through incubating the cells with media at a controlled pH. Both MATE1 and MATE2K transfected HEK293 cells transport substrate into the cell from a more acidic extracellular pH to a less acidic intracellular pH via secondary active transport. In light of this, providing the transfected cells are functional, it would be expected that CAR within the transfected cells would be higher than within the control cells, which were HEK293 cells treated identically to the transfected HEK293s with the exception that they were not transfected with any type of vector DNA.

In order to determine the best conditions in which to conduct the ^{14}C metformin accumulation, several conditions were optimised: incubation with ammonium chloride containing media prior to incubation with radiolabeled drug, pH of the media containing radiolabeled drug and incubation time with radiolabeled drug.

Incubation with ammonium chloride was trialed to determine if greater polarisation of extracellular to intracellular pH increased the level of CAR. In Figure 4.7 for MATE1 transfected cells and in Figure 4.8 for MATE2K transfected cells, a 10-minute incubation with ammonium chloride prior to incubation with radiolabeled drug was shown to increase the CAR of ^{14}C metformin within the HEK293 cells, compared to the cells not treated with ammonium chloride prior to incubation with ^{14}C metformin. This mimicked that previously observed by Tanihara *et al.* (Tanihara 2007).

As seen in Figure 4.7 and 4.8 incubation with ^{14}C metformin for 5 minutes produced a CAR that was observed to be statistically significant compared to control, for all conditions within MATE1 transfected cells and for MATE2K transfected cells incubated for 5 or 15 minutes at pH 7.4. As such, a 5-minute incubation with ^{14}C metformin was completed for all experiments after this point.

In contrast to the results observed by Tanihara *et al*., comparison of the cells treated with ^{14}C metformin with media at pH 7.4 showed a greater difference in CAR between the transfected and untreated (control) cells, compared to those treated in media at pH 8.4, and so all future experiments used media at pH 7.4 exclusively (Tanihara 2007).

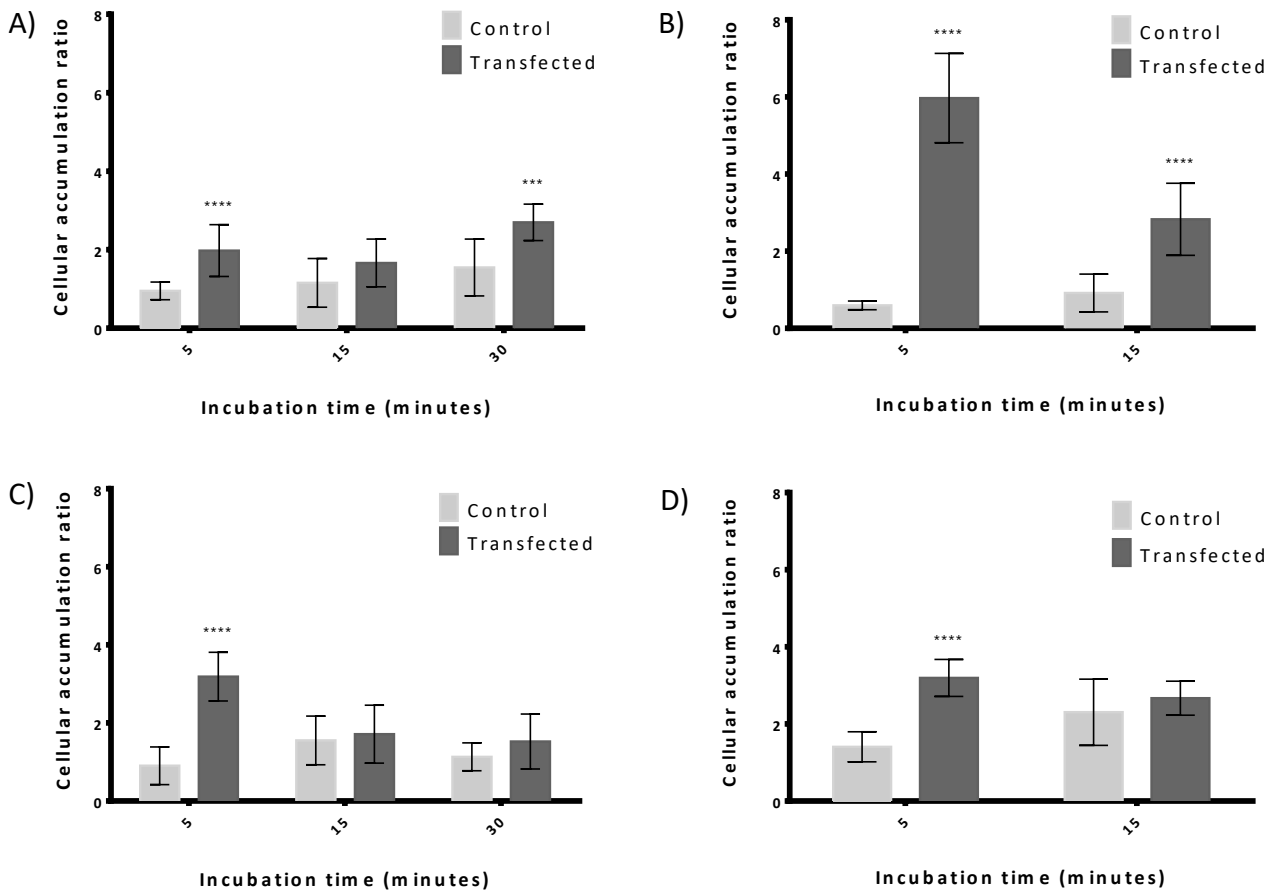

Figure 4.7: Cellular accumulation of ^{14}C metformin in HEK293 cells overexpressing MATE1.

Graph A: Accumulation at pH 7.4. Graph B: Cells incubated with ammonium chloride for 10 minutes prior to accumulation at pH 7.4. Graph C: Accumulation at pH 8.4. Graph D: Cells incubated with ammonium chloride for 10 minutes prior to accumulation at pH 8.4. Data points represents the mean ± SD, N = 3

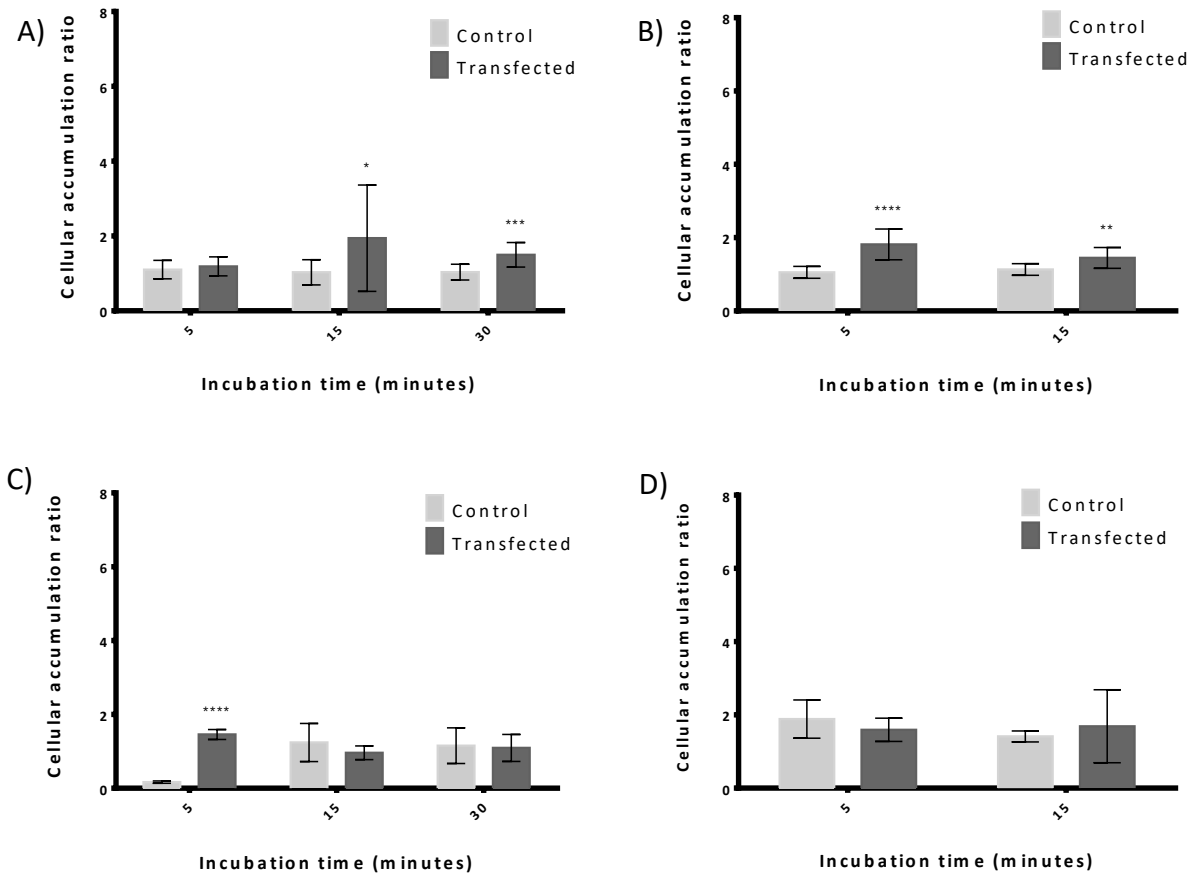

Figure 4.8: Cellular accumulation of ^{14}C metformin in HEK293 cells overexpressing MATE2K.

Graph A: Accumulation at pH 7.4. Graph B: Cells incubated with ammonium chloride for 10 minutes prior to accumulation at pH 7.4. Graph C: Accumulation at pH 8.4. Graph D: Cells incubated with ammonium chloride for 10 minutes prior to accumulation at pH 8.4. Data points represents the mean ± SD, N = 3

4.3.6 *Cell viability assay*

To ensure that cell death was not accountable for any differences observed in CAR between the control and transfected cells, cell viability was measured through a MTT assay. As shown in Figure 4.9, for all conditions cell viability was lower in the cells incubated with transfection reagents for a longer length of time post incubation. Furthermore, viability was comparable between conditions for each of the incubation time points. Cell viability was observed to be greater than 80% compared to untreated HEK293 cells for incubation times of 2 or 3 days post transfection. Given that the manufacturer protocol for the Lipofectamine 3000 reagent recommended a 3-day incubation post transfection before experimentation, and that the MTT assay showed cell viability to be to an adequate level 3 days post transfection, it was decided that within all experiments going forward all cell conditions would be incubated for 3 days post transfection prior to initiation of accumulation experiments.

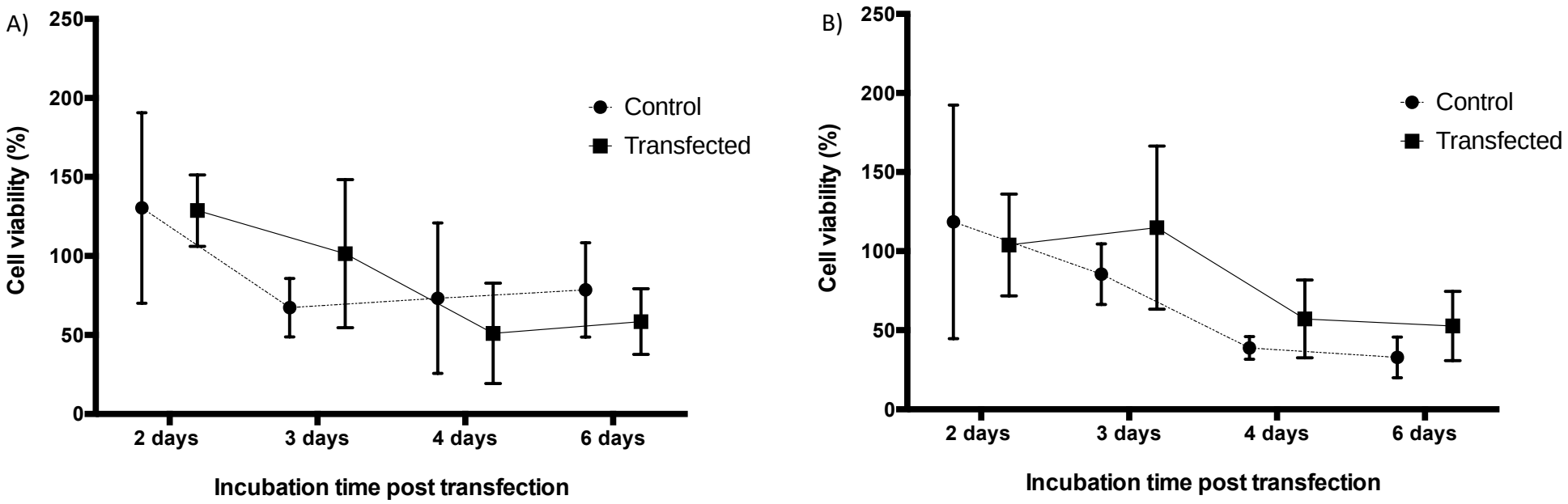

Figure 4.9: Cell viability of HEK293 cells post transfection.

Graph A: Cell viability for MATE1 plasmid DNA transfected HEK293 cells vs control cells. Graph B: Cell viability for MATE2K plasmid DNA transfected HEK293 cells vs control cells. Data points represents the mean ± SD, N = 6

4.4 DISCUSSION

The HEK293 cell line was selected as it represents the site of interest, the proximal tubule, and is established in the literature as a reproducible cell line for transfection (Graham 1977, Baldi 2007, Tanihara 2007, Dietmair 2012). HEK293 cells have previously been shown to express low levels of endogenous transporters (Ahlin 2009). The human protein atlas has previously demonstrated that MATE1, but not MATE2K, protein coding genes are expressed within HEK293 cells, through the use of RNA-seq to measure the transcript abundance of SLC47A1 and SLC47A2 (Thul 2017). Additionally, stable transfection of HEK293s with 4 drug transporters did not alter endogenous gene expression of transporters to a significant degree (Ahlin 2009). However, endogenous gene expression must still be considered on a case by case basis. This indicates that changes in cell culture conditions, in order to facilitate transfection, do not significantly alter transporter expression on the HEK293 cell membrane. The exponential growth, amino acid production and consumption of HEK293 cells has been shown to be the same within untreated and transfected protein producing HEK293s (Dietmair 2012). However, glucose consumption and production differs between the two cell cultures (Dietmair 2012). Differential regulation of genes involved in several metabolic pathways including glycolysis and oxidative phosphorylation, is also observed between untreated and recombinant protein producing HEK293s (Dietmair 2012).

HEK293 cell line transfection has been consistently utilised to study transporter morphology and function (Bai 1996, Bai 1997, Bai 1998, Otsuka 2005, Masuda 2006). Additionally, transfected HEK293s have been used to study numerous transporter-drug interactions (Tanihara 2007). As shown in the case of MATE1 and MATE2K and by Bai *et al.* who demonstrated the function, expression and morphology of the extracellular calcium-sensing receptor within transiently transfected HEK293 cells (Bai 1996, Bai 1997, Bai 1997, Bai 1998).

The transiently overexpressing MATE1 or MATE2K transporter cell lines described here could be used to study not only the interactions of TAF and TFV (See chapter 5) but also other drugs that may interact with these PTC transporters. This type of work has previously included the study of the inhibitory effect of the pharmacoenhancers COBI and RTV on creatinine transport by MATE1 (Lepist 2014). This interaction is of particular interest given that COBI may be prescribed as part of the single dose drug regimen STRIBILD, which also contains TDF, FTC and EVG. An elevation in creatinine concentration caused by inhibiting MATE1 could result in discontinuation of STRIBILD therapy, given that patients are already at increased risk of developing renal dysfunction when receiving a TDF-containing regimen.

This study demonstrates the functionality of two transiently transfected HEK293 cell lines overexpressing either the MATE1 or the MATE2K transporter. These cell lines will be used to study the potential effect of TAF or TFV on the transport of metformin or creatinine by MATE1 and MATE2K.

Chapter 5: The Effect of Tenofovir Alafenamide and Tenofovir on the Transport of MATE1 and MATE2K Substrates

5.1 INTRODUCTION

MATE1 and MATE2K are broad specificity proton/cation transporters studied in the kidney for a multitude of aims, including investigating multidrug resistance, drug-drug interactions and kidney toxicity (Tanihara 2007, Damme 2011, Lu 2016). Drug interactions with MATE transporters are wide ranging and have previously included ART, with the pharmacokinetic booster COBI inhibiting MATE1 and moderately inhibiting MATE2K (Tanihara 2007, Nies 2011, German 2012, Gutierrez 2014).

TAF has been shown to be a substrate of P-gp and BCRP within the small intestine and a substrate of the hepatic uptake transporters OATP1B1 and OATP1B3 (EuropeanMedicinesAgency 2015). TAF is not an inducer of P-gp or UGT1A1 and is unlikely to activate PXR xenobiotic receptors (EuropeanMedicinesAgency 2015). Furthermore, TAF induces CYP isoenzymes at a concentration of 10 μM but not at a concentration of 1 μM (EuropeanMedicinesAgency 2015). TAF is a minimal inhibitor of the renal transporters OCT1 and MATE1 but does not inhibit P-gp, BCRP, OAT1, OAT3 and OCT2 (EuropeanMedicinesAgency 2015). TFV is not a substrate of either MATE1 or MATE2K (Tanihara 2007) and previous studies have shown TFV does not inhibit OCT2 or MATE1 (EuropeanMedicinesAgency 2015).

The type 2 diabetes drug metformin is a common co-medication for several diseases such as CKD and cardiovascular disease (Plantinga 2010, Jellinger 2012). Metformin has previously been highlighted as unsuitable for use in patients with renal dysfunction, a known side effect of TDF therapy (Munar 2007, Moss 2014). In light of this, potential drug-drug interactions between TAF and metformin are of interest, as the use of this agent is anticipated to increase through the prescription of PrEP and the licensing of TAF as an alternative to TDF.

Creatinine's use as a biomarker for kidney dysfunction makes its efflux from PTCs a mechanism of interest, given that a diagnosis of renal impairment for HIV positive patients can result in discontinuation of TFV therapy in some circumstances (Röling 2006, Wyatt 2007). A lack of specific biological markers for renal toxicity hinders early detection and intervention in drug associated renal toxicity. Therefore, further understanding the way in which antiretroviral drugs can interfere with the mechanism of active secretion of creatinine via PTCs is important not only in terms of drug development but also for the relevance of serum creatinine as a clinical biomarker for renal toxicity. Multiple drugs have been reported to alter eGFR filtration rate with minimal evidence of actual kidney damage (Berglund 1975, Van Acker 1992, German 2012, Lepist 2014). This includes DTG which inhibits OCT2, the influx transporter of creatinine into PTCs, resulting in increased levels of serum creatinine without altering kidney function (Koteff 2013).

Cimetidine is a H_2 receptor antagonist known to inhibit MATE1 and MATE2K, as such it is frequently used as a model inhibitor of these transporters within transporter interaction studies (van Acker 1992, Otsuka 2005, Tanihara 2007, Tsuda 2009, Ito 2012, Elsby 2017). Metformin transport by MATE1 and MATE2K has been shown to be inhibited by cimetidine *in vitro* (Tanihara 2007, Tsuda 2009, Ito 2012, Elsby 2017) and *in vivo* (Somogyi 1987, Wang 2008). Furthermore, creatinine clearance is known to be influenced by cimetidine *in vivo*, with a reduction in creatinine clearance observed due to inhibition of tubular transport by cimetidine (van Acker 1992, Serdar 2001, Kabat-Koperska 2007).

This chapter sought to determine the effect of TFV and its prodrug TAF on the transport of metformin and creatinine by the MATE1 and MATE2K transporters. TDF and TAF release the active metabolite TFV through different metabolic pathways. TDF is rapidly metabolised in

plasma releasing TFV, whereas TAF is broken down by cathepsin A in peripheral blood mononuclear cells and carboxylesterase 1 in the liver (Birkus 2016). As such, renal exposure to TDF is minor and so the interaction of TDF with renal transporters was not included within this study. Inhibition of MATE1 or MATE2K by TAF or TFV has the potential to have ramifications beyond creatinine's use as a renal biomarker and an increase in metformin pharmacokinetics. As drug interactions may alter exposure to concomitantly prescribed drugs, metabolites and endogenous compounds, resulting in unanticipated drug-drug interactions and potential toxicity (Chu 2016).

5.2 METHODS

5.2.1 *Materials*

Lipofectamine 3000 transfection kit, OptiMEM media, Nunclon Delta Surface 24 well plate, FBS, DMEM, HBSS, Molecular Biology Grade Water and Poly-L-lysine solution were purchased from Sigma Aldrich (Dorset, UK). ^{14}C metformin and ^{14}C creatinine were purchased from American Radiolabeled Chemicals (St Louis, MO). HEK293 cells were purchased from ATCC-LGC (Middlesex, UK). TFV and TAF were purchased from FisherScientific (Leicestershire, UK).

5.2.2 *Cell culture*

HEK293 cells were cultured using the same method previously described in Chapter 4 (Section 4.2.4).

5.2.3 *Viability assay*

Cell viability was assessed using the same protocol outlined in Chapter 4 (Section 4.2.7).

5.2.4 *Uptake of radiolabeled drug*

A 24 well Nunclon Delta plate containing 200,000 HEK293 cells and 1 mL of DMEM per well, set up as previously described in Chapter 4 (Section 4.2.4), was transfected after 24 hours incubation at 37 °C, 5% CO_2, using a Lipofectamine 3000 reagent kit as previously outlined in Chapter 4 (Section 4.2.5). All cells were incubated at 37 °C, 5% CO_2 for 72 hours before conducting the accumulation experiment.

For the accumulation experiment, incubation media normalised to pH 7.4 using 1 M NaOH was prepared, containing 145 mM NaCl, 3 mM KCl, 1 mM $CaCl_2$, 0.5 mM $MgCl_2$, 5 mM D-

glucose, 5 mM HEPES and distilled water. The transfected HEK293 cells were pre-incubated with 200 µL of incubation media for 10 minutes at 37 °C, 5% CO_2. Incubation media was aspirated, and cells were treated with 200 µL of 30 mM ammonium chloride at 37 °C, 5% CO_2 for 10 minutes. Post ammonium chloride incubation, cells were incubated for 5 minutes with 200 µL of 9.9 µM ^{14}C metformin or 5 µM ^{14}C creatinine combined with either 500 µM cimetidine, TAF or TFV at concentrations ranging from 3.3 nM to 33 µM at pH 7.4 at 37 °C, 5% CO_2. A 500 µM concentration of cimetidine was chosen due to previous demonstration of maximum inhibition of MATE1 and MATE2K at this concentration (Ito 2012). TAF and TFV concentration ranges were selected to produce a full $\log_{10}$ concentration response curve.

After drug incubation, 100 µL of media was removed from each well and prepared for analysis within 4 mL of scintillation fluid. The remaining media was then removed from each well and cells were washed rapidly three times with 1 mL of ice-cold incubation medium at pH 7.4. 500 µL of 0.5 M NaOH was then added to each well. Cells were incubated for 10 minutes at 37 °C, 5% CO_2. A second 100 µL aliquot was then taken from each well of the plate and prepared for analysis through the addition of 4 mL of scintillation fluid. The radioactivity of each sample was then analysed using a Tri-Carb scintillation counter and QuantaSmart™ software (DPM Soultions Ltd, Chesterfield, UK). The cellular volume, intra- and extra-cellular concentration and CAR were calculated as described in Chapter 4 (Section 4.2.9).

5.2.5 *Statistical analysis*

The Shapiro-Wilk Test was used to test for normality, with $P \leq 0.05$ considered as statistically significant. An unpaired t test was then used to analyse potential differences in radiolabeled drug accumulation and percentage cell viability between conditions, with $P \leq 0.05$ considered to be statistically significant. EC_{50} values were calculated through fitting a sigmoidal

concentration-response model to the TAF or TFV concentration-response curves, using the following equation:

$$Y = \frac{\text{Bottom} + (\text{Top} - \text{Bottom})}{(1 + 10\text{^}((\text{LogEC50} - X)))}$$

All statistical analyses, chart production and sigmoidal concentration-response model production was carried out using GraphPad Prism 6 (GraphPad Software, La Jolla, CA).

5.3 RESULTS

5.3.1 *Cell viability assay*

To determine that the difference in CAR between experimental conditions was not due to cell death, cell viability was determined. HEK293 cells were incubated with either 500 µM cimetidine, TAF or TFV at the 5 highest concentrations to be included within the experiment, for 10 minutes under experimental conditions (Figure 5.1). Greater than 80% of the cell viability observed for the untreated cells was observed at each of these conditions and so all drug concentrations were deemed non-toxic and therefore suitable for the experiments.

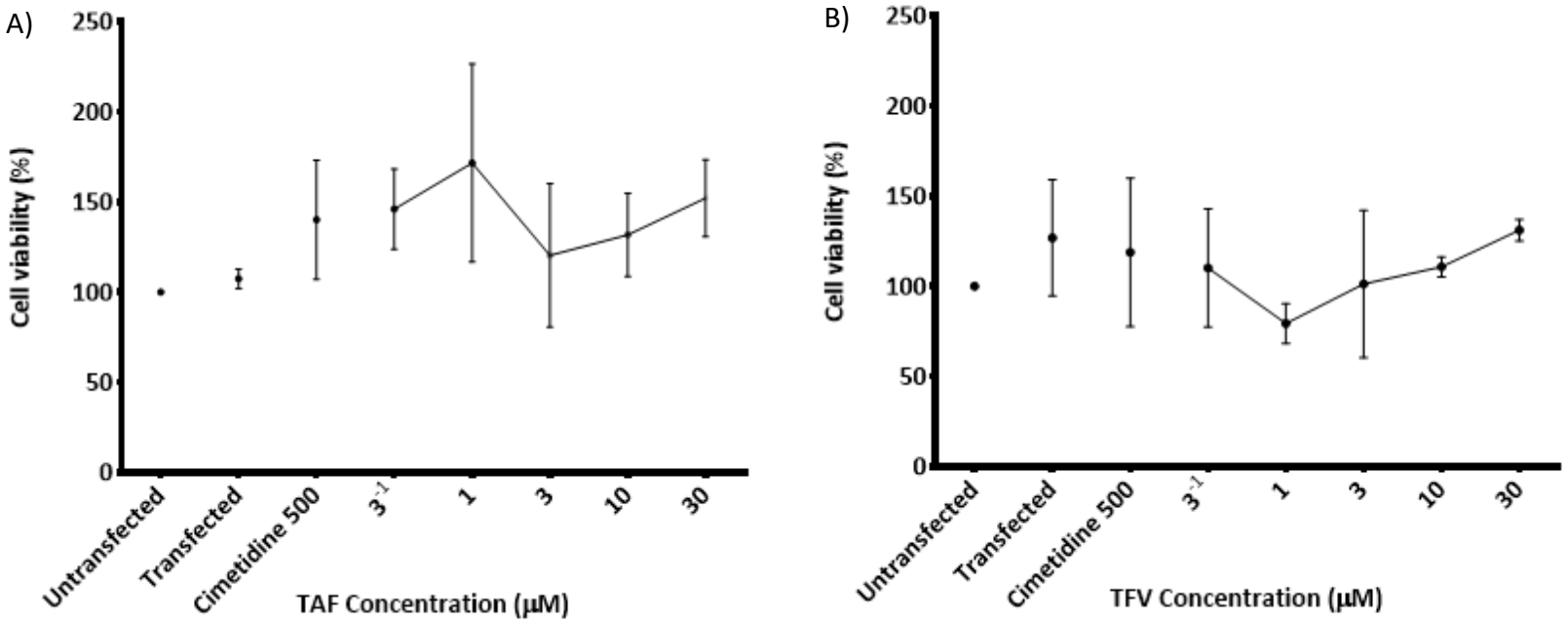

Figure 5.1: Cell viability assay.

Graph A: HEK293 cells incubated with TAF or cimetidine. Graph B: HEK293 cells incubated with TFV or cimetidine. Data points represent the mean ± SD, N = 3

5.3.2 ^{14}C *metformin cellular accumulation*

As shown in Figure 5.2 the CAR of ^{14}C metformin within the transiently transfected HEK293 cells was statistically significant compared to untreated cells within the MATE1 TAF incubation (P = 0.006), TFV incubation (P = 0.001) and MATE2K TAF incubation (P = 0.023) experiments, but not within the MATE2K TFV incubation (P = 0.904).

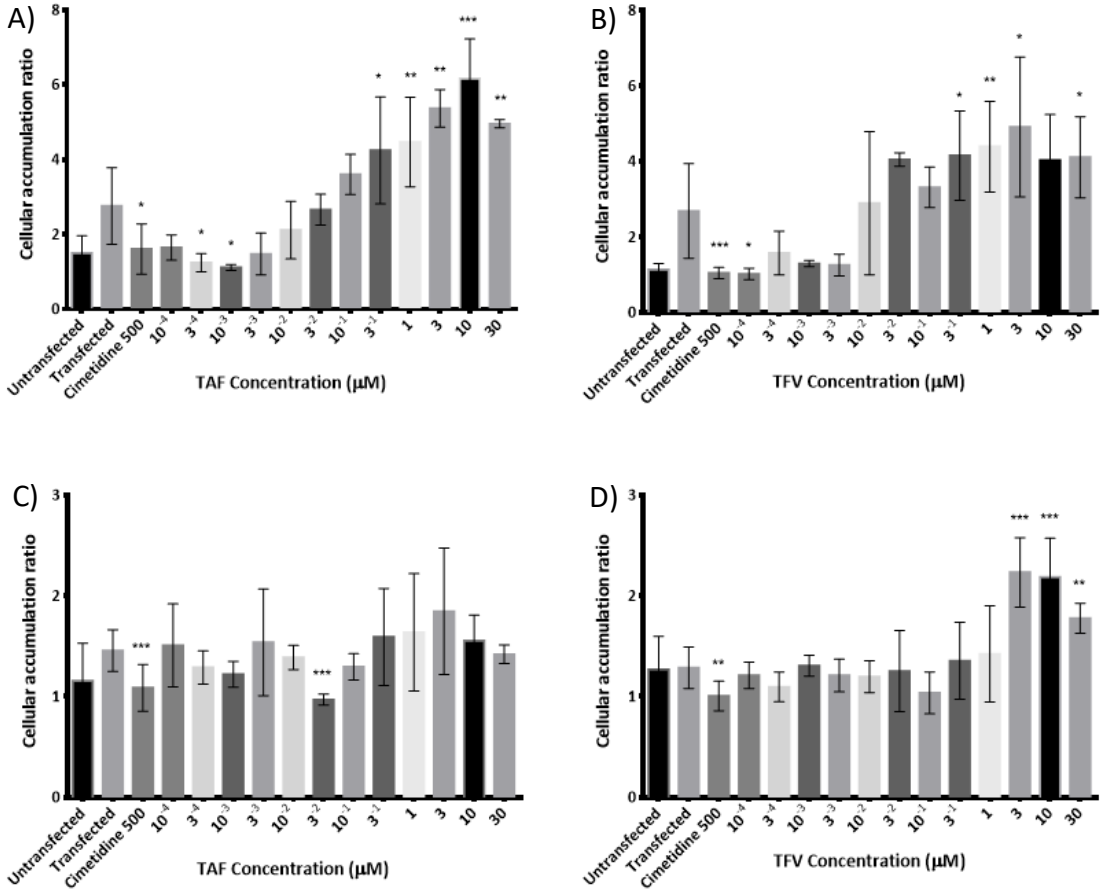

Figure 5.2: Effect of TAF or TFV on the cellular accumulation of ^{14}C metformin within cells overexpressing either the MATE1 or the MATE2K transporter.

Graph A: MATE1 overexpressing HEK293 cells incubated with TAF. Graph B: MATE1 overexpressing HEK293 cells incubated with TFV. Graph C: MATE2K overexpressing HEK293 cells incubated with TAF. Graph D: MATE2K overexpressing HEK293 cells incubated with TFV. Data points represents the mean ± SD, N = 3 from 3 experiments

Figure 5.3 demonstrates that incubation of ^{14}C metformin with cimetidine at concentrations ranging from 10^{-4} µM to 30 µM within HEK293 cells overexpressing either the MATE1 or MATE2K transporter, resulted in a CAR comparable to that observed in untreated HEK293 cells. Furthermore, inhibition of ^{14}C metformin accumulation for each cimetidine concentration was comparable to that observed after incubation with cimetidine 500 µM. Demonstrating the effective inhibition of the MATE1 and MATE2K transporter by cimetidine.

^{14}C metformin cellular accumulation in the presence of TAF or TFV at concentrations ranging from 0.3 µM to 30 µM combined with 500 µM cimetidine, was found to be comparable between untreated, MATE1 overexpressing and MATE2K overexpressing HEK293 cells (Figure 5.3). This indicates that the alterations in ^{14}C metformin accumulation observed within this chapter was mediated by TAF or TFV at either the MATE1 or MATE2K transporter, and not due to an off-target interaction.

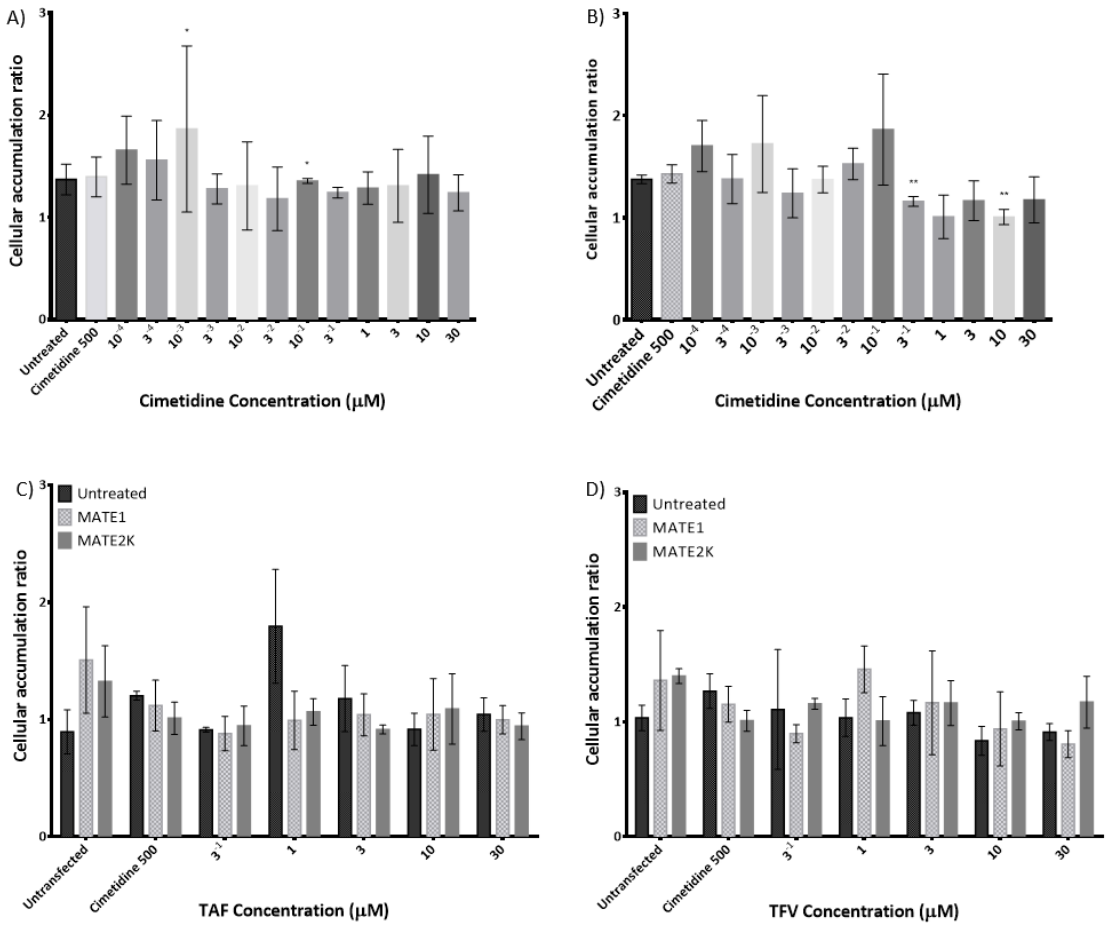

Figure 5.3: Comparison of ^{14}C metformin accumulation by cell type, post incubation with TAF or TFV with cimetidine.

Graph A: MATE1 overexpressing HEK293 cells incubated with cimetidine. Graph B: MATE2K overexpressing HEK293 cells incubated with cimetidine. Graph C: HEK293 cells untreated, expressing MATE1 or expressing MATE2K incubated with TAF and cimetidine. Graph D: HEK293 cells untreated, expressing MATE1 or expressing MATE2K incubated with TFV and cimetidine. Data points represent the mean ± SD, of N = 3 from 3 experiments

As seen in Figure 5.4 the CAR of ^{14}C metformin was observed to be higher in MATE1 overexpressing cells compared to untreated HEK293 cells or MATE2K overexpressing cells in the presence of either TAF or TFV.

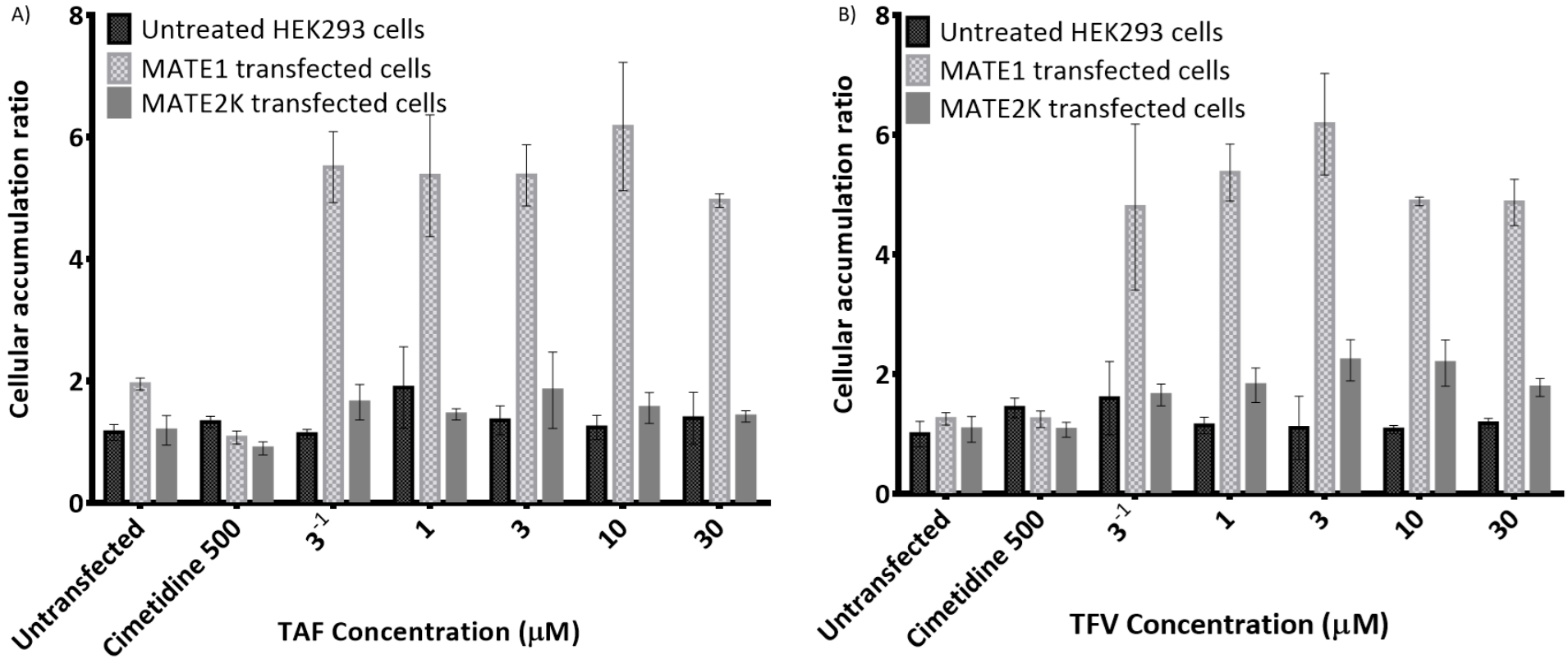

Figure 5.4: Comparison of ^{14}C metformin accumulation by cell type, post incubation with TAF or TFV.

Graph A: HEK293 cells untreated or expressing MATE1 or MATE2K incubated with TAF. Graph B: HEK293 cells untreated or expressing MATE1 or MATE2K incubated with TFV. Data points represent the mean ± SD, N = 3 from 3 experiments

As shown in Figure 5.2 Graph A, accumulation of ^{14}C metformin incubated with TAF at concentrations of 0.3 µM and above, within HEK293 cells transiently transfected to overexpress the MATE1 transporter, increased to a significant level ($P < 0.020$), compared to cells incubated with ^{14}C metformin alone. Figure 5.5 demonstrates the effect of TAF on MATE1 (EC_{50} =1.7 x 10^{-4} µM) mediated transport of ^{14}C metformin.

Cellular accumulation of ^{14}C metformin was elevated with increasing concentration of TFV from 0.3 µM and above ($P < 0.019$), up to the point of saturation at a concentration greater than 10 µM. Demonstrating the effect of TFV on the efflux of ^{14}C metformin by MATE1 (EC_{50} = 3.9 x 10^{-4} µM; Figure 5.2 and 5.5).

As shown in Figure 5.2, exposure to TAF did not alter the accumulation ratio of ^{14}C metformin within HEK293 cells transiently overexpressing MATE2K. Because of this, the sigmoidal concentration-response model applied in Figure 5.5 was unable to produce an R^2 value or EC_{50} value.

Accumulation of ^{14}C metformin in the presence of TFV at varied concentrations within MATE2K overexpressing HEK293 cells was shown to be comparable to that observed within MATE2K overexpressing HEK293s incubated with ^{14}C metformin in isolation up to a concentration of TFV at 1 µM (Figure 5.2). Incubation with TFV concentrations of 3 µM and above resulted in a higher CAR of ^{14}C metformin compared to MATE2K overexpressing cells incubated with ^{14}C metformin alone ($P < 0.003$; EC_{50} = 2.4 µM; Figure 5.2 and 5.5).

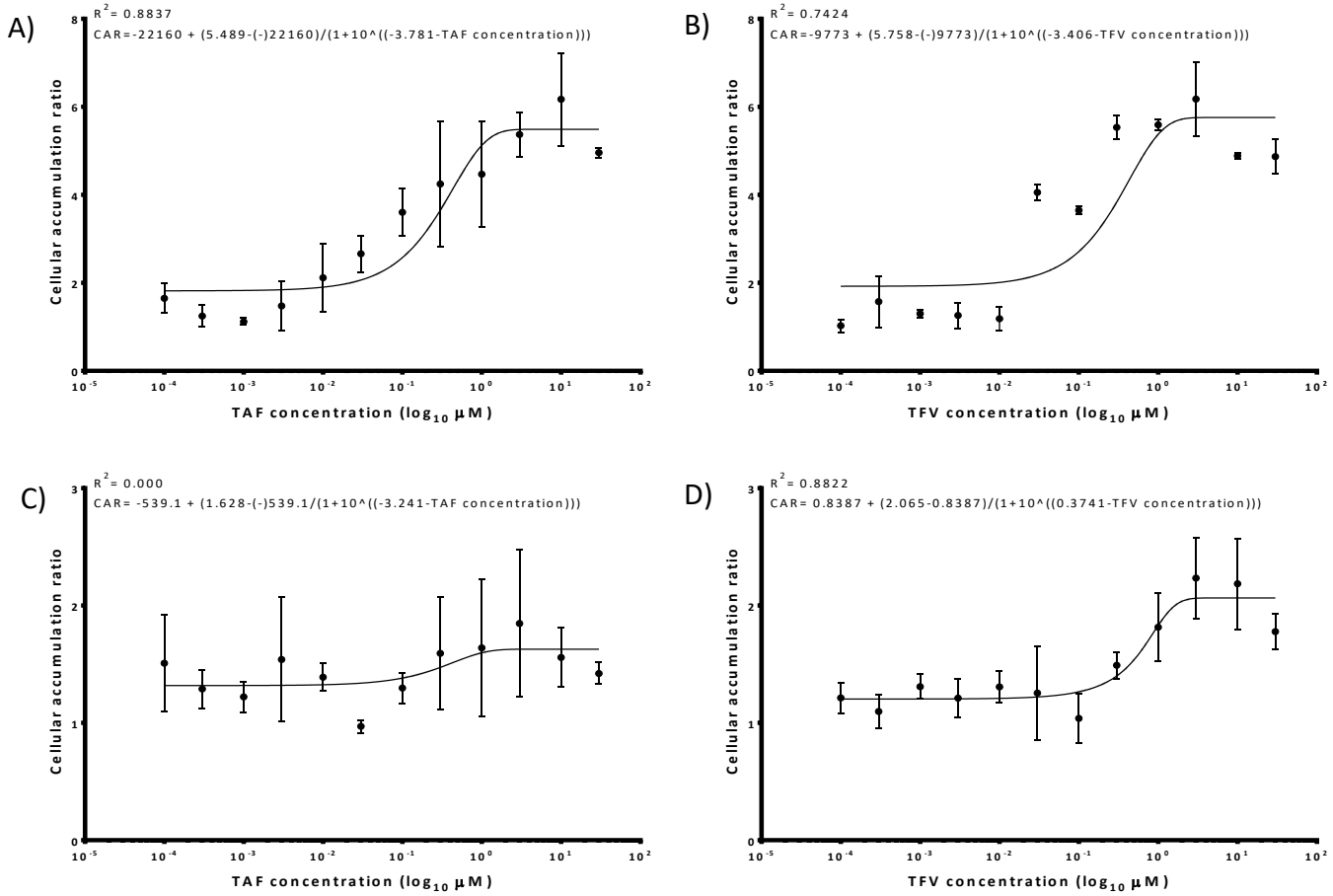

Figure 5.5: TAF or TFV concentration dependent accumulation of ^{14}C metformin.

A sigmoidal concentration response model fitted to calculate EC_{50}. Graph A: HEK293 cells overexpressing MATE1 incubated with TAF. Graph B: HEK293 cells overexpressing MATE1 incubated with TFV. Graph C: HEK293 cells overexpressing MATE2K incubated with TAF. Graph D: HEK293 cells overexpressing MATE2K incubated with TFV. Data points represent the mean ± SD, N = 3 from 3 experiments

5.3.3 *^{14}C creatinine cellular accumulation*

As shown in Figure 5.6 Graph A, accumulation of ^{14}C creatinine incubated with TAF at concentrations of 0.1 µM and above, within HEK293 cells transiently transfected to overexpress the MATE1 transporter, was decreased to a significant level ($P < 0.030$; $IC_{50} = 0.3$ nM; Figure 5.7), compared to cells incubated with ^{14}C creatinine alone. Cellular accumulation of ^{14}C creatinine was not altered by incubation with increasing concentration of TFV, within cells overexpressing the MATE1 transporter (Figure 5.6). However, Figure 5.7 Graph B indicates an inhibitory effect of TFV on the CAR of ^{14}C creatinine at concentrations greater than 3 µM, although not to a statistically significant degree.

Accumulation of ^{14}C creatinine in the presence of increasing concentrations of TAF within MATE2K overexpressing HEK293 cells was shown to be statistically significant to that observed in cells incubated with ^{14}C creatinine in isolation ($P \leq 0.039$; $IC_{50} = 2.3$ µM; Figure 5.6 and 5.7).

Figure 5.6 shows incubation of HEK293 cells overexpressing MATE2K with ^{14}C creatinine and TFV at concentrations ranging from 0.001-0.3 µM resulted in lower CAR of ^{14}C creatinine compared to cells incubated with ^{14}C creatinine alone ($P < 0.030$; $IC_{50} = 0.3$ µM; Figure 5.7).

As seen in Figure 5.8 the CAR of ^{14}C creatinine was lower in MATE1 overexpressing cells compared to MATE2K overexpressing cells in the presence of TAF. Indicating that the inhibitory effect of TAF is greater for MATE1 compared to MATE2K. In the presence of TFV there was a general trend of higher CAR of ^{14}C creatinine within MATE1 transfected cells compared to MATE2K.

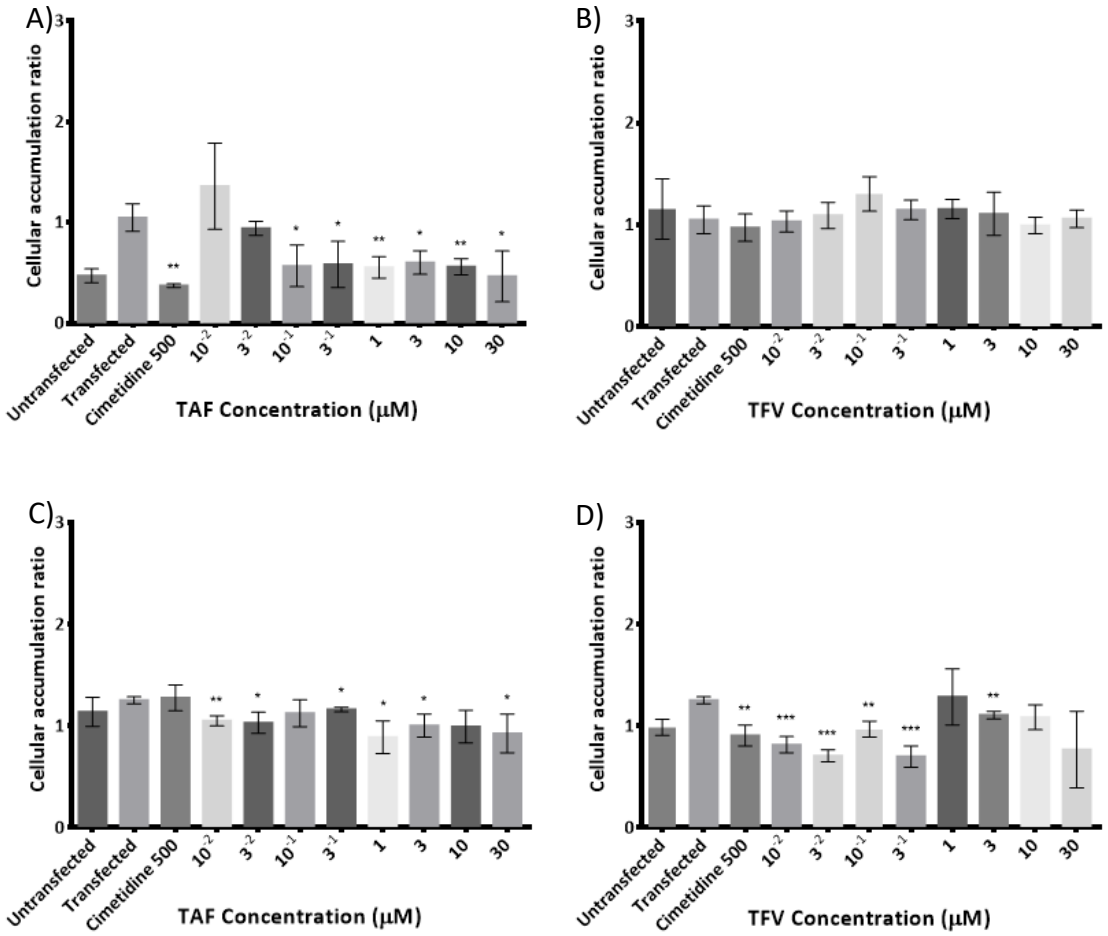

Figure 5.6: Effect of TAF or TFV on the cellular accumulation of ^{14}C creatinine within cells overexpressing either the MATE1 or MATE2K transporter.

Graph A: HEK293 cells overexpressing MATE1 incubated with TAF. Graph B: HEK293 cells overexpressing MATE1 incubated with TFV. Graph C: HEK293 cells overexpressing MATE2K incubated with TAF. Graph D: HEK293 cells overexpressing MATE2K incubated with TFV. Data points represent the mean ± SD, N = 3 from 3 experiments

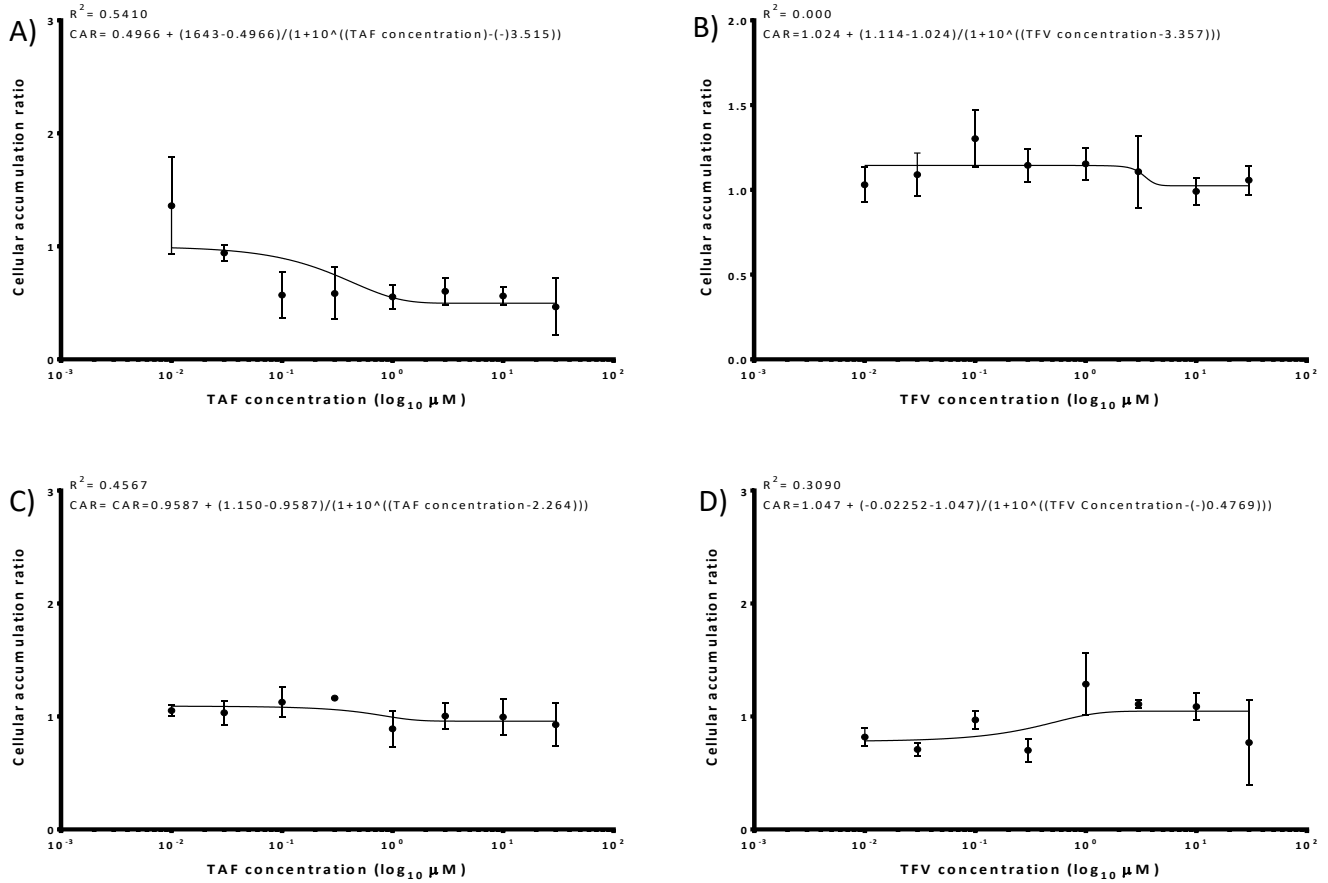

Figure 5.7: TAF or TFV concentration dependent accumulation of ^{14}C creatinine.

A sigmoidal concentration response model was fitted to calculate EC_{50}. Graph A: HEK293 cells overexpressing MATE1 incubated with TAF. Graph B: HEK293 cells overexpressing MATE1 incubated with TFV. Graph C: HEK293 cells overexpressing MATE2K incubated with TAF. Graph D: HEK293 cells overexpressing MATE2K incubated with TFV. Data points represent the mean ± SD, N = 3

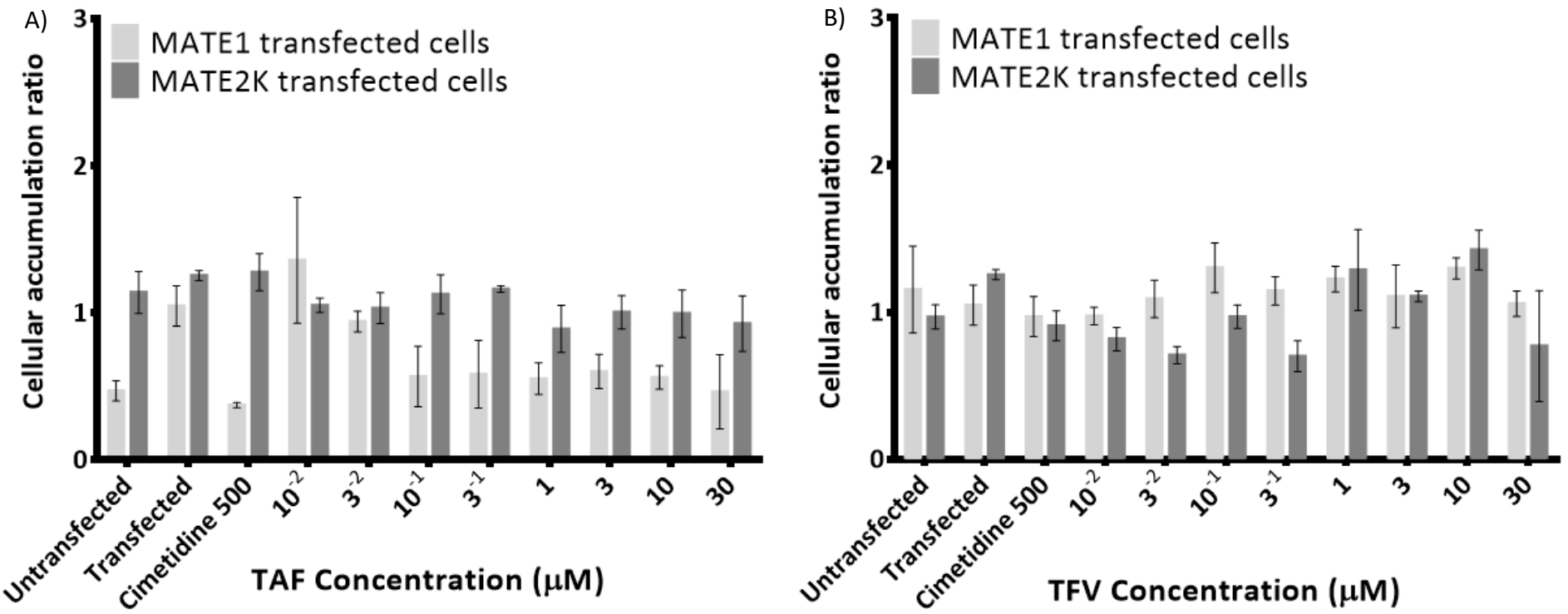

Figure 5.8: Comparison of ^{14}C creatinine accumulation by cell type, post incubation with TAF or TFV.

Graph A: HEK293 cells overexpressing either MATE1 or MATE2K incubated with TAF. Graph B: HEK293 cells overexpressing either MATE1 or MATE2K incubated with TFV. Data points represent the mean ± SD, N = 3

5.4 DISCUSSION

This chapter investigated the effect of TAF and TFV on the transport of metformin and creatinine by the MATE1 and MATE2K transporters, utilising a transiently transfected HEK293 cell line. The data demonstrated an effect of TAF on MATE1 mediated transport of metformin, and an effect of TFV on MATE1 and MATE2K mediated transport of metformin. Furthermore, our study showed an inhibitory effect of TAF for MATE1 and MATE2K mediated transport of creatinine and of TFV for MATE2K mediated transport of creatinine.

The effect of TAF on MATE1 mediated accumulation of metformin and MATE1 and MATE2K mediated accumulation of creatinine is of interest given the limited data currently available on the interaction of TAF with renal transporters. TAF has previously been shown to inhibit MATE1 to a marginal degree at concentrations 200 fold in excess to those achieved in plasma after dosing to patients (EuropeanMedicinesAgency 2015). Given that TAF is able to achieve higher intracellular concentrations and lower circulating concentrations of TFV compared to TDF treatment, and that TAF is minimally eliminated in urine as unchanged drug, TAF is projected to have fewer renal complications compared to TDF (Markowitz 2014, Bonora 2016). Although TAF is minimally eliminated in urine as unchanged drug, TAF exposure in patients with renal impairment has been observed to be elevated, which the authors hypothesise to be a result of reduced P-gp mediated transport of TAF, resulting in increased absorption (Custodio 2016). Unlike TFV, TAF has been shown not to be a substrate of OAT1 and OAT3, and so accumulation within PTCs through this mechanism is unlikely (Bam 2014). Multiple Phase 2 and 3 studies have demonstrated TAF to have a reduced impact on renal function compared to TDF containing regimens, and so the clinical impact of the observed

inhibition of creatinine transport may be limited but is nevertheless important in terms of developing understanding of TAF transporter interactions.

Accumulation of metformin within MATE1 or MATE2K overexpressing cells was elevated by incubation with TFV, with a 6,000-fold difference in EC_{50} value between MATE1 and MATE2K overexpressing cell lines. Given that MATE1 is the primary efflux transporter of metformin within PTCs (Tanihara 2007, Damme 2011) the higher impact of TFV on MATE1 compared to MATE2K could potentially result in a reduction in metformin pharmacokinetics, due to an increase in clearance of metformin. Incubation with TAF resulted in alterations in the accumulation of creatinine within MATE1 and MATE2K overexpressing cells. A 7,000-fold difference in TAF IC_{50} was observed between the two cells lines. The higher impact of TAF on MATE1 may result in elevation in serum creatinine, and thus a potential false indication of renal toxicity, as previously observed within patients who receive TDF (Yombi 2014). Study of TAF in combination with EVG/COBI and FTC within patients with renal impairment demonstrated no effect on eGFR in patients who had previously received TDF but did observe a worsening of eGFR (median change = -0.6 mL/min) in six ART naive patients (Pozniak 2016).

An inhibitory effect of TFV on MATE2K, but not MATE1, mediated creatinine transport was observed within this chapter. This effect on MATE1 was previously outlined by the European Medicines Agency (EuropeanMedicinesAgency 2015). Further study into the structural determinants for this inhibitor specificity would be of use given the broadly overlapping substrate specificity of the two transporters. As MATE1 but not MATE2K is expressed on HEK293 cells endogenously, inhibition of the endogenous MATE1 transporter on MATE2K overexpressing cells could be of use in future studies to show conclusively that any alterations in substrate transport are caused by interaction with MATE2K exclusively. This could be achieved through incubating the cells with famotidine, a selective MATE1 inhibitor,

before incubating the cells with MATE substrate and TAF or TFV. Additionally, development of a multiple-transporter expressing HEK293 cell line expressing both influx and efflux transporters of creatinine may be of use, enabling the study of the effect of TAF and TFV on the full transporter profile of creatinine within the kidney.

We observed probe substrate-specific differences in CAR between metformin and creatinine despite utilising the same assay conditions for both substrates and incubating both substrates with the same concentration range of TAF or TFV. Incubation of metformin with TAF or TFV was shown to elevate CAR within MATE1 overexpressing cells, with the same observed for metformin accumulation with TFV in MATE2K overexpressing cells. This indicates an activation effect of the antiretrovirals on substrate transport by MATE1 and MATE2K. However, in the case of creatinine, incubation with TAF within MATE1 overexpressing cells and with TAF or TFV in MATE2K overexpressing cells resulted in a reduction in CAR of creatinine. Indicating an inhibitory effect of TAF on MATE1 and MATE2K and of TFV on MATE2K.

The difference observed in TAF and TFV interactions with metformin and creatinine may be due to differential binding of the substrates to allosteric binding sites on the MATE transporters, occurring as a result of differences in the chemical compositions of the two substrates. A previous study has suggested that MATE substrates may influence the interaction of inhibitors with MATE transporters. This study demonstrated that the inhibitory effect of 3 salts in liquid state on MATE activity was dependent on the substrate being transported, suggesting a kinetically complex mechanism of substrate-inhibitor interaction with the transport protein (Martínez-Guerrero 2013). Additionally, probe substrate-specific differences in IC_{50} values have previously been seen within studies investigating MATE2K and OCT2 (Zolk 2009, Müller 2015, Shen 2015). These observations suggest that substrate

interactions with transporters may be a combination of competitive and allosteric interactions, as previously suggested for OCT (Gorboulev 2005). This could be explained through the potential presence of multiple binding sites on MATE transporters (Martínez-Guerrero 2013). Further studies are required to determine the exact mechanism underpinning the observations in this chapter. These studies could include biochemical and mechanistic studies to investigate the current mechanism by which MATE transporters select cations or drugs from the cytoplasm, which has yet to be elucidated (Lu 2016).

Since MATE function is determined *in vitro* through alteration of extracellular pH, interpretation of *in vitro* data assumes that there is equal affinity for transporter substrates and inhibitors at both the intra- and extra-cellular binding sites. Potential differences in CAR between creatinine and metformin may in part be attributed to preferential binding of metformin to the extracellular binding site of MATE transporters, and of creatinine to the intracellular binding site of MATE transporters, resulting in a higher level of transport of each substrate in the corresponding direction.

Finally, the clinical impact of these findings must be taken into consideration. Whilst TAF was shown to inhibit MATE1 and MATE2K transport of creatinine to a statistically significant level compared to control, at the full range of concentrations studied (10^{-2} – 30 μM), the clinical relevance of this interaction may be negligible in light of the fewer cases of TFV-associated renal dysfunction that have been reported with prescription of TAF over TDF (Yombi 2014). Nevertheless further knowledge of the way this recently approved ART drug interacts with endogenous substrates at a key site for excretion is of utility and provides further evidence for the unsuitability of creatinine as a reliable indicator of renal function (Moss 2014).

5.4.1 *Limitations*

Limitations of this chapter includes the use of a restricted number of MATE1 and MATE2K substrates. Given that *in vitro* inhibition data for some antiretroviral drugs has previously been shown to be highly variable, with the IC_{50} value for RTV with MATE1 showing a 193-fold variability between studies, (Chu 2016) data on a greater number of substrate-drug interactions will aid interpretation. Future studies could include other established and novel probe substrates for the study of MATE inhibition. Including the frequently studied retinol-binding protein and the more recently used endogenous probe N-methylnicotimide (NMN), which has the same transporter profile as creatinine and has previously been used within multiple studies as an endogenous probe for drug-drug interactions involving MATEs (Yombi 2014, Chu 2016).

Chapter 6: The Effect of Gene Variants on Levonorgestrel Pharmacokinetics when Combined with Antiretroviral Therapy Containing Efavirenz or Nevirapine

6.1 INTRODUCTION

Hormonal contraceptives and ART are critical components of healthcare for the estimated 17 million women living with HIV and are key pillars in the effort to globally reduce mother-to-child HIV transmission. The subdermal LNG implant is a highly effective and desirable method of contraception (Lehtovirta 2007, Heikinheimo 2011). LNG is released from the implant initially at 100 mcg/day, decreasing to 40 mcg/day within one year and to 30 mcg/day within three years, providing relatively stable daily drug concentrations over this timeframe (Kopp 2003). Notably, the use of contraceptive implants is rapidly expanding in low and middle income countries (Phillips 2013). In these same settings, the WHO recommends ART containing two NRTIs in combination with EFV as a first-line regimen for HIV treatment (WHO 2016). The use of EFV-based ART in women of childbearing potential has expanded in the past decade, first following characterisation of the lower than expected level of fetal risk during in-utero EFV exposure (Ford 2011, WHO 2012, WHO 2013), and subsequently due to recent WHO recommendations for universal use of ART, irrespective of CD4+ cell count (WHO 2010). Considered an alternate first-line option, NVP is still used by many women in low and middle income countries (WHO 2016). In light of this, identifying safe and efficacious combinations of both therapies with hormonal contraceptives in HIV positive women is a critical public health priority.

A significant drug-drug interaction between the LNG implant and EFV-based ART in HIV-positive Ugandan women, which resulted in 47% lower LNG concentrations compared to control participants, and a high rate of unintended pregnancy, in women receiving EFV-based ART [3 (15%) of 20 participants] has previously been described (Scarsi 2016). Induction of CYP3A4 and CYP3A5 mediated metabolism of LNG is the proposed mechanism of the observed interaction with EFV. No pharmacokinetic interaction or unintended pregnancies

were observed in women receiving NVP-based ART within the same study. These findings are supported by a retrospective cohort study of Kenyan women that found a three-fold higher adjusted pregnancy incidence in HIV-positive women receiving the implant plus EFV-based ART compared to those receiving NVP-based ART (Patel 2015).

LNG, EFV and NVP are substrates of CYP enzymes; LNG is metabolised by CYP3A4 and CYP3A5, (Moreno 2012) EFV is metabolised by CYP2B6 with minor contributions from CYP2A6, CYP3A4, and UGT2B7, (Bélanger 2009, Ogburn 2010) while NVP is metabolised by CYP2B6, CYP3A4 and partially by CYP2D6 (Cammett 2009, Fan-Havard 2013). The nuclear receptor genes *NR1I2* and *NR1I3* are known to regulate the expression and activity of several CYPs, including CYP2B6 and CYP3A4 (Zhang 2001, Wyen 2011, Swart 2012). SNPs within the genes expressing the aforementioned proteins have been associated with alterations in EFV and NVP pharmacokinetics, as outlined in Chapter 1 (Section 1.6 and Section 1.8).

The primary objective of this secondary study analysis was to ascertain the contributory effect of SNPs in key genes of interest in LNG, EFV, and NVP metabolism (*CYP2B6*, *CYP2A6*, *NR1I2* and *NR1I3)* on plasma LNG pharmacokinetics when the subdermal implant was given in combination with EFV or NVP based ART (EFV and NVP groups, respectively) in HIV-positive women. Since these SNPs have been shown to influence NNRTI pharmacokinetics, our underlying hypothesis was that there would be consequences of different NNRTI concentrations for the degree of CYP3A induction, and therefore a genetic basis for the subsequent magnitude of the interaction with LNG.

6.2 METHODS

6.2.1 *Ethical approval*

All study procedures followed the Helsinki Declaration of 1975 and were approved by ethics boards at the Joint Clinical Research Centre Kampala, Uganda National Council for Science and Technology, and the University of Nebraska Medical Centre. The study was registered on clinicaltrials.gov (NCT01789879).

6.2.2 *Study design and cohort*

This was a prospective pharmacokinetic evaluation of HIV-positive Ugandan women receiving EFV-based ART (EFV group, n = 20) or NVP-based ART (NVP group, n = 20). For the pharmacogenetic study, all participants in the EFV and NVP group were included (n = 40) and the ART-naïve group was excluded. The two-rod (75 mg/rod) LNG sub-dermal implant was inserted in all patients upon study entry. Inclusion criteria for the EFV and NVP groups included prescription of EFV or NVP plus 2 NRTIs for 30 days or longer and a HIV-RNA of < 400 copies/mL (Habtewold 2011).

6.2.3 *Sample and data collection*

Over a total of 48 weeks, a plasma sample was collected at weeks 1, 4, 12, 24, 36 and 48 to assess LNG, NVP and EFV pharmacokinetics. Follow-up was interrupted for 9 subjects between weeks 36-44 after 3 pregnancies were identified in the EFV group. The primary endpoint for the pharmacokinetic analysis was 24 weeks. Timing of blood sample collection for the EFV group was based on EFV mid-dosing interval at 12-14 hours post dose and for the NVP group based on the end dosing interval of 11-13 hours post dose. pharmacokinetic parameters included AUC from entry to week 24 ($AUC_{0\text{-}24\ weeks}$), maximum concentration (C_{max}), time to C_{max} (T_{max}) and minimum concentration (C_{min}). C_{max} and C_{min} represent the

highest and lowest concentrations observed over the entire study period. AUC was calculated using the trapezoidal rule (Phoenix WinNonlin, Certara®). LNG concentrations were analysed by a validated LC-MS/MS method; EFV and NVP plasma concentrations were determined using high performance liquid chromatography (HPLC) assays with ultraviolet detection as previously outlined by Scarsi *et al*. (Scarsi 2016).

6.2.4 *Genotyping*

Genomic DNA was extracted from whole blood through use of the manufacturers' protocol (E.Z.N.A Blood DNA Mini Kit; Omega bio-tek; Norcross, GA) as outlined in Chapter 2 (Section 2.2.6). Extracted DNA was quantified using NanoDrop (Thermo Fisher Scientific, Wilmington, DE). Genotyping was completed using real-time allelic discrimination PCR assay on a DNA Engine Chromo4 system (Bio-Rad Laboratories, Hercules, CA). The PCR protocol followed denaturation at 95 °C for 10 minutes, followed by 50 cycles of amplification at 92 °C for 15 seconds and annealing at 60 °C for 1 minute 30 seconds. Taqman Genotyping Master mix and assays *CYP2B6* 516G>T (rs3745274), *CYP2B6* 983T>C (rs28399499), *CYP2B6* 15582C>T (rs4803419), *CYP2A6* -48A>C (rs28399433) *CYP2A6*9B* 1836G>T (rs8192726) *NR1I2* 63396C>T (rs2472677), *NR1I3* 540C>T (rs2307424) and *NR1I3* 1089T>C (rs3003596) were purchased from Life Technologies (Paisley, Renfrewshire, UK). Opticon Monitor v.3.1 software (Bio-Rad Laboratories) was used to obtain allelic discrimination plots and identify genotypes.

6.2.5 *Statistical analysis*

Compliance with Hardy-Weinberg equilibrium was tested as outlined in Chapter 2 Section 2.2.6. Genotypes were coded for regression analyses as 0 = homozygous common allele, 1 = heterozygous and 2 = homozygous variant allele. Categorical variables were described using relative frequencies, whilst continuous variables were described using median and IQR. The

Shapiro-Wilk Test was used to test for normality, with $P \leq 0.05$ considered as statistically significant. A univariate analysis through linear regression was carried out in order to identify independent variables associated with LNG pharmacokinetic parameters within the EFV group, or the NVP group separately. Variables with $P \leq 0.2$ for the univariate analysis were carried through to a linear backwards multivariate analysis were $P \leq 0.05$ was deemed to be statistically significant. All statistical analyses were carried out using IBM SPSS Statistics v.22 (IBM Armonk, NY). All charts were produced using GraphPad Prism 6 (GraphPad Software, La Jolla, CA).

6.3 RESULTS

6.3.1 *Patient characteristics*

All women in the EFV and NVP group from the primary study were included in this analysis (n = 40) (Scarsi 2016). Patient characteristics and genotype frequencies are summarised in Table 6.1. The median (IQR) age and weight of all patients was 31 years (29-34 years) and 59 kg (53-68 kg). All SNPs were in Hardy-Weinberg equilibrium, except *CYP2B6* 15582C>T (rs4803419; $P < 0.001$, $X^2 = 20.6$) and *NR1I3* 540C>T (rs2307424; $P < 0.001$, $X^2 = 12.4$), which compromises their interpretation. Univariate and multiple regression analysis for LNG pharmacokinetic parameters based on EFV and NVP groups are presented in Table 6.3. All patients in the EFV group (n = 20) received EFV 600 mg daily plus 2 NRTIs for a median (IQR) of 10.5 months (6.3-37.8 months) prior to study entry. Patients in the NVP group (n = 20) received NVP 200 mg twice daily plus 2 NRTIs for a median (IQR) of 30.5 months (13.5-80.3 months) prior to study entry.

Table 6.1: Characteristics of the study participants at entry.

Characteristics	Total (n = 40)			Efavirenz group (n = 20)			Nevirapine group (n = 20)		
Age (years)	31.0 (29.0-34.0)			31.0 (28.3-34.0)			32.5 (31.0-35.8)		
Weight (kg)	59.0 (53.0-68.0)			59.5 (52.3-63.8)			59.5 (54.3-69.8)		
CD4 count (cells/mm^3)	579.0 (464.0-731.0)			556.5 (477.3-663.5)			626.0 (399.8-857.3)		
Albumin concentration at baseline (g/L)	43.7 (41.5-46.5)			43.3 (40.7-45.1)			43.1 (41.8-45.6)		
SHBG at baseline (nmol/L)	105.0 (82.3-136.0)			100.0 (79.4-125.9)			100.0 (100.0-125.9)		
Genotype frequencies									
CYP2B6 516G>T (rs3745274) (n [%])	**GG**	**GT**	**TT**	**GG**	**GT**	**TT**	**GG**	**GT**	**TT**
	17 (43)	22 (55)	1 (2)	8 (40)	11 (55)	1 (5)	9 (45)	11 (55)	0 (0)
CYP2B6 983T>C (rs28399499) (n [%])	**TT**	**CT**	**CC**	**TT**	**CT**	**CC**	**TT**	**CT**	**CC**
	32 (80)	7 (18)	1 (2)	17 (85)	3 (15)	0 (0)	15 (75)	4 (20)	1 (5)
CYP2B6 15582C>T (rs4803419) (n [%])	**CC**	**CT**	**TT**	**CC**	**CT**	**TT**	**CC**	**CT**	**TT**
	11 (28)	28 (70)	1 (2)	5 (25)	15 (75)	0 (0)	6 (30)	13 (65)	1 (5)
*CYP2A6*9B* 1836G>T (rs8192726) (n [%])	**GG**	**GT**	**TT**	**GG**	**GT**	**TT**	**GG**	**GT**	**TT**
	31 (82)	9 (18)	0 (0)	16 (80)	4 (20)	0 (0)	15 (75)	5 (25)	0 (0)
CYP2A6 48A>C (rs28399433) (n [%])	**AA**	**AC**	**CC**	**AA**	**AC**	**CC**	**AA**	**AC**	**CC**
	29 (78)	10 (22)	1 (2)	15 (75)	5 (25)	0 (0)	14 (70)	5 (25)	1 (5)
NR1I2 63396C>T (rs2472677) (n [%])	**CC**	**CT**	**TT**	**CC**	**CT**	**TT**	**CC**	**CT**	**TT**
	25 (63)	12 (30)	3 (7)	13 (65)	6 (30)	1 (5)	12 (60)	6 (30)	2 (10)
NR1I3 540C>T (rs2307424) (n [%])	**CC**	**CT**	**TT**	**CC**	**CT**	**TT**	**CC**	**CT**	**TT**
	10 (25)	30 (75)	0 (0)	6 (30)	14 (70)	0 (0)	4 (20)	16 (80)	0 (0)
NR1I3 1089T>C (rs3003596) (n [%])	**TT**	**CT**	**CC**	**TT**	**CT**	**CC**	**TT**	**CT**	**CC**
	14 (35)	22 (55)	4 (10)	6 (30)	12 (60)	2 (10)	8 (40)	10 (50)	2 (10)

Values shown as median (IQR) and percentage of population. SHBG: sex hormone-binding globulin.

6.3.2 *Levonorgestrel, efavirenz and nevirapine pharmacokinetics*

LNG C_{max}, T_{max}, C_{min}, and $AUC_{0\text{-}24week}$ are summarised by study group and SNP in Table 6.2. EFV $C_{12\text{-}14h}$ (mg/L) was 76% higher in homozygous *CYP2B6* 516 TT participants compared to those who were homozygous for the G allele. Within the NVP group NVP $C_{11\text{-}13h}$ (mg/L) was 5% lower in heterozygous *CYP2B6* 516 CT participants compared to homozygotes for the G allele.

Table 6.2: Levonorgestrel, efavirenz and nevirapine pharmacokinetic, summarised by associated *CYP2B6*, *NR1I2* or *CYP2A6* genotype.

LNG C_{max} (pg/mL)	***CYP2B6* 516G>T (rs3745274)**			***CYP2B6* 15582C>T (rs4803419)**			***CYP2A6* 1836G>T (rs8192726)**			***NR1I2* 63396C>T (rs2472677)**		
	GG	GT	TT	CC	CT	TT	GG	GT	TT	CC	CT	TT
EFV group	692.6 (486.8-888.0)	402.4 (223.1-1027.7)	200.6	692.6 (501.1-706.6)	486.8 (347.1-775.3)	-	486.8 (359.7-706.6)	585.2 (223.1-1405.4)	-	486.8 (347.1-775.3)	463.0 (419.8-1027.7)	585.2
NVP group	1310.8 (1070.0-2530.1)	1449.5 (1053.4-1837.0)	-	1097.9 (814.90-2157.0)	1449.5 (1070.0-1836.9)	1267.2	1449.5 (1267.2-1836.9)	1097.9 (1070.0-1543.1)	-	1436.4 (1054.4-1877.4)	1310.8 (1303.2-818.5)	1466.5(776.0-2157.0)
LNG T_{max} (wk)												
EFV group	1.0 (1.0-1.0)	1.00 (1.0-1.0)	4.0	1.0 (1.0-1.0)	1.0 (1.0-12.0)	-	1.0 (1.0-4.0)	1.0 (1.0-36.0)	-	1.0 (1.0-12.0)	1.0 (1.0-1.0)	1.0
NVP group	1.0 (1.0-1.0)	1.0 (1.0-12.0)	-	1.0 (1.0-1.0)	1.0 (1.0-1.0)	1.0	1.0 (1.0-1.0)	1.0 (1.0-1.0)	-	1.0 (1.0-1.0)	1.0 (1.0-1.0)	6.5 (1.0-12.0)
LNG C_{min} (pg/mL)												
EFV group	272.2 (189.5-377.9)	202.2 (175.9-359.7)	121.8	299.0 (273.0-307.3)	208.1 (188.2-274.2)	-	224.7 (188.2-307.3)	202.2 (189.5-1405.4)	-	223.1 (188.2-359.7)	202.2 (189.1-299.0)	189.5
NVP group	553.7 (365.2-1094.1)	562.6 (504.4-807.7)	-	504.4 (343.7-714.0)	562.38 (512.46-986.40)	526.4	562.4 (504.4-807.7)	725.0 (540.2-986.4)	-	540.2 (501.0-957.0)	562.6 (562.4-986.4)	599.3 (512.5-686.2)
LNG $AUC_{0\text{-}24weeks}$ (pg*wk/mL)												
EFV group	10114.6 (8069.3-12862.2)	6311.8 (6569.7-14937.7)	3622.1	10114.6 (8500.0-12798.8)	7754.4 (5676.9-9435.6)	-	7754.4 (6311.8-11399.6)	8069.3 (4321.3-11070.0)	-	6830.6 (5677.0-11340.0)	7754.4 (7371.6-10114.6)	8069.3
NVP group	19970.2 (15259.3-30339.9)	15965.4 (15729.6-26301.1)	-	15761.9 (11338.7-22478.4)	20167.2 (15729.6-27442.0)	19970.2	19970.2 (15761.9-26301.1)	16948.7 (15258.3-21199.9)	-	16948.7 (15730.0-26301.1)	16759.1 (15258.3-27442.0)	19189.4 (15900.4-22478.4)
EFV $C_{12\text{-}14h}$ (mg/L)	2.1 (1.4-2.6)	2.6 (2.1-6.9)	8.7	2.4 (2.2-2.6)	2.4 (1.8-5.1)	-	2.4 (1.8-3.0)	2.4 (2.0-6.6)	-	2.6 (2.1-6.6)	2.2 (2.0-2.4)	1.62
NVP $C_{11\text{-}13h}$ (mg/L)	6.5 (4.4-7.4)	6.2 (5.1-10.0)	-	6.8 (5.9-8.3)	6.1 (5.0-8.3)	8.0	6.1 (5.1-8.4)	6.6 (5.5-7.1)	-	6.8 (4.8-8.4)	6.2 (5.5-6.9)	7.1 (5.9-8.3)

EFV $C_{12\text{-}14h}$ (mg/L) and NVP $C_{11\text{-}13h}$ (mg/L) determined from individual participants geometric mean value calculated from concentration measured at study entry, week 1, 4, 12, 24, 36 and 48 and summarised for the group as median (IQR). LNG: levonorgestrel. EFV: efavirenz. NVP: nevirapine

6.3.3 *Efavirenz group*

6.3.3.1 Non-significant associations

No associations between *CYP2B6* 516G>T (rs3745274) and LNG T_{max} and log_{10} LNG C_{min} were observed within this study. *CYP2B6* 983T>C (rs28399499) was not associated with log_{10} LNG C_{max} and log_{10} LNG $AUC_{0\text{-}24weeks}$. *CYP2B6* 15582C>T (rs4803419) was not associated with LNG T_{max}, log_{10} LNG C_{min} or log_{10} LNG C_{max}. *CYP2A6*9B* 1836G>T (rs8192726) and *NR1I3* 1089T>C (rs3003596) were only associated with LNG T_{max} and log_{10} LNG C_{min} respectively. No associations were seen between *CYP2A6* 48A>C (rs28399433), *NR1I2* 63396C>T (rs2472677), *NR1I3* 540C>T (rs2307424) and any pharmacokinetic parameters of LNG. No relationship was seen between age and log_{10} LNG C_{max}, LNG T_{max} and log_{10} LNG C_{min}. Weight, log_{10} sex hormone-binding globulin (SHBG) and albumin concentration at baseline were not associated with any LNG pharmacokinetic parameters. log_{10} CD4 was only associated with log_{10} LNG $AUC_{0\text{-}24weeks}$. Figure 6.1 shows all non-significant interactions between SNPs and LNG pharmacokinetic parameters.

6.3.3.2 Relationships observed from univariate analysis

Through univariate regression analysis a trend between *CYP2B6* 983T>C (rs28399499) and higher log_{10} LNG C_{min} and T_{max} (P = 0.114, β = 0.2; P = 0.069, β = 17.7; respectively) was observed. *NR1I3* 1089T>C (rs3003596) was seen to be linked with higher log_{10} LNG C_{min} (P = 0.143, β = 0.1). A trend was seen between *CYP2A6*9B* 1836G>T (rs8192726) and lower T_{max} (P = 0.195, β = 11.5). Age was linked with lower log_{10} LNG C_{max} (P = 0.049, β = 0.0), and a relationship between log_{10} CD4 and higher log_{10} LNG $AUC_{0\text{-}24weeks}$ (P = 0.085, β = 0.5) was seen. However, these associations did not persist through multivariate regression analysis. Figure 6.2 shows all factors linked with LNG pharmacokinetic parameters and genetics found through univariate linear regression analysis only.

Consistent with previous reports, through univariate linear regression analysis, *CYP2B6* 516G>T was linked with higher EFV concentration (P = 0.011, β = 0.3), meaning that $C_{12\text{-}14h}$ values were 2.1, 2.6 and 8.7 mg/L in GG, GT and TT genotype groups, respectively (76% difference between homozygote groups). Additionally, a correlation was seen between higher EFV $C_{12\text{-}14h}$ ($\log_{10}$ mg/L) and lower LNG $\log_{10}$ $AUC_{0\text{-}24week}$ (P = 0.003, β = 0.0).

6.3.3.3 Significant associations from multivariate analysis

After multivariate analysis, *CYP2B6* 516G>T (rs3745274) was associated with lower $\log_{10}$ LNG C_{max} (P = 0.021, β = -0.2) and $\log_{10}$ LNG $AUC_{0\text{-}24weeks}$ (P = 0.023, β = -0.1). This meant that LNG C_{max} median values were 692.8, 402.4 and 200.6 pg/mL in the GG, GT and TT genotype groups, respectively (71% difference between homozygote groups) and LNG $AUC_{0\text{-}24weeks}$ median values were 10114.6, 6311.8 and 3622.1 pg*wk/mL in the GG, GT and TT genotype groups, respectively (64% difference between homozygote groups). *CYP2B6* 15582C>T (rs4803419) was associated with lower $\log_{10}$ LNG $AUC_{0\text{-}24weeks}$ (P = 0.021, β = -0.2), resulting in LNG $AUC_{0\text{-}24weeks}$ median values of 10114.6 and 7754.4 pg*wk/mL in the CC and CT genotype groups, respectively (23% difference between groups). Figure 6.3 illustrates the LNG $AUC_{0\text{-}24weeks}$ within the EFV group according to these genotypes. In addition to these genetic associations, age was inversely associated with $\log_{10}$ LNG $AUC_{0\text{-}24weeks}$ (P = 0.039, β = 0.0 per 1 year; Table 6.3).

6.3.3.4 Levonorgestrel pharmacokinetics by metaboliser status

Additional assessment of LNG pharmacokinetic parameters with *CYP2B6* SNPs was completed through assignment of a *CYP2B6* metaboliser status. In our patient population, the following genotypes were absent: intermediate metaboliser: 15582 TT, 516 GG, 983 TT and 15582 CC, 516 GG, 983 CT. No patients met the criteria to be assigned as a slow

metaboliser. Statistical analysis through multiple linear regression linked *CYP2B6* extensive metaboliser status with greater $\log_{10}$ LNG $AUC_{0\text{-}24\ weeks}$ (P = 0.002, β = 0.7) and higher $\log_{10}$ LNG C_{max} (P = 0.049, β = 0.483). Figure 6.4 shows EFV plasma and serum LNG concentration separated by CYP2B6 metaboliser status.

6.3.3.5 Pharmacodynamic outcome in the EFV group

Three women in the EFV group became pregnant between study weeks 36 and 48 (3 (15%) of 20 participants). Pharmacogenetic characteristics of these three patients were as follows for the statistically significant genotypes within the EFV group: One woman was both homozygous TT for *CYP2B6* 516G>T (rs3745274) and heterozygous CT for *CYP2B6* 15582C>T (rs4803419). She was the only patient who possessed both of these genotypes in the study group, and her LNG concentration at the study visit prior to pregnancy (week 36) was 122 pg/mL (LNG $AUC_{0\text{-}24weeks}$ 3622 pg*wk/mL). The other two women were heterozygous CT for *CYP2B6* 516G>T and homozygous CC for *CYP2B6* 1582C>T. They were the only patients in the EFV group who possessed these genotypes, and their LNG concentration prior to pregnancy (week 36) were 299 and 303 pg/mL (LNG $AUC_{0\text{-}24weeks}$ 10,115 and 8500 pg*wk/mL), respectively. Figure 6.5 shows the relationship between EFV plasma concentration and serum LNG concentration based on *CYP2B6* 516G>T (rs3745274) and *CYP2B6* 15582C>T (rs4803419) genotype.

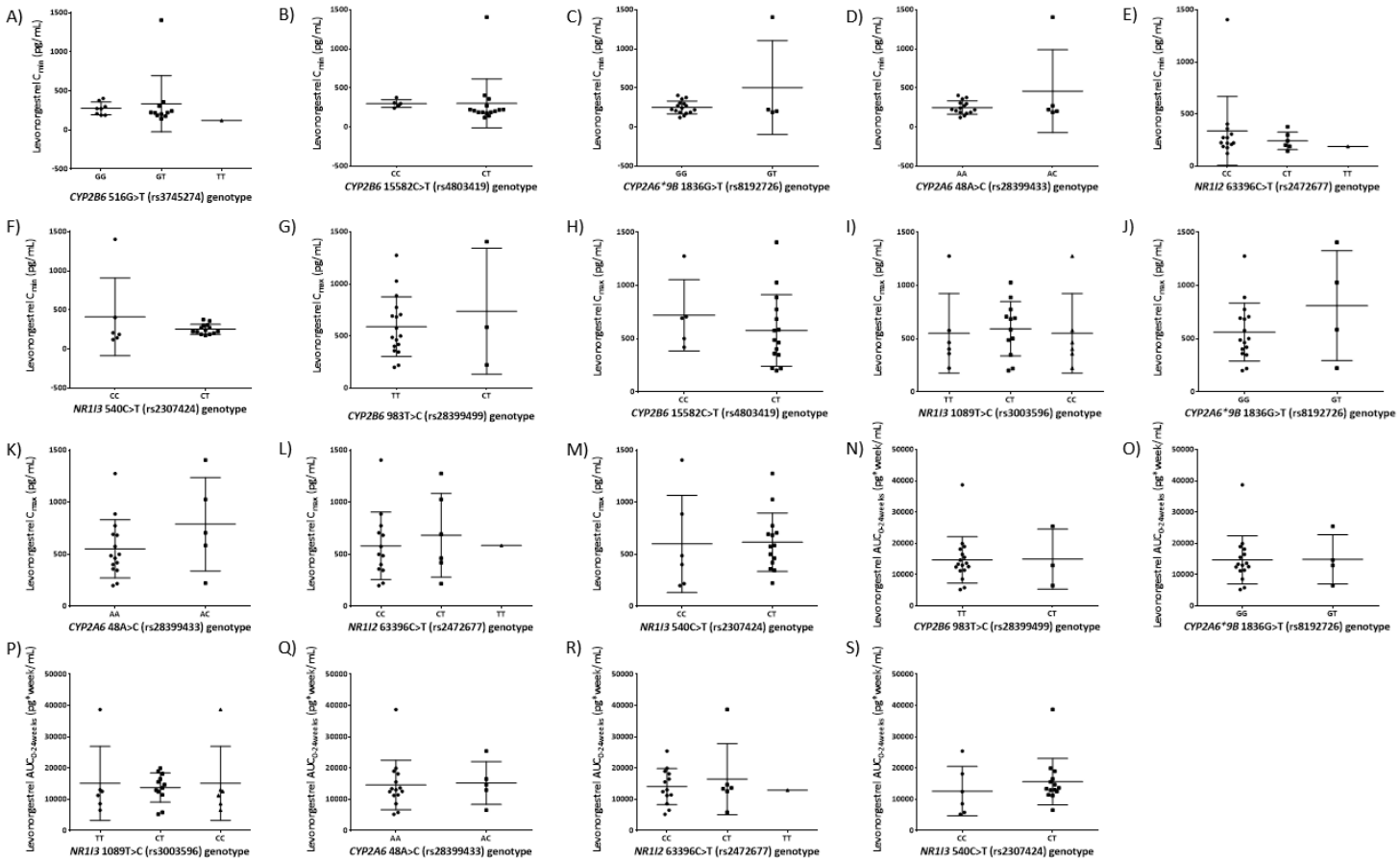

Figure 6.1: Non-significant associations for SNPs within the EFV group.

Graphs A-F: Non-significant relationships between SNPs and LNG C_{min}. Graphs G-M: Non-significant relationships between SNPs and LNG C_{max}. Graphs N-S: Non-significant relationships between SNPs and LNG $AUC_{0\text{-}24\ weeks}$. Data points represent the mean ± SD

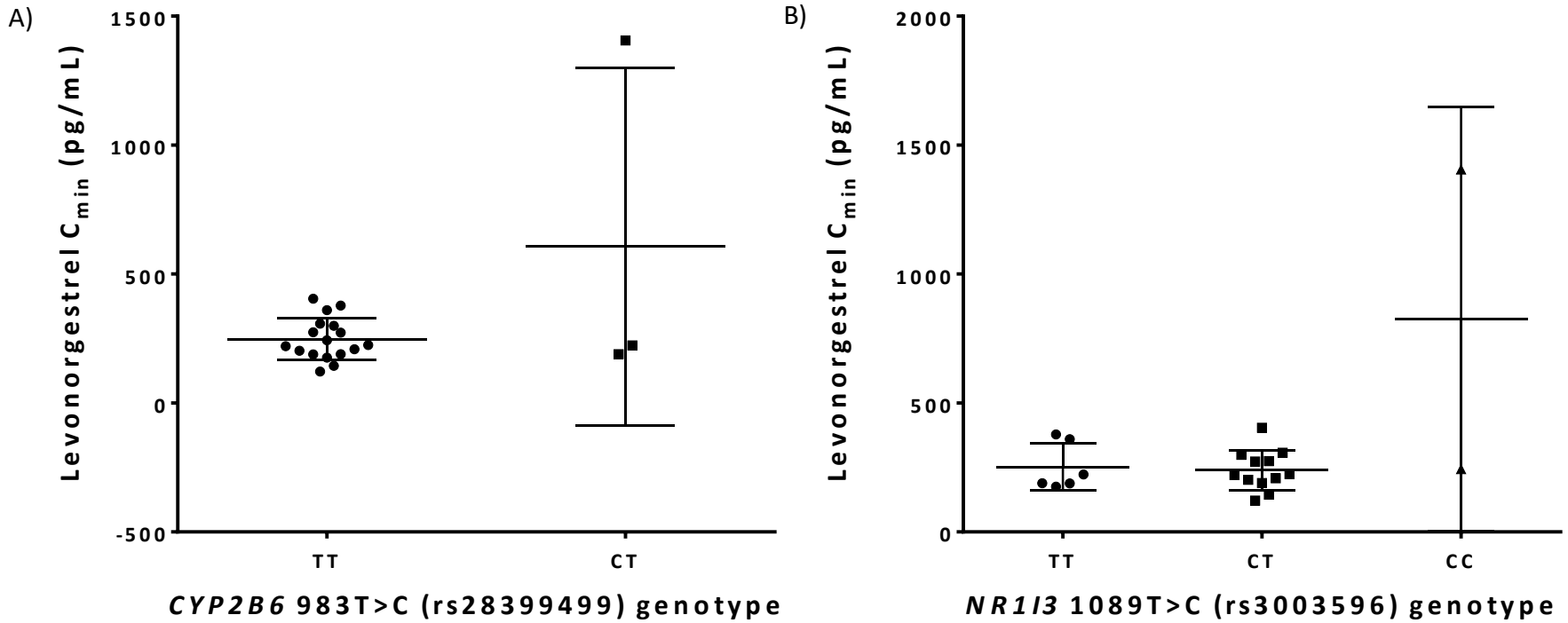

Figure 6.2: Relationships between levonorgestrel pharmacokinetic parameters and patient genotypes, within the EFV group, determined through univariate analysis.

Graphs A and B: Relationship between SNPs and LNG C_{min}. All relationships found to be significant ($P \leq 0.2$) through univariate regression analysis only. Data points represent the mean ± SD

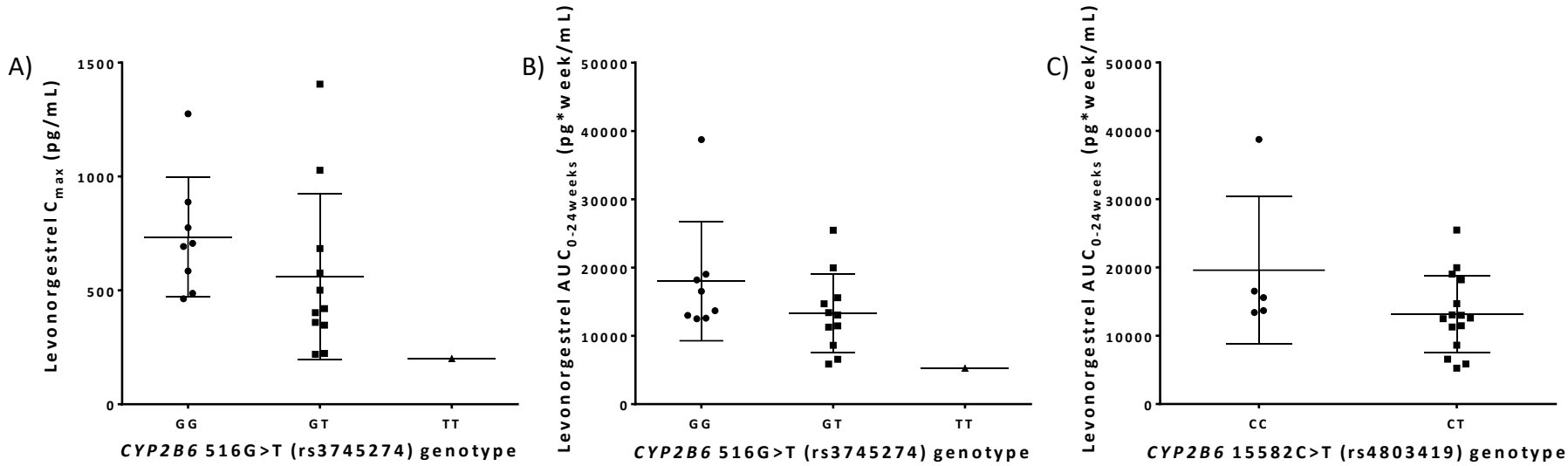

Figure 6.3: Levonorgestrel pharmacokinetic parameters compared by statistically significant genotype, within the EFV group, determined through multivariate analysis.

Graph A: Significant relationship between SNP and LNG C_{max}. Graphs B and C: Significant relationships between SNPs and LNG $AUC_{0\text{-}24\ weeks}$. All relationships found to be statistically significant ($P \leq 0.05$) through multivariate regression analysis. Data points represent the mean ± SD

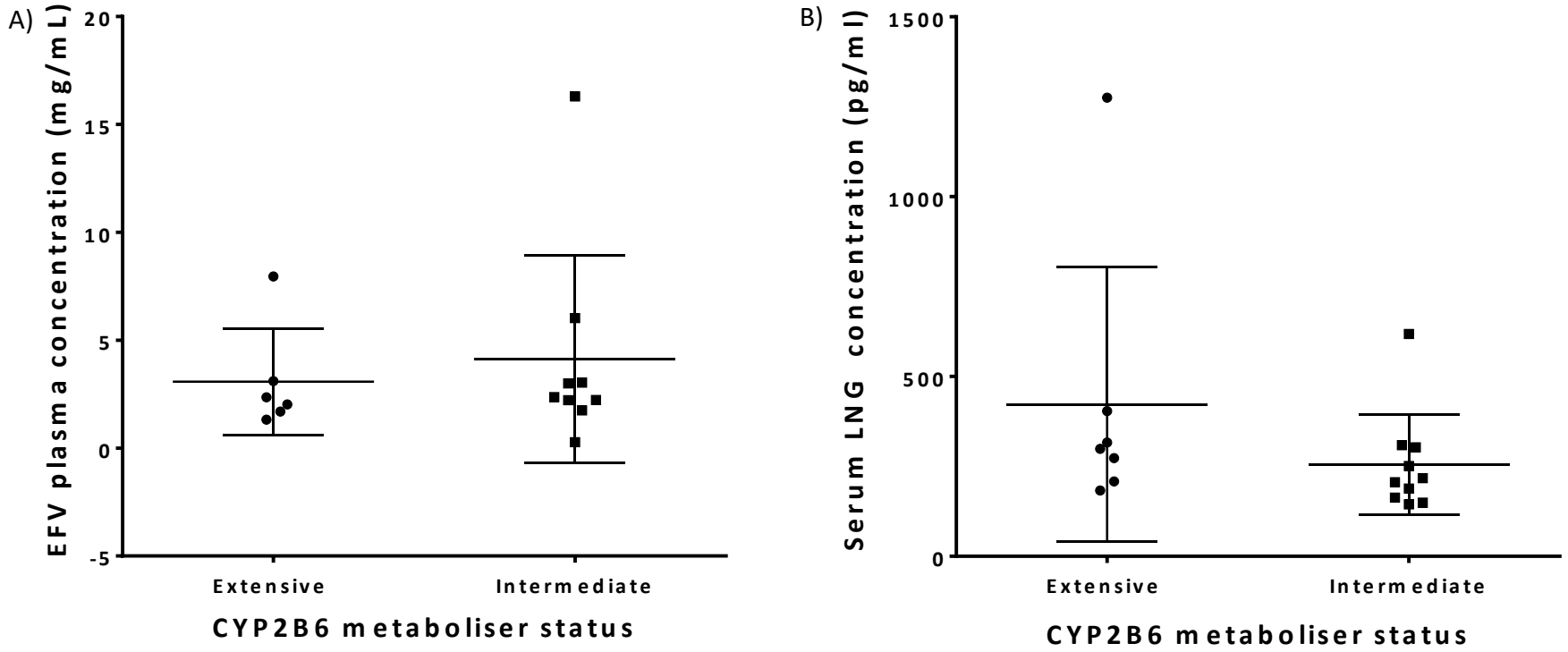

Figure 6.4: Efavirenz and levonorgestrel concentration at week 24 based on CYP2B6 metaboliser status.

Graph A: Relationship between CYP2B6 metaboliser status and EFV plasma concentration at week 24 of study. Graph B: Relationship between CYP2B6 metaboliser status and LNG serum concentration at week 24 of study. Data points represent the mean ± SD

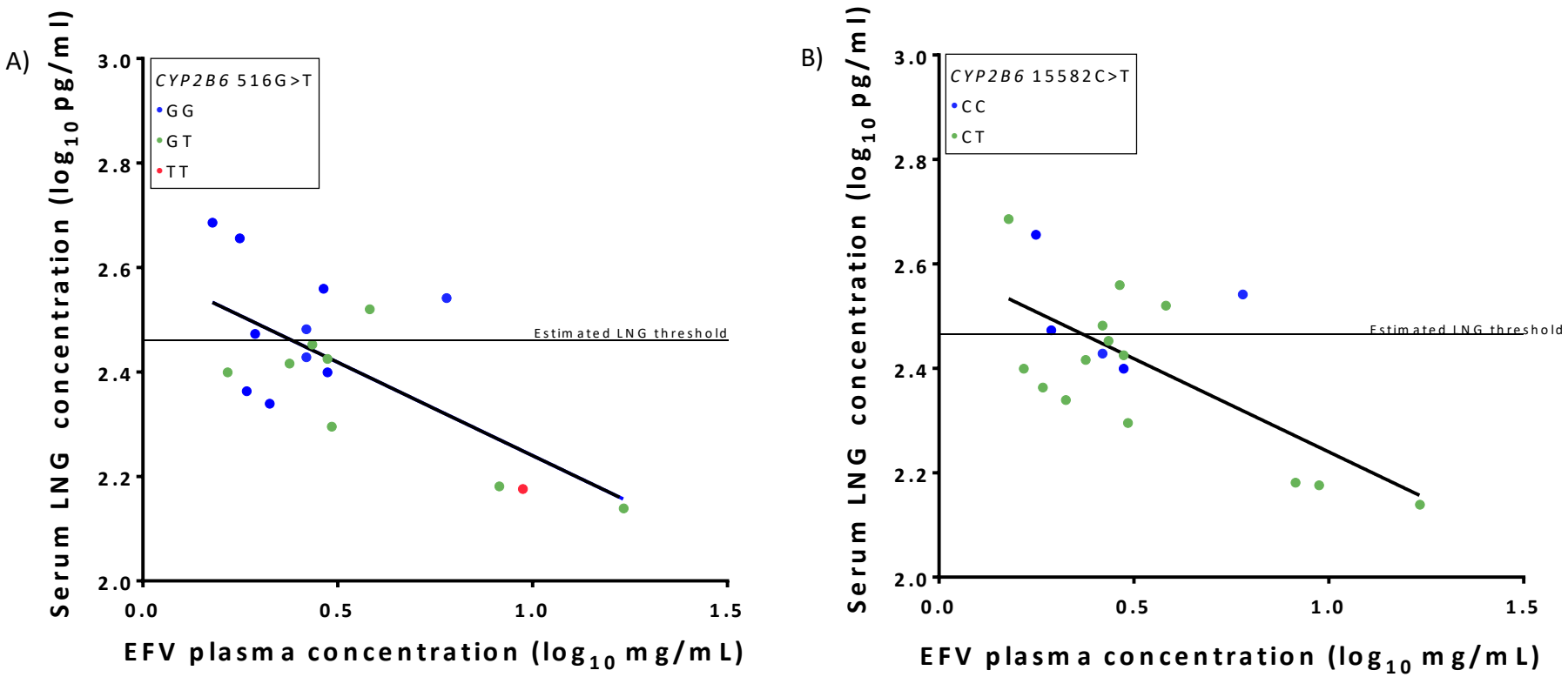

Figure 6.5: Relationship between efavirenz and levonorgestrel concentrations at week 24 based on *CYP2B6* 516G>T and *CYP2B6* 15582C>T genotype.

Graph A: Relationship between plasma EFV and serum LNG concentration at week 24 of study colour coded by *CYP2B6* 516G>T genotype. Graph B: Relationship between plasma EFV and serum LNG concentration at week 24 of study colour coded by *CYP2B6* 15582C>T genotype.

6.3.4 *Nevirapine group*

6.3.4.1 Non-significant associations

Through univariate and multivariate linear regression analysis *CYP2B6* 516G>T (rs3745274) was not associated with LNG T_{max}. *NR1I2* 63396C>T (rs2472677) was not associated with log_{10} LNG C_{max}, log_{10} LNG C_{min} or log_{10} LNG $AUC_{0\text{-}24weeks}$. No associations were observed between *CYP2B6* 983T>C (rs28399499), *CYP2B6* 15582C>T (rs4803419), *CYP2A6*9B* 1836G>T (rs8192726), *CYP2A6* 48A>C (rs28399433), *NR1I3* 540C>T (rs2307424) or *NR1I3* 1089T>C (rs3003596) and any parameters of LNG pharmacokinetics. Figure 6.6 shows all non-significant associations between SNPs and pharmacokinetics of LNG within the NVP group.

Age was not associated with log_{10} LNG C_{min} or log_{10} LNG $AUC_{0\text{-}24weeks}$. Log_{10} weight was not associated with log_{10} LNG C_{max} or log_{10} LNG $AUC_{0\text{-}24weeks}$. SHBG was not associated with LNG T_{max}. Log_{10} CD4 count and albumin concentration at baseline were not associated with any parameters of LNG pharmacokinetics.

6.3.4.2 Trends observed from univariate analysis

A trend was observed between *CYP2B6* 516G>T (rs3745274) and higher log_{10} LNG $AUC_{0\text{-}24weeks}$ through univariate linear regression analysis (P = 0.179, β = 0.1) within the NVP group. Age was correlated with lower LNG T_{max} (P = 0.043, β = -0.3). Log_{10} weight was linked with lower log_{10} LNG C_{min} (P = 0.168, β = -0.8). Log_{10} CD4 count was linked with lower LNG T_{max} (P = 0.157, β = -3.5) and log_{10} LNG $AUC_{0\text{-}24weeks}$ (P = 0.034, β = -0.3). Albumin concentration at baseline was linked with log_{10} LNG C_{max} (P = 0.076, β = 0.0). However, these relationships were not significant when carried through to multivariate linear regression analysis. Figure 6.7 shows the relationship between *CYP2B6* 516G>T (rs3745274) genotype and LNG AUC found to be associated through univariate regression analysis only.

6.3.4.3 Significant associations from multivariate analysis

As shown in Figure 6.8, *CYP2B6* 516G>T (rs3745274) was associated with higher log_{10} LNG C_{max} (*P* = 0.034, β = 0.1) and log_{10} LNG C_{min} (*P* = 0.048, β = 0.1). Resulting in LNG C_{max} median values of 1310.8 and 1449.5 pg/mL in the GG and GT genotype groups, respectively (10% difference between homozygote groups) and LNG C_{min} median values of 553.7 and 562.6 pg/mL in the GG and GT genotype groups (2% difference between groups). *NR1I2* 63396C>T was associated with delayed LNG T_{max} (*P* = 0.003, β = 1.6) with a median value of 1.0, 1.0 and 6.5 weeks in the CC, CT and TT genotype groups. Additionally, log_{10} weight (*P* = 0.002, β = -15.9) and albumin concentration at baseline (*P* = 0.003, β = -0.3) were associated with shorter LNG T_{max}. Log_{10} SHBG was associated with higher log_{10} LNG $AUC_{0\text{-}24weeks}$ (*P* = 0.004, β = 0.5), log_{10} LNG C_{min} (*P* = 0.011, β = 0.5) and log_{10} LNG C_{max} (*P* = 0.007, β = 0.5). Age was associated with higher log_{10} LNG C_{max} (*P* = 0.044, β = 0.0) (Table 6.3).

No other genetic associations were observed in any of the groups; however, the sample size was insufficient to robustly assess the *CYP2B6* 983T>C variant (rs28399499).

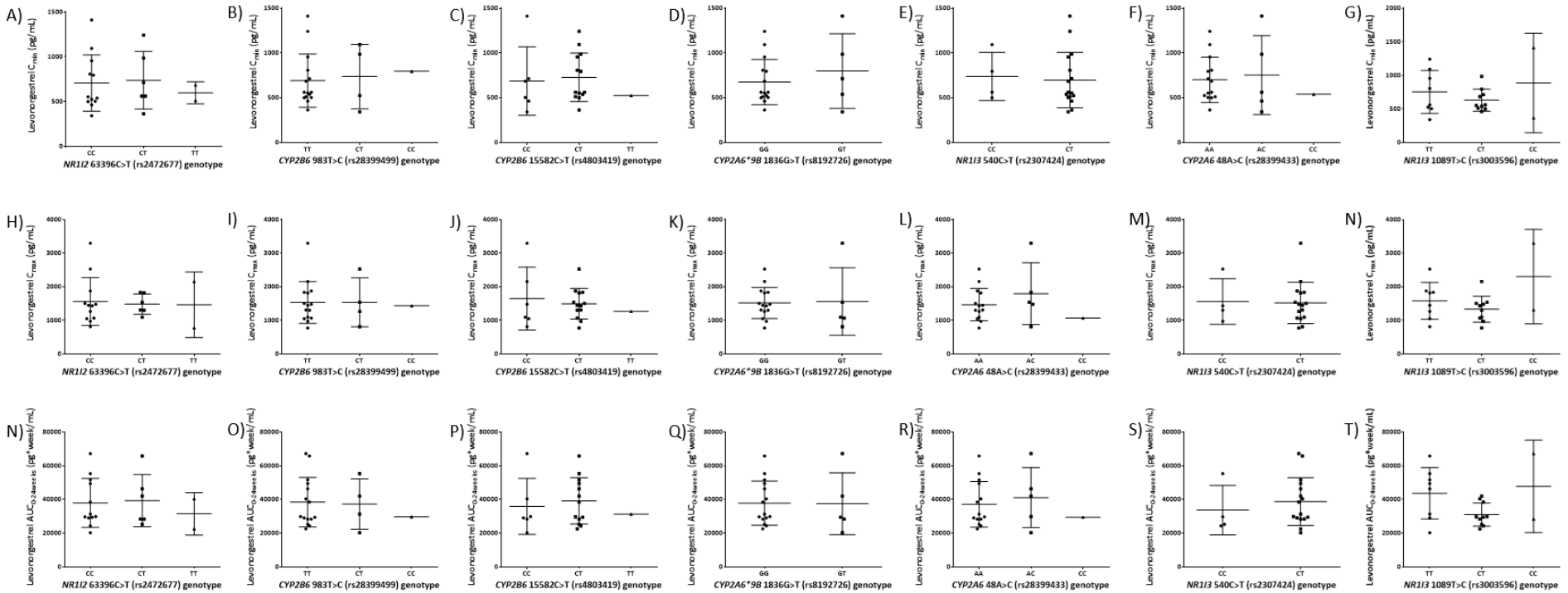

Figure 6.6: Non-significant associations for SNPs within the NVP group.

Graphs A-G: Non-significant relationships between SNPs and LNG C_{min}. Graphs H-M: Non-significant relationships between SNPs and LNG C_{max}. Graphs N-T: Non-significant relationships between SNPs and LNG $AUC_{0\text{-}24\ weeks}$. Data points represent the mean ± SD

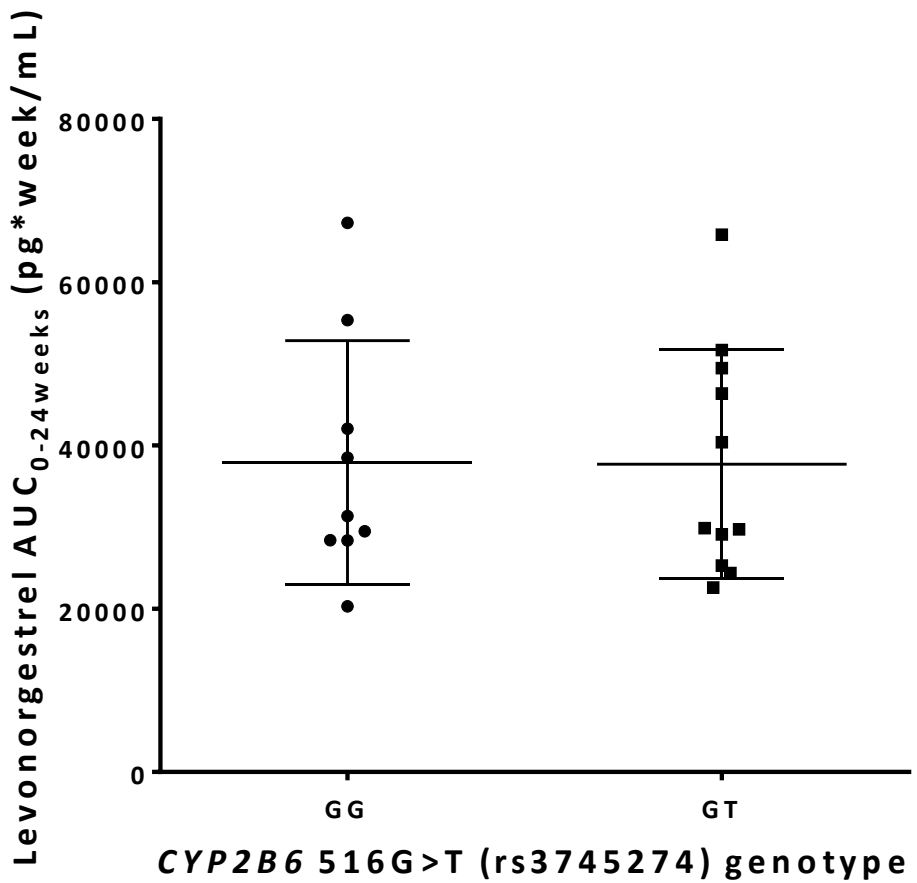

Figure 6.7: Relationship between *CYP2B6* 516G>T and levonorgestrel $AUC_{0\text{-}24weeks,}$ within the nevirapine group, determined through univariate analysis.

Relationship found to be significant ($P \leq 0.2$) through univariate regression analysis only. Data points represent the mean ± SD

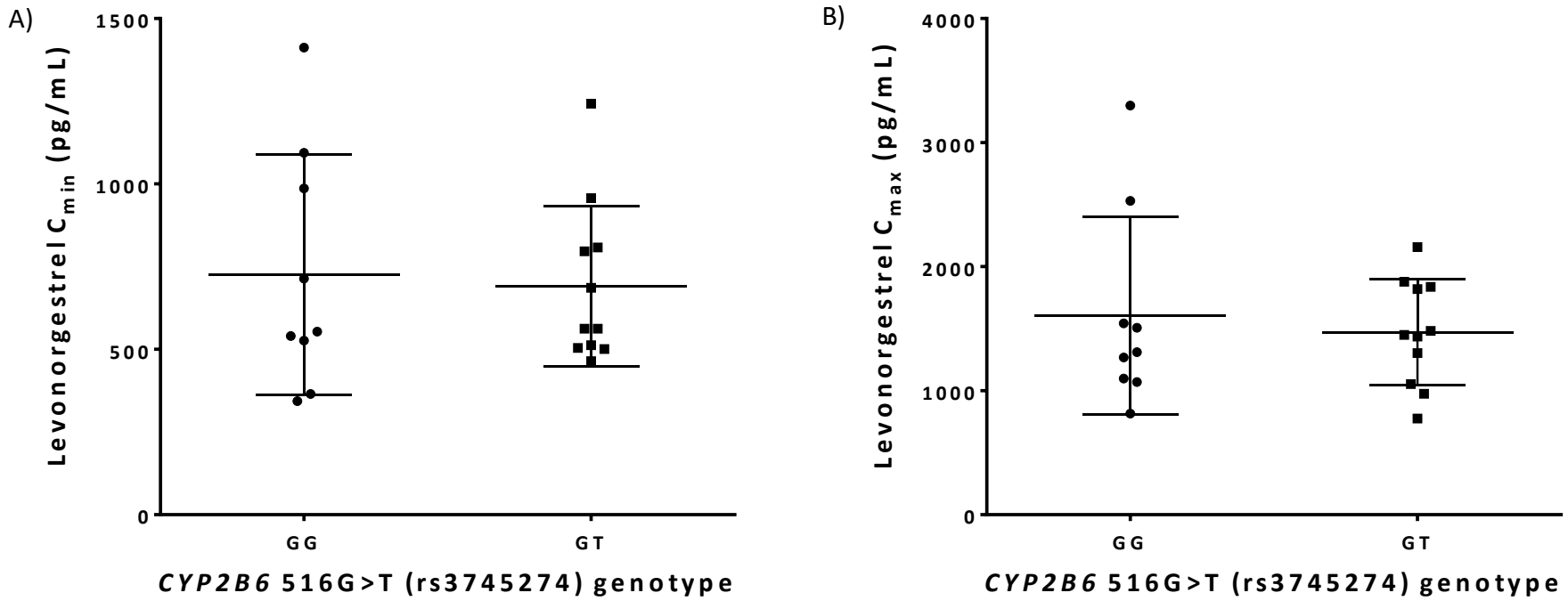

Figure 6.8: Levonorgestrel pharmacokinetic parameters compared by statistically significant genotype, within the nevirapine group, determined through multivariate analysis.

Graph A: Significant relationship between *CYP2B6* 516G>T and LNG C_{min}. Graph B: Significant relationship between *CYP2B6* 516G>T and LNG C_{max}. All relationships found to be statistically significant ($P \leq 0.05$) through multivariate regression analysis. Data points represent the mean ± SD

Table 6.3: Univariate and multivariate linear regression analysis from each study group.

Efavirenz group						
$\log_{10} C_{max}$	Univariate linear regression			Multivariate linear regression		
	P value	β value (95% CI)	r^2	*P* value	β value (95% CI)	r^2
Age (years)	0.049	-0.3 (-0.01,0.0)	0.2			
***CYP2B6* 516G>T (rs3745274)**	0.021	-0.2 (-0.4,0.0)	0.3	**0.021**	**-0.2 (-0.4,0.0)**	**0.3**
$\log_{10} AUC_{0\text{-}24\ weeks}$	Univariate linear regression			Multivariate linear regression		
	P value	β (pg/mL) (95% CI)	r^2	*P* value	β (pg/mL) (95% CI)	r^2
Age (years)	0.028	-0.0 (0.0,0.0)	0.2	**0.039**	**-0.0 (-0.0,0.0)**	**0.8**
CD4 ($\log_{10}$ cells/mm^3)	0.085	0.5 (-0.1,1.1)	0.2			
***CYP2B6* 516G>T (rs3745274)**	<0.000	-0.2 (-0.3,-0.1)	**0.5**	**0.023**	**-0.1 (-0.2,0.0)**	**0.8**
***CYP2B6* 15582C>T (rs4803419)**	0.058	-0.2 (-0.3,0.0)	**0.2**	**0.021**	**-0.2 (-0.3,0.0)**	**0.8**
Nevirapine Group						
$\log_{10} C_{max}$	Univariate linear regression			Multivariate linear regression		
	P value	β value (95% CI)	r^2	*P* value	β value (95% CI)	r^2
Age (years)	0.056	0.0 (0.0,0.0)	0.2	**0.044**	**0.0 (0.0,0.3)**	**0.6**
Albumin concentration at baseline (g/L)	0.076	0.0 (0.0,0.0)	0.2			
SHBG at baseline ($\log_{10}$ pg/mL)	0.017	0.5 (0.1,0.9)	0.3	**0.007**	**0.5 (0.0,0.8)**	**0.6**
***CYP2B6* 516G>T (rs3745274)**	0.115	0.1 (0.0,0.2)	0.1	**0.034**	**0.1 (0.0,0.2)**	**0.6**
T_{max}	Univariate linear regression			Multivariate linear regression		
	P value	β value (95% CI)	r^2	*P* value	β value (95% CI)	r^2
Age (years)	0.043	-0.3 (-0.5,0.0)	0.2			
Weight ($\log_{10}$ kg)	0.029	-17.0 (-31.9,-0.2)	0.2	**0.002**	**-15.9 (-24.9,-6.9)**	**0.8**
CD4 ($\log_{10}$ cells/mm^3)	0.157	-3.5 (-8.5,1.5)	0.1			
Albumin concentration at baseline (g/L)	0.001	-0.5 (-0.8,0.2)	0.4	**0.003**	**-0.3 (-0.5,-0.1)**	**0.8**
***NR1I2* 63396C>T (rs2472677)**	0.013	2.0 (0.5,3.5)	0.3	**0.003**	**1.6 (0.6,2.6)**	**0.8**
$\log_{10} C_{min}$	Univariate linear regression			Multivariate linear regression		

	P value	β value (95% CI)	r^2	*P* value	β value (95% CI)	r^2
Weight (log_{10} kg)	0.168	-0.8 (-1.8,0.3)	0.1			
SHBG at baseline (log_{10} nmol/L)	0.022	0.5 (0.1,0.9)	0.3	**0.011**	**0.5 (0.1,0.9)**	**0.6**
***CYP2B6* 516G>T (rs3745274)**	0.118	0.1 (0.0,0.2)	0.1	**0.048**	**0.1 (0.0,0.2)**	**0.6**
$\underline{log_{10} AUC_{0\text{-}24\ weeks}}$	Univariate linear regression			Multivariate linear regression		
	P value	β value (95% CI)	r^2	*P* value	β value (95% CI)	r^2
CD4 (log_{10} cells/mm^3)	0.034	-0.3 (-0.5,0.0)	0.2			
SHBG at baseline (log_{10} pg/mL)	0.008	0.5 (0.1,0.8)	0.3	**0.004**	**0.5 (0.2,0.8)**	**0.5**
CYP2B6 516G>T (rs3745274)	0.179	0.1 (0.0,0.0)	0.1			

Univariate linear regression analysis ($P \leq 0.2$) was completed, all statistically significant results where then carried through to multivariate linear regression analysis ($P \leq 0.05$). All statistically significant variables from multivariate linear regression shown in bold type.

β is the regression coefficient and represents incremental change in the log_{10} LNG pharmacokinetic parameter per unit change in a patient characteristic (e.g. per kg body weight or per allele carried). Therefore, if β = 0.5 an increase per unit in the patient characteristic results in the log_{10} LNG pharmacokinetic parameter increasing by a factor of 0.5.

6.4 DISCUSSION

The impact of this investigation is greatest for women receiving a combination of EFV based ART with an LNG subdermal implant. Women receiving this drug combination are at risk for suboptimal LNG exposure, which results in a higher rate of contraceptive failures (Patel 2015, Scarsi 2016). For women who are heterozygous or homozygous for *CYP2B6* 516G>T or *CYP2B6* 15582C>T, which were associated with lower LNG AUC when combined with EFV, this drug-drug interaction will be more pronounced. This was evidenced by the three patients who became pregnant in the EFV group, who all possessed at least one of these genotypes. Importantly, the patient who possessed both these genotypes had the lowest LNG exposure of any study participant. Nine additional women in the EFV group were heterozygous for either *CYP2B6* 516G>T or *CYP2B6* 15582C>T and had LNG exposure (median LNG $AUC_{0\text{-}24weeks}$ 6831 pg*wk/mL), consistent with those women who became pregnant, indicating that they were also at risk for contraceptive failure. We hypothesise that high EFV plasma concentrations associated with these SNPs may result in greater EFV induction of *CYP3A4*, resulting in increased LNG metabolism and lower LNG exposure in the patients who were heterozygous or homozygous for *CYP2B6* 516G>T or *CYP2B6* 15582C>T. Further contributing to this effect may be the modest inhibitory effect of LNG on *CYP2B6* (Palovaara 2003, Walsky 2006). It is possible that LNG may inhibit CYP2B6 activity, resulting in high EFV concentrations and further inhibition of CYP3A4.

Within the NVP group, the significant association between *CYP2B6* 516G>T and higher LNG $\log_{10} C_{max}$ and LNG $\log_{10} C_{min}$ was surprising, given that NVP is an inducer of CYP3A4, the enzyme believed to be primarily responsible for LNG metabolism. In a previous study of three HIV-positive Malawian women receiving 30 µg ethinyl estradiol/300 µg norgestrel (a racemic mixture of LNG and dextronorgestrel) and NVP based ART, higher LNG exposure was also

observed compared to HIV uninfected women (Stuart 2011). Notably, two of the three women were heterozygous for *CYP2B6* 516G>T. Furthermore, *CYP2B6* 516G>T has been associated with elevated NVP concentrations in previous studies (Rotger 2005, Penzak 2007). Therefore, the association between *CYP2B6* 516G>T and LNG pharmacokinetic parameters could be attributed to NVP-mediated inhibition of LNG metabolism by CYP3A4, or potential inhibition of CYP3A5. However, this result must be interpreted with caution, given that overall exposure (as measured by AUC) was not associated with the same SNP. Further investigation is required to determine the mechanism underpinning this finding.

We observed an association between *NR1I2* 63396C>T (rs2472677) and delayed LNG T_{max} in patients receiving NVP, which has the potential to result in suboptimal LNG concentrations. Previously, *NR1I2* 63396C>T (in linkage disequilibrium with *NR1I2* 63704G>A, 63813(CAAA)n/(CA)n, and *NR1I2* 65104T>C) has been associated with higher *NR1I2* expression, elevated *CYP3A4* expression, and unboosted ATV plasma concentrations (Lamba 2008, Siccardi 2008, Schipani 2010). *NR1I2* 63396C>T may be directly or indirectly associated with inducibility of CYP3A4 and hence reduced LNG metabolism. This is supported by observations in primary human hepatocytes where the 63396 T allele was associated with higher basal activity but lower rifampicin-mediated inducibility of CYP3A4 (Lamba 2008).

LNG pharmacokinetics demonstrate high inter-individual variability, often attributed to variations in protein binding (Coukell 1998) and bodyweight (Sivin 1997, Sivin 1997, Sivin 2001). Although we did not observe a consistent association with weight and LNG pharmacokinetics, this may be related to the lower median body weight of HIV-infected Ugandan women compared to those in other studied populations. LNG is highly protein-bound to SHBG and albumin (Coukell 1998). Elevated $\log_{10}$ SHBG concentration has previously been associated with higher serum LNG concentration (Abdalla 1992). However,

the observed association of $\log_{10}$ SHBG concentration at baseline with higher LNG $\log_{10} C_{max}$, LNG $\log_{10} C_{min}$ and LNG $\log_{10} AUC_{0\text{-}24weeks}$, and of albumin concentration at baseline with lower T_{max} within the NVP group, may reflect some influence of baseline protein binding on overall LNG exposure.

The study demonstrates pharmacogenetic associations with LNG pharmacokinetics when administered as a LNG subdermal implant in HIV positive women receiving EFV or NVP based ART. Despite the EFV interaction with LNG, effectiveness of the LNG subdermal implant may still be higher for oral contraception, due to improved medication adherence (Patel 2015, Shelton 2015). Notwithstanding, any increased risk of pregnancy when receiving contraception is important, given the impact that unintended pregnancy has for women living with HIV. Based upon our findings, screening for SNPs associated with low LNG exposure in patients receiving EFV represents a novel approach to identify women at the highest risk for an unintended pregnancy. Added pharmacogenetic knowledge would allow clinicians to personalise counseling of women on their choice of a contraceptive method based on individualised risks and benefits. Overall, this study highlights the potential role of affordable, accessible and clinically relevant pharmacogenetic screening in resource-constrained settings. Future studies with larger populations and a more diverse range of ethnicities, should focus upon prospective evaluation of the relationship between pharmacogenetics and the effectiveness of the LNG implant in the presence of EFV-related drug-drug interactions.

6.4.1 *Limitations*

A limitation of this study was the relatively small sample size, particularly related to *CYP2B6* 15582C>T (rs4803419) and *NR1I3* 540C>T (rs2307424), as both SNPs were not in Hardy-Weinberg equilibrium. An increase in sample size would be of use in light of the low number

of patients within the statistically significant patient populations. With some variant genotypes represented by a single outlier. Given that the frequency of the variant alleles for some of the SNPs included within this analysis are low within the general population, as discussed in Chapter 1 (Table 1.2), a greater study population size would enable us to determine if these associations persist outside of the original study group. Additionally, the consequences of the T_{max} associations are unclear, but should in any case be interpreted cautiously given the intermittent measurement of LNG pharmacokinetics during the study period.

Chapter 7: General Discussion

7.1 CONTEXT OF WORK

The work within this thesis sits within the context of a wider research environment. As outlined in Figure 7.1 the clinical trial process is divided into 4 phases. Pre-clinical studies are completed through a range of methodologies. These studies include, but are not limited to, toxicology studies utilising *in vitro* cell lines, determination of pharmacokinetic parameters through *in vivo* studies in non-human animal models and defining a starting dose via physiologically-based pharmacokinetic modelling. Phase I is designed to study the absorption, distribution, metabolism and excretion of the drug and assesses drug safety within a small cohort of healthy volunteers. Phase II focuses on drug efficacy, through comparing the novel drug to a standard treatment or placebo within a randomised trial. Phase III involves larger scale testing of the therapeutic agent with randomised blind trials involving thousands of patients. These studies provide more information about the adverse effects of the drug and its effectiveness in comparison to drugs already on the market. Phase IV occurs post regulatory approval and is an ongoing process. Pharmacogenetics studies including those described in Chapters 2, 3 and 6 fit within Phase IV post-marketing research. As does the *in vitro* cell line work completed in Chapters 4 and 5. Phase IV studies are essential to continuously assess the suitability of the recommended drug dosage, and the occurrence of adverse drug responses or drug-drug interactions that were not observed within the previous phases. They also allow for the mechanisms by which these events occurred to be investigated, and there are numerous examples of how clinical management has been optimised through such careful ongoing analysis.

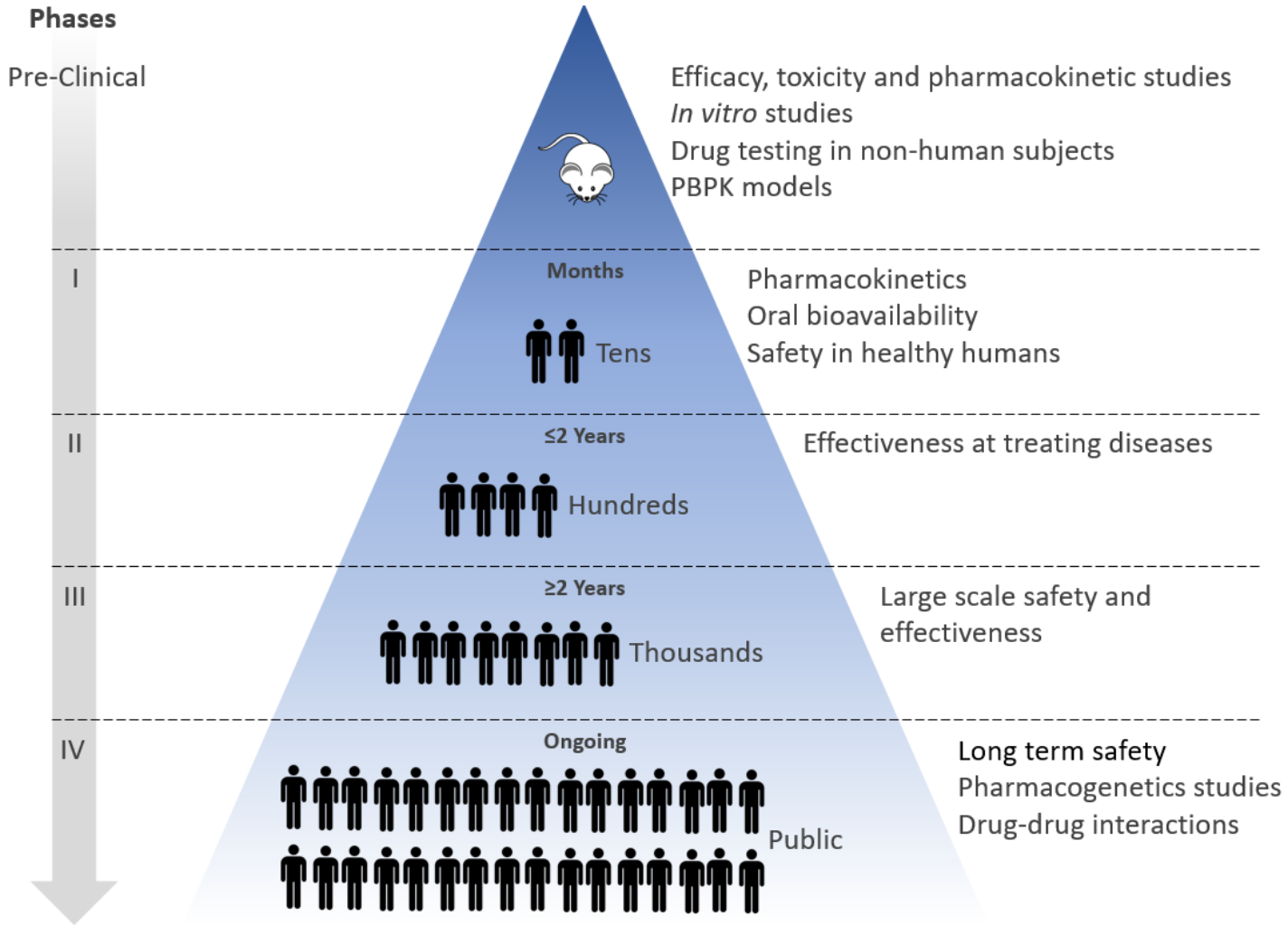

Figure 7.1: Clinical trial process from pre-clinical experimentation through to approval for general use.

7.2 EXPANDING USE OF ANTIRETROVIRALS

The interactions studied within Chapters 2, 3, 4 and 5 within this thesis are of particular relevance in light of the UNAIDS 90:90:90 target. This target has galvanised global initiatives to provide improved testing, access to sustained ART and achievement of viral suppression through innovative projects which target at risk populations (UNAIDS 2016). An example of this is The Global Fund initiative to reduce HIV incidence within adolescent girls and young women in high HIV burden settings, who represent a disproportionate number of new HIV cases (TheGlobalFund 2017). Current projections by UNAIDS indicate that the 90:90:90 target is achievable (UNAIDS 2016), however, a standardised monitoring and evaluation system is required in order to accurately evaluate the progress towards these targets (Granich 2017). More work is still needed to ensure all targets are reached and further ingenuity and investment is required. Nevertheless, progression towards 27 million additional people receiving treatment by 2020 (Williams 2017) will not only benefit patients in at risk groups, particularly in high HIV burden settings, but also enable a greater understanding of drug toxicity and drug-drug interactions within these previously understudied populations. It is important to consider the positive impact that greater access to ART will have on the study of pharmacogenetic interactions, providing a more diverse and larger pool of patients from which interactions can occur and be investigated.

As access to PrEP is increased, through drug assistance programs such as PEPFAR DREAMS or access via government run infrastructure such as in that seen in Brazil and Scotland, the incidence of drug-drug interactions and toxicity not previously observed in trials focusing solely on HIV positive participants are likely to increase. There is a need to consider the implications that PrEP use could have for a patients' pre-existing drug regimen, whether in

the form of a contraceptive or for the treatment of a comorbidity. This problem is demonstrated within Chapter 6, where the indirect effect of EFV on LNG pharmacokinetics resulted in LNG treatment failure. At the time of writing, no data is currently available from earlier implementer sites in the UK that discusses the number of incidents of drug-drug interactions that led to discontinuation of PrEP. The release of this data would provide an invaluable foundation from which to base guidance on PrEP prescription in patients with pre-existing clinical needs.

7.3 PHARMACOGENETICS CLINICAL IMPLEMENTATION

7.3.1 *Clinical implementation*

A number of barriers to implementation need to be overcome in order for stratified medicine to be realised (Duthey 2013). A general consensus on what criteria must be met in order for a SNP to be considered as having clinical value must be agreed. Furthermore, a multidisciplinary strategy should be used to prepare clinical practitioners for the process and realities of providing care based on stratified approaches. Once clear guidelines have been established for the clinical relevance of a SNP, regulatory authorities can use preexisting tools and methods to disseminate this knowledge to practitioners in the field. Furthermore, these guidelines can be incorporated into the current clinical trials framework, outlined in Figure 7.1, enabling pharmacogenetic interactions to be considered throughout drug development. Through these processes being implemented there is an increased likelihood of pharmacogenetic research having a greater impact, and a global effort to understand subpopulation differences will enable patients to benefit globally from research outcomes.

Pharmacogenetics studies have yielded clinically impactful data, as summarised in Chapter 1 (Section 1.4 and Table 1.1). Clinical guidelines for abacavir use are currently implemented

based on *HCP5* 733T>G (rs2395029) genotype. The single nucleotide polymorphism *HCP5* 733T>G (rs2395029) known as the *HLA-B*57-01* allele, is found in ~6% of patients and has been strongly associated with a significantly increased risk of developing abacavir hypersensitivity. Hypersensitivity presents as two or more of the following: fever, rash, gastrointestinal symptoms, fatigue, cough, and dyspnea, and results in discontinuation of abacavir therapy (Martin 2012, Dean 2015). The FDA and the European Medicines Agency now recommend genetic pre-screening for *HLA-B*57-01* for all patients before initiating abacavir-containing regimens (Martin 2012). Abacavir hypersensitivity has been observed in both Caucasian and Hispanic populations, but Black ethnicity populations have been shown to have a lowered risk of developing abacavir hypersensitivity (Mallal 2002, Symonds 2002, Hughes 2004, Martin 2004). This monogenic association has a categorical phenotype and provides an example of a direct link between a single SNP and a phenotype in the form of an adverse event. More often pharmacokinetic associations are complex interactions involving multiple genes and environmental factors, which contribute to a phenotype in varying degrees depending on the other variables instigating an effect. As such determining the degree of effect of a single SNP on a change in pharmacokinetics within a general population is difficult to do conclusively.

7.3.2 Influence of proteins

The interplay between transporter, enzyme and transcription factor expression and co-regulation, creates an intricate network of regulation that can influence study results. The complexity of these interactions coupled with variation in environmental factors feeds ambiguity for some variants. Given that less than 1% of all SNPs result in variations in proteins, the task of 'sifting for gold' is a laborious one (Venter 2001). Nevertheless, ground has been made in revealing SNPs that explain a proportion of inter-individual response. The next challenge will be to determine the overall impact of multiple polymorphisms in

combination. One example of this utilises the *CYP2B6* 516G>T SNP found to be statistically significant in Chapter 6. *CYP2B6* 516G>T, *CYP2B6* 983T>C and 15582C>T genotypes are used to define a person's EFV metaboliser status as a slow, intermediate or extensive metaboliser based on the presence or absence of the variant allele for each polymorphism. Further work is also required to understand how multiple variants in multiple loci across multiple chromosomes may be implemented in unison.

7.3.2 *Ethnicity*

Chapters 2 and 6 include pharmacogenetic analysis within African populations of single ethnicities. To achieve the definitive goal of pharmacogenetic studies, a stratified medicine approach that would enable the prescription and dosage of drugs to be founded on a sound understanding of how subpopulation genetics would influence their response, further work must be completed. As technology becomes cheaper and therefore more broadly accessible, it is hoped that the frequency of studies involving small or remote populations should increase over time. For this to happen it is imperative that a collaborative approach continues be adopted such as those being promoted through the H3Africa initiative. This provides the exchange of technology, knowledge and experience to broaden research across diverse populations. There is also a need to account for environmental and cultural differences, and the socio-economic factors that may influence an individual's response to antiretroviral drugs, which cannot be underestimated. Additionally, thought needs to be given to the way in which ethnicity is defined within studies, with a move away from self-classified ethnicity towards genetically-defined ethnicity, as more priority is given to investigating differences in response within population groups with overlapping ethnicity classifications.

7.4 CONCLUSIONS

Through conducting pharmacogenetics studies involving multi-ethnic populations receiving one of two first line HIV therapy drugs TFV or EFV, this thesis sought to gain insight into the degree of influence a patient's genetics has on their drug response. This response was defined as incidence of toxicity, alteration in drug pharmacokinetics or degree of drug-drug interaction. Furthermore, the work aimed to determine the effect of transporter interactions at the site of TFV toxicity, the proximal tubule, and the impact this had on the transport of two substrates.

These studies yielded valuable information surrounding the contribution of pharmacogenetics to the drug-drug interaction observed between EFV and LNG and defined a genetic association between TFV transporter SNPs and TFV plasma and urine concentrations. Both interactions have potential ramifications for a patient's overall response to ART, and build on current knowledge of how a patient's genetics can contribute to achieving sustained virological response. The work investigating the effect of TAF and TFV on MATE1 and MATE2K transport of metformin and creatinine produced novel data on the effect of TAF and TFV on the MATE2K mediated transport of metformin and creatinine. Demonstrating inhibition of MATE2K by TFV at a concentration of 0.01 μM and above. These studies have clinical impact through further elucidating potential mechanisms of toxicity caused by antiretroviral drug regimens and thus improving patient safety.

Further work is required to fully define the transporter profile of TFV in terms of its metabolism and excretion, in light of its prevailing use in ART. The release of advisory guidelines by regulatory bodies, including the FDA and EMA, on the need to assess clinically relevant transporters during drug development is thought to have led to the observed

increase in transporter related information on prescribing information (Sheetal Agarwal 2013). However, future work may benefit from the full transporter profile of newly developed antiretroviral drugs being evaluated. Section 7.3 of this chapter explores several factors that must be considered in order for personalised medicine to be implemented. The use of pharmacogenetics-based therapeutic recommendations in drug labels has been shown to be lacking (Lee 2017). The inclusion of pharmacogenetic evaluation into the drug development process and labelling information for novel drugs could potentially lead to rapid development in our knowledge of how genetics influence drug response and reduce adverse events in patients receiving ART.

REFERENCES

Abdalla, K., et al. (1992). "Interrelationship of serum levonorgestrel and sex hormone-binding globulin levels following vaginal and oral administration of combined steroid contraceptive tablets." Contraception **45**(2): 111-118.

Ahlin, G., et al. (2009). "Endogenous gene and protein expression of drug-transporting proteins in cell lines routinely used in drug discovery programs." Drug Metabolism and Disposition **37**(12): 2275-2283.

Albermann, N., et al. (2005). "Expression of the drug transporters MDR1/ABCB1, MRP1/ABCC1, MRP2/ABCC2, BCRP/ABCG2, and PXR in peripheral blood mononuclear cells and their relationship with the expression in intestine and liver." Biochemical pharmacology **70**(6): 949-958.

AntiretroviralGuidelinesforAdults&Adolescents (2017). Guidelines for the Use of Antiretroviral Agents in Adults and Adolescents Living with HIV. , US Department of Health and Human Services.

Antoniou, T., et al. (2005). "Incidence of and risk factors for tenofovir‐induced nephrotoxicity: a retrospective cohort study." HIV medicine **6**(4): 284-290.

Apolinário, T., et al. (2017). "ARTICLE Intermediate alleles of Huntington's disease HTT gene in different populations worldwide: a systematic review." Genetics and molecular research: GMR **16**(2).

Apostolova, N., et al. (2017). "Efavirenz: What is known about the cellular mechanisms responsible for its adverse effects." European journal of pharmacology **812**: 163-173.

Apostolova, N., et al. (2015). "Efavirenz and the CNS: what we already know and questions that need to be answered." Journal of antimicrobial chemotherapy **70**(10): 2693-2708.

Baheti, G., et al. (2013). "Age-related differences in plasma and intracellular tenofovir concentrations in HIV-1 infected children, adolescents and adults." AIDS (London, England) **27**(2): 221.

Bai, M., et al. (1997). "Markedly reduced activity of mutant calcium-sensing receptor with an inserted Alu element from a kindred with familial hypocalciuric hypercalcemia and neonatal severe hyperparathyroidism." Journal of Clinical Investigation **99**(8): 1917.

Bai, M., et al. (1997). "In vivo and in vitro characterization of neonatal hyperparathyroidism resulting from a de novo, heterozygous mutation in the Ca2+-sensing receptor gene: normal maternal calcium homeostasis as a cause of secondary hyperparathyroidism in familial benign hypocalciuric hypercalcemia." Journal of Clinical Investigation **99**(1): 88.

Bai, M., et al. (1996). "Expression and characterization of inactivating and activating mutations in the human Ca2+ o-sensing receptor." Journal of Biological Chemistry **271**(32): 19537-19545.

Bai, M., et al. (1998). "Dimerization of the extracellular calcium-sensing receptor (CaR) on the cell surface of CaR-transfected HEK293 cells." Journal of Biological Chemistry **273**(36): 23605-23610.

Baldi, L., et al. (2007). "Recombinant protein production by large-scale transient gene expression in mammalian cells: state of the art and future perspectives." Biotechnology letters **29**(5): 677-684.

Bam, R. A., et al. (2014). "Tenofovir alafenamide is not a substrate for renal organic anion transporters (OATs) and does not exhibit OAT-dependent cytotoxicity." Antiviral Therapy **19**(7): 687-692.

Barditch-Crovo, P., et al. (2001). "Phase I/II trial of the pharmacokinetics, safety, and antiretroviral activity of tenofovir disoproxil fumarate in human immunodeficiency virus-infected adults." Antimicrob Agents Chemother **45**(10): 2733-2739.

Barrett, J., et al. (2002). Population pharmacokinetic meta-analysis with efavirenz.

Barrios, A., et al. (2004). "Tenofovir-related nephrotoxicity in HIV-infected patients." Aids **18**(6): 960-963.

Barry, M., et al. (1999). "Pharmacokinetics and potential interactions amongst antiretroviral agents used to treat patients with HIV infection." Clinical pharmacokinetics **36**(4): 289-304.

Baxi, S., et al. (2017). "Evaluating the association of single-nucleotide polymorphisms with tenofovir exposure in a diverse prospective cohort of women living with HIV." The pharmacogenomics journal.

Baxi, S. M., et al. (2014). "Common Clinical Conditions–Age, Low BMI, Ritonavir Use, Mild Renal Impairment-Affect Tenofovir Pharmacokinetics in a Large Cohort of HIV-Infected Women." AIDS (London, England) **28**(1): 59.

Bélanger, A.-S., et al. (2009). "Glucuronidation of the antiretroviral drug efavirenz by UGT2B7 and an in vitro investigation of drug-drug interaction with zidovudine." Drug Metabolism and Disposition **37**(9): 1793-1796.

Bennett, W. M. and G. A. Porter (1971). "Endogenous creatinine clearance as a clinical measure of glomerular filtration rate." Br Med J **4**(5779): 84-86.

Berglund, F., et al. (1975). "Effect of trimethoprim-sulfamethoxazole on the renal excretion of creatinine in man." The Journal of urology **114**(6): 802-808.

Betts, S., et al. (2015). "Expression of CYP3A4 and CYP3A7 in human foetal tissues and its correlation with nuclear receptors." Basic & clinical pharmacology & toxicology **117**(4): 261-266.

Birdwell, K. A., et al. (2015). "Clinical pharmacogenetics implementation consortium (CPIC) guidelines for CYP3A5 genotype and tacrolimus dosing." Clinical Pharmacology & Therapeutics **98**(1): 19-24.

Birkus, G., et al. (2016). "Intracellular activation of tenofovir alafenamide and the effect of viral and host protease inhibitors." Antimicrob Agents Chemother **60**(1): 316-322.

Boffito, M., et al. (2017). "Antiretroviral dose optimization: the future of efavirenz 400 mg dosing." Current Opinion in HIV and AIDS **12**(4): 339-342.

Bonora, S., et al. (2016). "Elvitegravir, cobicistat, emtricitabine and tenofovir alafenamide for the treatment of HIV in adults." Expert opinion on pharmacotherapy **17**(3): 409-419.

Borges, K. (2010). "International Society of Genetic Genealogy." Session **3**: 20.

Brown, K. C., et al. (2012). "Exploration of CYP450 and drug transporter genotypes and correlations with nevirapine exposure in Malawians." Pharmacogenomics **13**(1): 113-121.

Burk, O., et al. (2004). "The induction of cytochrome P450 3A5 (CYP3A5) in the human liver and intestine is mediated by the xenobiotic sensors pregnane X receptor (PXR) and constitutively activated receptor (CAR)." Journal of Biological Chemistry **279**(37): 38379-38385.

Calza, L., et al. (2013). "Incidence of renal toxicity in HIV-infected, antiretroviral-naive patients starting tenofovir/emtricitabine associated with efavirenz, atazanavir/ritonavir, or lopinavir/ritonavir." Scandinavian journal of infectious diseases **45**(2): 147-154.

Cammett, A. M., et al. (2009). "Pharmacokinetic assessment of nevirapine and metabolites in human immunodeficiency virus type 1-infected patients with hepatic fibrosis." Antimicrob Agents Chemother **53**(10): 4147-4152.

Carrie, B. J., et al. (1980). "Creatinine: an inadequate filtration marker in glomerular diseases." The American journal of medicine **69**(2): 177-182.

Cascorbi, I. (2011). P-glycoprotein: tissue distribution, substrates, and functional consequences of genetic variations. Drug Transporters, Springer**:** 261-283.

Caudle, K. E., et al. (2013). "Clinical Pharmacogenetics Implementation Consortium guidelines for dihydropyrimidine dehydrogenase genotype and fluoropyrimidine dosing." Clinical Pharmacology & Therapeutics **94**(6): 640-645.

Chadwick, D. R., et al. (2015). "Tenofovir is associated with increased tubular proteinuria and asymptomatic renal tubular dysfunction in Ghana." BMC nephrology **16**(1): 1.

Chadwick, D. R., et al. (2015). "Tenofovir is associated with increased tubular proteinuria and asymptomatic renal tubular dysfunction in Ghana." BMC nephrology **16**(1): 195.

Chesnoy, S. and L. Huang (2000). "Structure and function of lipid-DNA complexes for gene delivery." Annual review of biophysics and biomolecular structure **29**(1): 27-47.

Cho, D.-Y., et al. (2016). "Rifampin enhances cytochrome P450 (CYP) 2B6-mediated efavirenz 8-hydroxylation in healthy volunteers." Drug metabolism and pharmacokinetics **31**(2): 107-116.

Chu, X., et al. (2016). "The complexities of interpreting reversible elevated serum creatinine levels in drug development: does a correlation with inhibition of renal transporters exist?" Drug Metabolism and Disposition: dmd. 115.067694.

Cihlar, T., et al. (2007). "Short communication Molecular assessment of the potential for renal drug interactions between tenofovir and HIV protease inhibitors." Antiviral Therapy **12**: 267-272.

Coelho, A. V., et al. (2013). "ABCB1 and ABCC1 variants associated with virological failure of first‐line protease inhibitors antiretroviral regimens in Northeast Brazil patients." The Journal of Clinical Pharmacology **53**(12): 1286-1293.

Cooper, R. D., et al. (2010). "Systematic review and meta-analysis: renal safety of tenofovir disoproxil fumarate in HIV-infected patients." Clinical Infectious Diseases **51**(5): 496-505.

Coresh, J., et al. (2003). "Prevalence of chronic kidney disease and decreased kidney function in the adult US population: Third National Health and Nutrition Examination Survey." American journal of kidney diseases **41**(1): 1-12.

Cortes, C. P., et al. (2013). "Correlates of efavirenz exposure in Chilean patients affected with human immunodeficiency virus reveals a novel association with a polymorphism in the constitutive androstane receptor." Therapeutic drug monitoring **35**(1): 78-83.

Coukell, A. J. and J. A. Balfour (1998). "Levonorgestrel subdermal implants." Drugs **55**(6): 861-887.

Cressey, T. R., et al. (2012). "Efavirenz pharmacokinetics during the third trimester of pregnancy and postpartum." Journal of acquired immune deficiency syndromes (1999) **59**(3): 245.

Csajka, C., et al. (2003). "Population pharmacokinetics and effects of efavirenz in patients with human immunodeficiency virus infection." Clinical Pharmacology & Therapeutics **73**(1): 20-30.

Custodio, J. M., et al. (2016). "Pharmacokinetics and safety of tenofovir alafenamide in HIV-uninfected subjects with severe renal impairment." Antimicrob Agents Chemother **60**(9): 5135-5140.

Dalal, B., et al. (2015). "Individualization of antiretroviral therapy-Pharmacogenomic aspect." The Indian journal of medical research **142**(6): 663.

Dalwadi, D. A., et al. (2016). "Molecular mechanisms of serotonergic action of the HIV-1 antiretroviral efavirenz." Pharmacological research **110**: 10-24.

Damme, K., et al. (2011). "Mammalian MATE (SLC47A) transport proteins: impact on efflux of endogenous substrates and xenobiotics." Drug metabolism reviews **43**(4): 499-523.

De Waal, R., et al. (2017). "Changes in estimated glomerular filtration rate over time in South African HIV‐1‐infected patients receiving tenofovir: a retrospective cohort study." Journal of the International AIDS Society **20**(1).

Dean, L. (2015). "Abacavir Therapy and HLA-B* 57: 01 Genotype."

Dean, L. (2015). "Irinotecan Therapy and UGT1A1 Genotype."

Dietmair, S., et al. (2012). "A multi-omics analysis of recombinant protein production in Hek293 cells." PloS one **7**(8): e43394.

Duthey, B. (2013). "Priority Medicines for Europe and the World" A public health approach to innovation." WHO Background paper **6**.

Elgar, G. and T. Vavouri (2008). "Tuning in to the signals: noncoding sequence conservation in vertebrate genomes." Trends in genetics **24**(7): 344-352.

Elsby, R., et al. (2017). "Mechanistic in vitro studies confirm that inhibition of the renal apical efflux transporter multidrug and toxin extrusion (MATE) 1, and not altered absorption, underlies the increased metformin exposure observed in clinical interactions with cimetidine, trimethoprim or pyrimethamine." Pharmacology research & perspectives **5**(5).

ENCORE1 (2014). "Efficacy of 400 mg efavirenz versus standard 600 mg dose in HIV-infected, antiretroviral-naive adults (ENCORE1): a randomised, double-blind, placebo-controlled, non-inferiority trial." The Lancet **383**(9927): 1474-1482.

Estrella, M. M. and D. M. Fine (2010). "Screening for chronic kidney disease in HIV-infected patients." Advances in chronic kidney disease **17**(1): 26-35.

EuropeanMedicinesAgency (2015). Assessment report Genvoya International non-proprietary name: elvitegravir / cobicistat / emtricitabine / tenofovir alafenamide Procedure No. EMEA/H/C/004042/0000. C. f. M. P. f. H. U. (CHMP).

Ezinga, M., et al. (2014). "Long-term treatment with tenofovir: prevalence of kidney tubular dysfunction and its association with tenofovir plasma concentration." Antivir Ther **19**(8): 765-771.

Fafin, C., et al. (2012). "Increased time exposure to tenofovir is associated with a greater decrease in estimated glomerular filtration rate in HIV patients with kidney function of less than 60 mL/min/1.73 m2." Nephron Clinical Practice **120**(4): c205-c214.

Fan-Havard, P., et al. (2013). "Pharmacokinetics of phase I nevirapine metabolites following a single dose and at steady state." Antimicrob Agents Chemother **57**(5): 2154-2160.

Ford, N., et al. (2011). "Safety of efavirenz in the first trimester of pregnancy: an updated systematic review and meta-analysis." Aids **25**(18): 2301-2304.

Fulco, P. P. and M. A. Kirian (2003). "Effect of tenofovir on didanosine absorption in patients with HIV." Annals of Pharmacotherapy **37**(9): 1325-1328.

Gao, X., et al. (2007). "Nonviral gene delivery: what we know and what is next." The AAPS journal **9**(1): E92-E104.

Gatch, M. B., et al. (2013). "The HIV Antiretroviral Drug Efavirenz has LSD-Like Properties." Neuropsychopharmacology **38**: 2373.

GenomesProjectConsortium (2012). "An integrated map of genetic variation from 1,092 human genomes." Nature **491**(7422): 56-65.

GenomesProjectConsortium (2015). "A global reference for human genetic variation." Nature **526**(7571): 68-74.

German, P., et al. (2012). "Effect of cobicistat on glomerular filtration rate in subjects with normal and impaired renal function." JAIDS Journal of Acquired Immune Deficiency Syndromes **61**(1): 32-40.

Giacomet, V., et al. (2013). "Tenofovir-induced renal tubular dysfunction in vertically HIV-infected patients associated with polymorphisms in ABCC2, ABCC4 and ABCC10 genes." The Pediatric infectious disease journal **32**(10): e403-e405.

GileadSciences (2016). Center for drug evaluation and research: labelling Vemlidy (Tenofovir Alafenamide Fumarate).

Goicoechea, M., et al. (2008). "Greater tenofovir-associated renal function decline with protease inhibitor-based versus nonnucleoside reverse-transcriptase inhibitor-based therapy." Journal of Infectious Diseases **197**(1): 102-108.

Gorboulev, V., et al. (2005). "Subtype-specific affinity for corticosterone of rat organic cation transporters rOCT1 and rOCT2 depends on three amino acids within the substrate binding region." Molecular pharmacology **67**(5): 1612-1619.

Graham, F., et al. (1977). "Characteristics of a human cell line transformed by DNA from human adenovirus type 5." Journal of General Virology **36**(1): 59-72.

Granich, R., et al. (2017). "Status and methodology of publicly available national HIV care continua and 90-90-90 targets: A systematic review." PLoS medicine **14**(4): e1002253.

Gupta, S. K. (2008). "Tenofovir-associated Fanconi syndrome: review of the FDA adverse event reporting system." AIDS patient care and STDs **22**(2): 99-103.

Gutierrez, F., et al. (2014). "Renal tubular transporter-mediated interactions of HIV drugs: implications for patient management." AIDS reviews **16**(4): 199-212.

Haas, D. W., et al. (2009). "Associations between CYP2B6 polymorphisms and pharmacokinetics after a single dose of nevirapine or efavirenz in African Americans." Journal of Infectious Diseases **199**(6): 872-880.

Haas, D. W., et al. (2004). "Pharmacogenetics of efavirenz and central nervous system side effects: an Adult AIDS Clinical Trials Group study." Aids **18**(18): 2391-2400.

Habtewold, A., et al. (2011). "Long-term effect of efavirenz autoinduction on plasma/peripheral blood mononuclear cell drug exposure and CD4 count is influenced by UGT2B7 and CYP2B6 genotypes among HIV patients." Journal of antimicrobial chemotherapy **66**(10): 2350-2361.

Hall, A. M., et al. (2011). "Tenofovir-associated kidney toxicity in HIV-infected patients: a review of the evidence." American journal of kidney diseases **57**(5): 773-780.

Hariparsad, N., et al. (2004). "Induction of CYP3A4 by efavirenz in primary human hepatocytes: comparison with rifampin and phenobarbital." The Journal of Clinical Pharmacology **44**(11): 1273-1281.

Heikinheimo, O., et al. (2011). "The levonorgestrel-releasing intrauterine system in human immunodeficiency virus–infected women: a 5-year follow-up study." American Journal of Obstetrics and Gynecology **204**(2): 126. e121-126. e124.

Herlitz, L. C., et al. (2010). "Tenofovir nephrotoxicity: acute tubular necrosis with distinctive clinical, pathological, and mitochondrial abnormalities." Kidney Int **78**(11): 1171-1177.

Herlitz, L. C., et al. (2010). "Tenofovir nephrotoxicity: acute tubular necrosis with distinctive clinical, pathological, and mitochondrial abnormalities." Kidney Int **78**(11): 1171-1177.

Heyn, P., et al. (2015). "Introns and gene expression: cellular constraints, transcriptional regulation, and evolutionary consequences." Bioessays **37**(2): 148-154.

Hoetelmans, R. M., et al. (2007). "Pharmacokinetic interaction between TMC114/ritonavir and tenofovir disoproxil fumarate in healthy volunteers." British journal of clinical pharmacology **64**(5): 655-661.

Hofmann, M. H., et al. (2008). "Aberrant splicing caused by single nucleotide polymorphism c. 516G> T [Q172H], a marker of CYP2B6* 6, is responsible for decreased expression and activity of CYP2B6 in liver." Journal of Pharmacology and Experimental Therapeutics **325**(1): 284-292.

Holzinger, E. R., et al. (2012). "Genome-wide association study of plasma efavirenz pharmacokinetics in AIDS Clinical Trials Group protocols implicates several CYP2B6 variants." Pharmacogenetics and genomics **22**(12): 858.

Hughes, A. R., et al. (2004). "Association of genetic variations in HLA-B region with hypersensitivity to abacavir in some, but not all, populations." Pharmacogenomics **5**(2): 203-211.

Hui, K., et al. (2016). "Dose optimization of efavirenz based on individual CYP2B6 polymorphisms in Chinese patients positive for HIV." CPT: pharmacometrics & systems pharmacology **5**(4): 182-191.

Huisman, M. T., et al. (2002). "Multidrug resistance protein 2 (MRP2) transports HIV protease inhibitors, and transport can be enhanced by other drugs." Aids **16**(17): 2295-2301.

Iacovacci, G., et al. (2017). "Forensic data and microvariant sequence characterization of 27 Y-STR loci analyzed in four Eastern African countries." Forensic Science International: Genetics **27**: 123-131.

Imaoka, T., et al. (2007). "Functional involvement of multidrug resistance-associated protein 4 (MRP4/ABCC4) in the renal elimination of the antiviral drugs adefovir and tenofovir." Molecular pharmacology **71**(2): 619-627.

Ito, S., et al. (2012). "Competitive inhibition of the luminal efflux by multidrug and toxin extrusions, but not basolateral uptake by organic cation transporter 2, is the likely mechanism underlying the pharmacokinetic drug-drug interactions caused by cimetidine in the kidney." Journal of Pharmacology and Experimental Therapeutics **340**(2): 393-403.

Izzedine, H., et al. (2006). "Association between ABCC2 gene haplotypes and tenofovir-induced proximal tubulopathy." Journal of Infectious Diseases **194**(11): 1481-1491.

Jellinger, P., et al. (2012). "American Association of Clinical Endocrinologists' guidelines for management of dyslipidemia and prevention of atherosclerosis." Endocrine practice **18**(Supplement 1): 1-78.

Jose, S., et al. (2014). "Incomplete reversibility of estimated glomerular filtration rate decline following tenofovir disoproxil fumarate exposure." Journal of Infectious Diseases **210**(3): 363-373.

Jülg, B. D., et al. (2005). "Progression of renal impairment under therapy with tenofovir." Aids **19**(12): 1332-1333.

Kabat-Koperska, J., et al. (2007). "Creatinine Clearance after Cimetidine Administration—Is It Useful in the Monitoring of the Function of Transplanted Kidney?" Renal failure **29**(6): 667-672.

Karras, A., et al. (2003). "Tenofovir-related nephrotoxicity in human immunodeficiency virus-infected patients: three cases of renal failure, Fanconi syndrome, and nephrogenic diabetes insipidus." Clinical Infectious Diseases **36**(8): 1070-1073.

Kearney, B. P., et al. (2006). "Pharmacokinetics and safety of tenofovir disoproxil fumarate on coadministration with lopinavir/ritonavir." JAIDS Journal of Acquired Immune Deficiency Syndromes **43**(3): 278-283.

Keinan, A. and A. G. Clark (2012). "Recent explosive human population growth has resulted in an excess of rare genetic variants." science **336**(6082): 740-743.

Kile, D. A., et al. (2012). "A population pharmacokinetic-pharmacogenetic analysis of atazanavir." AIDS research and human retroviruses **28**(10): 1227-1234.

Kiser, J., et al. (2008). "The effect of lopinavir/ritonavir on the renal clearance of tenofovir in HIV‐infected patients." Clinical Pharmacology & Therapeutics **83**(2): 265-272.

Kiser, J. J., et al. (2008). "Clinical and genetic determinants of intracellular tenofovir diphosphate concentrations in HIV-infected patients." JAIDS Journal of Acquired Immune Deficiency Syndromes **47**(3): 298-303.

Kohler, J. J., et al. (2009). "Tenofovir renal toxicity targets mitochondria of renal proximal tubules." Laboratory investigation **89**(5): 513-519.

Kopp, J. B. and C. Winkler (2003). "HIV-associated nephropathy in African Americans1." Kidney Int **63**: S43-S49.

Koteff, J., et al. (2013). "A phase 1 study to evaluate the effect of dolutegravir on renal function via measurement of iohexol and para‐aminohippurate clearance in healthy subjects." British journal of clinical pharmacology **75**(4): 990-996.

Kunimoto, Y., et al. (2016). "Plasma tenofovir trough concentrations are associated with renal dysfunction in Japanese patients with HIV infection: a retrospective cohort study." Journal of Pharmaceutical Health Care and Sciences **2**(1): 22.

Lamba, J., et al. (2008). "Novel single nucleotide polymorphisms in the promoter and intron 1 of human pregnane X receptor/NR1I2 and their association with CYP3A4 expression." Drug Metabolism and Disposition **36**(1): 169-181.

Lamorde, M., et al. (2017). "Pharmacokinetics, pharmacodynamics and pharmacogenetics of efavirenz 400 mg once daily during pregnancy and post-partum." Clinical Infectious Diseases.

Lee, J. C. and R. D. Marosok (2003). "Acute tubular necrosis in a patient receiving tenofovir." Aids **17**(17): 2543-2544.

Lee, S., et al. (2017). "Pharmacogenetic Information Reflected in Cpic and Dpwg Guideline and its Application on Drug Labels." Clinical therapeutics **39**(8): e57-e58.

Lehtovirta, P., et al. (2007). "Experience with the levonorgestrel-releasing intrauterine system among HIV-infected women." Contraception **75**(1): 37-39.

Lepist, E.-I., et al. (2012). "Cobicistat boosts the intestinal absorption of transport substrates including HIV protease inhibitors and GS-7340 in vitro." Antimicrob Agents Chemother: AAC. 01089-01012.

Lepist, E.-I., et al. (2012). "Cobicistat boosts the intestinal absorption of transport substrates, including HIV protease inhibitors and GS-7340, in vitro." Antimicrob Agents Chemother **56**(10): 5409-5413.

Lepist, E.-I., et al. (2014). "Contribution of the organic anion transporter OAT2 to the renal active tubular secretion of creatinine and mechanism for serum creatinine elevations caused by cobicistat." Kidney Int.

Lepist, E.-I., et al. (2014). "Contribution of the organic anion transporter OAT2 to the renal active tubular secretion of creatinine and mechanism for serum creatinine elevations caused by cobicistat." Kidney Int **86**(2): 350-357.

Lewis, C. M. (2002). "Genetic association studies: design, analysis and interpretation." Briefings in bioinformatics **3**(2): 146-153.

Lewis, W. and M. C. Dalakas (1995). "Mitochondrial toxicity of antiviral drugs." Nature medicine **1**(5): 417-422.

Liptrott, N. J., et al. (2012). "Association of ABCC10 polymorphisms with nevirapine plasma concentrations in the German Competence Network for HIV/AIDS." Pharmacogenetics and genomics **22**(1): 10.

López-Cortés, L. F., et al. (2002). "Pharmacokinetic interactions between efavirenz and rifampicin in HIV-infected patients with tuberculosis." Clinical pharmacokinetics **41**(9): 681-690.

Lu, M. (2016). "Structures of multidrug and toxic compound extrusion transporters and their mechanistic implications." Channels **10**(2): 88-100.

Luo, G., et al. (2002). "CYP3A4 induction by drugs: correlation between a pregnane X receptor reporter gene assay and CYP3A4 expression in human hepatocytes." Drug Metabolism and Disposition **30**(7): 795-804.

Ma, J. D., et al. (2010). "HLA-B* 5701 testing to predict abacavir hypersensitivity." PLoS Currents Evidence on Genomic Tests.

Maddalena Cerrone, X. W., Megan Neary, Christine Weaver, Serge Fedele, Isaac Day-Weber, Andrew Owen, Andrew Hill, Myra McClure, Marta Boffito (2018). Pharmacokinetics of efavirenz 400mg with isoniazid/rifampicin in people with HIV. . Conference on Retroviruses and Opportunistic Infections (CROI) Boston (MA) USA.

Malik, A., et al. (2005). "Acute renal failure and Fanconi syndrome in an AIDS patient on tenofovir treatment—case report and review of literature." Journal of Infection **51**(2): E61-E65.

Mallal, S., et al. (2002). "Association between presence of HLA-B* 5701, HLA-DR7, and HLA-DQ3 and hypersensitivity to HIV-1 reverse-transcriptase inhibitor abacavir." The Lancet **359**(9308): 727-732.

Markowitz, M., et al. (2014). "Phase I/II study of the pharmacokinetics, safety and antiretroviral activity of tenofovir alafenamide, a new prodrug of the HIV reverse transcriptase inhibitor tenofovir, in HIV-infected adults." Journal of antimicrobial chemotherapy **69**(5): 1362-1369.

Marques, S. C. and O. N. Ikediobi (2010). "The clinical application of UGT1A1 pharmacogenetic testing: gene-environment interactions." Human genomics **4**(4): 238.

Marth, G., et al. (2003). "Sequence variations in the public human genome data reflect a bottlenecked population history." Proceedings of the National Academy of Sciences **100**(1): 376-381.

Martin, A. M., et al. (2004). "Pharmacogenetics of antiretroviral therapy: genetic variation of response and toxicity." Pharmacogenomics **5**(6): 643-655.

Martin, M., et al. (2012). "Clinical pharmacogenetics implementation consortium guidelines for HLA‐B genotype and abacavir dosing." Clinical Pharmacology & Therapeutics **91**(4): 734-738.

Martínez-Guerrero, L. J. and S. H. Wright (2013). "Substrate-dependent inhibition of human MATE1 by cationic ionic liquids." Journal of Pharmacology and Experimental Therapeutics **346**(3): 495-503.

Marzolini, C., et al. (2016). "Cobicistat versus ritonavir boosting and differences in the drug–drug interaction profiles with co-medications." Journal of antimicrobial chemotherapy **71**(7): 1755-1758.

Marzolini, C., et al. (2001). "Efavirenz plasma levels can predict treatment failure and central nervous system side effects in HIV-1-infected patients." Aids **15**(1): 71-75.

Masuda, S., et al. (2006). "Identification and functional characterization of a new human kidney–specific H+/organic cation antiporter, kidney-specific multidrug and toxin extrusion 2." Journal of the American Society of Nephrology **17**(8): 2127-2135.

Mauss, S., et al. (2005). "Antiretroviral therapy with tenofovir is associated with mild renal dysfunction." Aids **19**(1): 93-95.

McCormack, S., et al. (2016). "Pre-exposure prophylaxis to prevent the acquisition of HIV-1 infection (PROUD): effectiveness results from the pilot phase of a pragmatic open-label randomised trial." The Lancet **387**(10013): 53-60.

McLeod, H., et al. (2000). "Genetic polymorphism of thiopurine methyltransferase and its clinical relevance for childhood acute lymphoblastic leukemia." Leukemia **14**(4): 567.

Moreno, I., et al. (2012). "Influence of CYP3A4/5 polymorphisms in the pharmacokinetics of levonorgestrel: a pilot study." Biomédica **32**(4): 570-577.

Moss, D. M., et al. (2011). "Raltegravir is a substrate for SLC22A6: a putative mechanism for the interaction between raltegravir and tenofovir." Antimicrob Agents Chemother **55**(2): 879-887.

Moss, D. M., et al. (2014). "The role of drug transporters in the kidney: lessons from tenofovir." Frontiers in pharmacology **5**: 248.

Moss, D. M., et al. (2011). "Raltegravir is a substrate for SLC22A6: a putative mechanism for the interaction between raltegravir and tenofovir." Antimicrob Agents Chemother **55**(2): 879-887.

Motohashi, H. and K.-i. Inui (2013). "Organic cation transporter OCTs (SLC22) and MATEs (SLC47) in the human kidney." The AAPS journal **15**(2): 581-588.

Mpondo, B. C., et al. (2014). "Impact of antiretroviral therapy on renal function among HIV-infected Tanzanian adults: a retrospective cohort study." PloS one **9**(2): e89573.

Müller, F., et al. (2015). "N1-methylnicotinamide as an endogenous probe for drug interactions by renal cation transporters: studies on the metformin–trimethoprim interaction." European Journal of Clinical Pharmacology **71**(1): 85-94.

Munar, M. Y. and H. Singh (2007). "Drug dosing adjustments in patients with chronic kidney disease." American family physician **75**(10).

Nelson, M. R., et al. (2007). "The safety of tenofovir disoproxil fumarate for the treatment of HIV infection in adults: the first 4 years." Aids **21**(10): 1273-1281.

Neumanova, Z., et al. (2014). "Interactions of tenofovir and tenofovir disoproxil fumarate with drug efflux transporters ABCB1, ABCG2, and ABCC2; role in transport across the placenta." Aids **28**(1): 9-17.

Ngaimisi, E., et al. (2013). "Importance of ethnicity, CYP2B6 and ABCB1 genotype for efavirenz pharmacokinetics and treatment outcomes: a parallel-group prospective cohort study in two sub-Saharan Africa populations." PloS one **8**(7): e67946.

Nguyen, C. M., et al. (2011). "Thiopurine methyltransferase (TPMT) genotyping to predict myelosuppression risk." PLoS Currents Evidence on Genomic Tests.

Nies, A. T., et al. (2011). Organic cation transporters (OCTs, MATEs), in vitro and in vivo evidence for the importance in drug therapy. Drug Transporters, Springer**:** 105-167.

Nightingale, S., et al. (2016). "Efavirenz and Metabolites in Cerebrospinal Fluid: Relationship with CYP2B6 c. 516G→ T Genotype and Perturbed Blood-Brain Barrier Due to Tuberculous Meningitis." Antimicrob Agents Chemother **60**(8): 4511-4518.

Nishijima, T., et al. (2011). "Impact of small body weight on tenofovir-associated renal dysfunction in HIV-infected patients: a retrospective cohort study of Japanese patients." PloS one **6**(7): e22661.

Nishijima, T., et al. (2012). "Single nucleotide polymorphisms in ABCC2 associate with tenofovir-induced kidney tubular dysfunction in Japanese patients with HIV-1 infection: a pharmacogenetic study." Clinical Infectious Diseases **55**(11): 1558-1567.

Ogburn, E. T., et al. (2010). "Efavirenz primary and secondary metabolism in vitro and in vivo: identification of novel metabolic pathways and cytochrome P450 2A6 as the principal catalyst of efavirenz 7-hydroxylation." Drug Metabolism and Disposition **38**(7): 1218-1229.

Orrell, C., et al. (2011). "Efavirenz and rifampicin in the South African context: is there a need to dose increase efavirenz with concurrent rifampicin therapy?" Antiviral Therapy **16**(4): 527.

Ortega, V. E. and D. A. Meyers (2014). "Pharmacogenetics: implications of race and ethnicity on defining genetic profiles for personalized medicine." Journal of Allergy and Clinical Immunology **133**(1): 16-26.

Otsuka, M., et al. (2005). "A human transporter protein that mediates the final excretion step for toxic organic cations." Proceedings of the National Academy of Sciences of the United States of America **102**(50): 17923-17928.

Owen, A., et al. (2004). "Short communication Expression of pregnane-X-receptor transcript in peripheral blood mononuclear cells and correlation with MDR1 mRNA." Antiviral Therapy **9**: 819-821.

Palovaara, S., et al. (2003). "Inhibition of cytochrome P450 2B6 activity by hormone replacement therapy and oral contraceptive as measured by bupropion hydroxylation." Clinical Pharmacology & Therapeutics **74**(4): 326-333.

Patel, R. C., et al. (2015). "Pregnancy rates in HIV-positive women using contraceptives and efavirenz-based or nevirapine-based antiretroviral therapy in Kenya: a retrospective cohort study." The Lancet HIV **2**(11): e474-e482.

Penzak, S., et al. (2007). "Cytochrome P450 2B6 (CYP2B6) G516T influences nevirapine plasma concentrations in HIV‐infected patients in Uganda." HIV medicine **8**(2): 86-91.

Phillips, S. J., et al. (2013). "Effect of hormonal contraceptive methods on HIV disease progression: a systematic review." Aids **27**(5): 787-794.

Pinillos, F., et al. (2016). "Case report: Severe central nervous system manifestations associated with aberrant efavirenz metabolism in children: the role of CYP2B6 genetic variation." BMC infectious diseases **16**(1): 56.

Plantinga, L. C., et al. (2010). "Prevalence of chronic kidney disease in US adults with undiagnosed diabetes or prediabetes." Clinical Journal of the American Society of Nephrology: CJN. 07891109.

Polgar, O., et al. (2008). "ABCG2: structure, function and role in drug response." Expert opinion on drug metabolism & toxicology **4**(1): 1-15.

Pozniak, A., et al. (2016). "Switching to tenofovir alafenamide, coformulated with elvitegravir, cobicistat, and emtricitabine, in HIV-infected patients with renal impairment: 48-week results from a single-arm, multicenter, open-label phase 3 study." Journal of acquired immune deficiency syndromes (1999) **71**(5): 530.

Pratt, V. M., et al. (2015). "Report of New Haplotype for ABCC2 Gene: rs17222723 and rs8187718 in cis." The Journal of Molecular Diagnostics **17**(2): 201-205.

Pushpakom, S. P., et al. (2011). "Genetic variants of ABCC10, a novel tenofovir transporter, are associated with kidney tubular dysfunction." Journal of Infectious Diseases **204**(1): 145-153.

Quesada, P. R., et al. (2015). "Incidence and risk factors for tenofovir-associated renal toxicity in HIV-infected patients." International journal of clinical pharmacy **37**(5): 865-872.

Quesada, P. R., et al. (2015). "Incidence and risk factors for tenofovir-associated renal toxicity in HIV-infected patients." International journal of clinical pharmacy: 1-8.

Ray, A. S., et al. (2016). "Tenofovir alafenamide: a novel prodrug of tenofovir for the treatment of human immunodeficiency virus." Antiviral research **125**: 63-70.

Rifkin, B. S. and M. A. Perazella (2004). "Tenofovir-associated nephrotoxicity: Fanconi syndrome and renal failure." The American journal of medicine **117**(4): 282-284.

Roberts, R., et al. (2016). "ABCG2 loss-of-function polymorphism predicts poor response to allopurinol in patients with gout." The pharmacogenomics journal.

Rodríguez-Nóvoa, S., et al. (2010). "Impairment in kidney tubular function in patients receiving tenofovir is associated with higher tenofovir plasma concentrations." Aids **24**(7): 1064-1066.

Rodríguez-Nóvoa, S., et al. (2009). "Predictors of kidney tubular dysfunction in HIV-infected patients treated with tenofovir: a pharmacogenetic study." Clinical Infectious Diseases **48**(11): e108-e116.

Rodriguez, S., et al. (2009). "Hardy-Weinberg equilibrium testing of biological ascertainment for Mendelian randomization studies." American journal of epidemiology **169**(4): 505-514.

Röling, J., et al. (2006). "HIV-Associated Renal Diseases and Highly Active Antiretroviral Therapy—Induced Nephropathy." Clinical Infectious Diseases **42**(10): 1488-1495.

Rostand, S. G., et al. (1982). "Racial differences in the incidence of treatment for end-stage renal disease." New England Journal of Medicine **306**(21): 1276-1279.

Rotger, M., et al. (2005). "Influence of CYP2B6 polymorphism on plasma and intracellular concentrations and toxicity of efavirenz and nevirapine in HIV-infected patients." Pharmacogenetics and genomics **15**(1): 1-5.

Rungtivasuwan, K., et al. (2015). "Influence of ABCC2 and ABCC4 polymorphisms on tenofovir plasma concentrations in Thai HIV-infected patients." Antimicrob Agents Chemother **59**(6): 3240-3245.

Russo, G., et al. (2016). "Pharmacogenetics of non-nucleoside reverse transcriptase inhibitors (NNRTIs) in resource-limited settings: Influence on antiretroviral therapy response and concomitant anti-tubercular, antimalarial and contraceptive treatments." Infection, Genetics and Evolution **37**: 192-207.

Sax, P. E., et al. (2015). "Tenofovir alafenamide versus tenofovir disoproxil fumarate, coformulated with elvitegravir, cobicistat, and emtricitabine, for initial treatment of HIV-1 infection: two randomised, double-blind, phase 3, non-inferiority trials." The Lancet **385**(9987): 2606-2615.

Scarsi, K. K., et al. (2016). "Unintended pregnancies observed with combined use of the levonorgestrel contraceptive implant and efavirenz-based antiretroviral therapy: a three-arm pharmacokinetic evaluation over 48 weeks." Clinical Infectious Diseases **62**(6): 675-682.

Scarsi, K. K., et al. (2016). "Unintended pregnancies observed with combined use of the levonorgestrel contraceptive implant and efavirenz-based antiretroviral therapy: a three-arm pharmacokinetic evaluation over 48 weeks." Clinical Infectious Diseases **62**(6): 675-682.

Scherzer, R., et al. (2012). "Association of tenofovir exposure with kidney disease risk in HIV infection." AIDS (London, England) **26**(7): 867.

Schipani, A., et al. (2010). "Population pharmacokinetic modeling of the association between 63396C→ T pregnane X receptor polymorphism and unboosted atazanavir clearance." Antimicrob Agents Chemother **54**(12): 5242-5250.

Schipani, A., et al. (2011). "Integration of population pharmacokinetics and pharmacogenetics: an aid to optimal nevirapine dose selection in HIV-infected individuals." Journal of antimicrobial chemotherapy: dkr087.

Schlaeger, E.-J., et al. (1998). Transient transfection in mammalian cells. New Developments and New Applications in Animal Cell Technology, Springer**:** 105-112.

Schooley, R. T., et al. (2002). "Tenofovir DF in antiretroviral-experienced patients: results from a 48-week, randomized, double-blind study." Aids **16**(9): 1257-1263.

Scott, S. A., et al. (2013). "Clinical Pharmacogenetics Implementation Consortium guidelines for CYP2C19 genotype and clopidogrel therapy: 2013 update." Clinical Pharmacology & Therapeutics **94**(3): 317-323.

Scourfield, A., et al. (2012). "Discontinuation of Atripla as first-line therapy in HIV-1 infected individuals." Aids **26**(11): 1399-1401.

Serdar, M. A., et al. (2001). "A practical approach to glomerular filtration rate measurements: creatinine clearance estimation using cimetidine." Annals of Clinical & Laboratory Science **31**(3): 265-273.

Shaw, J.-P., et al. (1997). "Metabolism and pharmacokinetics of novel oral prodrugs of 9-[(R)-2-(phosphonomethoxy) propyl] adenine (PMPA) in dogs." Pharmaceutical research **14**(12): 1824-1829.

Sheetal Agarwal, L. C., Lei Zhang (2013). "An Overview of Transporter Information in Package Inserts of Recently Approved New Molecular Entities." Pharmaceutical research(30): 899-910.

Shelton, J. D. (2015). "Reduced Effectiveness of Contraceptive Implants for Women Taking the Antiretroviral Efavirenz (EFV): Still Good Enough and for How Long?" Global Health: Science and Practice **3**(4): 528-531.

Shen, H., et al. (2015). "Characterization of organic anion transporter 2 (SLC22A7): a highly efficient transporter for creatinine and species-dependent renal tubular expression." Drug Metabolism and Disposition **43**(7): 984-993.

Siccardi, M., et al. (2008). "Association of a single-nucleotide polymorphism in the pregnane X receptor (PXR 63396C→ T) with reduced concentrations of unboosted atazanavir." Clinical Infectious Diseases **47**(9): 1222-1225.

Sivin, I., et al. (1997). "First week drug concentrations in women with levonorgestrel rod or Norplant capsule implants." Contraception **56**(5): 317-321.

Sivin, I., et al. (1997). "Levonorgestrel concentrations during use of levonorgestrel rod (LNG ROD) implants." Contraception **55**(2): 81-85.

Sivin, I., et al. (2001). "Levonorgestrel concentrations during 7 years of continuous use of Jadelle contraceptive implants." Contraception **64**(1): 43-49.

Slatkin, M. (2008). "Linkage disequilibrium—understanding the evolutionary past and mapping the medical future." Nature Reviews Genetics **9**(6): 477-485.

Solus, J. F., et al. (2004). "Genetic variation in eleven phase I drug metabolism genes in an ethnically diverse population." Pharmacogenomics **5**(7): 895-931.

Somogyi, A., et al. (1987). "Reduction of metformin renal tubular secretion by cimetidine in man." British journal of clinical pharmacology **23**(5): 545-551.

Stray, K. M., et al. (2013). "Evaluation of the effect of cobicistat on the in vitro renal transport and cytotoxicity potential of tenofovir." Antimicrob Agents Chemother **57**(10): 4982-4989.

Stuart, G. S., et al. (2011). "Combined oral contraceptives and antiretroviral PK/PD in Malawian women: pharmacokinetics and pharmacodynamics of a combined oral contraceptive and a generic combined formulation antiretroviral in Malawi." Journal of acquired immune deficiency syndromes (1999) **58**(2): e40-43.

Svärd, J., et al. (2010). "Nuclear receptor-mediated induction of CYP450 by antiretrovirals: functional consequences of NR1I2 (PXR) polymorphisms and differential prevalence in whites and sub-Saharan Africans." JAIDS Journal of Acquired Immune Deficiency Syndromes **55**(5): 536-549.

Swart, M., et al. (2012). "ABCB1 4036A> G and 1236C> T polymorphisms affect plasma efavirenz levels in South African HIV/AIDS patients." Frontiers in genetics **3**: 236.

Swart, M., et al. (2012). "PXR and CAR single nucleotide polymorphisms influence plasma efavirenz levels in South African HIV/AIDS patients." BMC medical genetics **13**(1): 1.

Swart, M., et al. (2012). "PXR and CAR single nucleotide polymorphisms influence plasma efavirenz levels in South African HIV/AIDS patients." BMC medical genetics **13**(1): 112.

Symonds, W., et al. (2002). "Risk factor analysis of hypersensitivity reactions to abacavir." Clinical therapeutics **24**(4): 565-573.

Tanihara, Y., et al. (2007). "Substrate specificity of MATE1 and MATE2-K, human multidrug and toxin extrusions/H+-organic cation antiporters." Biochemical pharmacology **74**(2): 359-371.

Tanihara, Y., et al. (2007). "Substrate specificity of MATE1 and MATE2-K, human multidrug and toxin extrusions/H< sup>+</sup>-organic cation antiporters." Biochemical pharmacology **74**(2): 359-371.

TheGlobalFund (2017). Technical Brief: Adolescent Girls and Young Women in High-HIV Burden Settings.

Thul, P. J., et al. (2017). "A subcellular map of the human proteome." science **356**(6340): eaal3321.

Tong, L., et al. (2007). "Effects of human immunodeficiency virus protease inhibitors on the intestinal absorption of tenofovir disoproxil fumarate in vitro." Antimicrob Agents Chemother **51**(10): 3498-3504.

Tsuchiya, K., et al. (2016). "Brief report: high peak level of plasma raltegravir concentration in patients with ABCB1 and ABCG2 genetic variants." JAIDS Journal of Acquired Immune Deficiency Syndromes **72**(1): 11-14.

Tsuda, M., et al. (2009). "Involvement of human multidrug and toxin extrusion 1 in the drug interaction between cimetidine and metformin in renal epithelial cells." Journal of Pharmacology and Experimental Therapeutics **329**(1): 185-191.

Ufer, M., et al. (2008). "Influence of CYP3A4, CYP3A5, and ABCB1 genotype and expression on budesonide pharmacokinetics: a possible role of intestinal CYP3A4 expression." Clinical Pharmacology & Therapeutics **84**(1).

UNAIDS (2016). 90-90-90 On the right track towards the global target.

UnitedNations (2014). 90-90-90: an ambitious treatment target to help end the AIDS epidemic. Geneva: UNAIDS.

Urakami, Y., et al. (2004). "Creatinine transport by basolateral organic cation transporter hOCT2 in the human kidney." Pharmaceutical research **21**(6): 976-981.

Van Acker, B., et al. (1992). "Creatinine clearance during cimetidine administration for measurement of glomerular filtration rate." The Lancet **340**(8831): 1326-1329.

van Acker, B. A., et al. (1992). "Creatinine clearance during cimetidine administration for measurement of glomerular filtration rate." The Lancet **340**(8831): 1326-1329.

Van Gelder, J., et al. (2002). "Intestinal absorption enhancement of the ester prodrug tenofovir disoproxil fumarate through modulation of the biochemical barrier by defined ester mixtures." Drug Metabolism and Disposition **30**(8): 924-930.

van Luin, M., et al. (2009). "Efavirenz dose reduction is safe in patients with high plasma concentrations and may prevent efavirenz discontinuations." JAIDS Journal of Acquired Immune Deficiency Syndromes **52**(2): 240-245.

Venter, J. C., et al. (2001). "The sequence of the human genome." science **291**(5507): 1304-1351.

Vyhlidal, C. A., et al. (2006). "Nuclear receptor expression in fetal and pediatric liver: correlation with CYP3A expression." Drug Metabolism and Disposition **34**(1): 131-137.

Walsky, R. L., et al. (2006). "Evaluation of 227 drugs for in vitro inhibition of cytochrome P450 2B6." The Journal of Clinical Pharmacology **46**(12): 1426-1438.

Wang, J., et al. (2006). "Identification of a novel specific CYP2B6 allele in Africans causing impaired metabolism of the HIV drug efavirenz." Pharmacogenetics and genomics **16**(3): 191-198.

Wang, Z.-J., et al. (2008). "OCT2 polymorphisms and in-vivo renal functional consequence: studies with metformin and cimetidine." Pharmacogenetics and genomics **18**(7): 637-645.

Wanga, V., et al. (2015). "Genome-wide Association Study of Tenofovir Pharmacokinetics and Creatinine Clearance in AIDS Clinical Trials Group Protocol A5202." Pharmacogenetics and genomics **25**(9): 450.

Wen, C., et al. (2015). "Genome‐wide association study identifies ABCG2 (BCRP) as an allopurinol transporter and a determinant of drug response." Clinical Pharmacology & Therapeutics **97**(5): 518-525.

Wenning, L. A., et al. (2008). "Lack of a significant drug interaction between raltegravir and tenofovir." Antimicrob Agents Chemother **52**(9): 3253-3258.

WHO (2010). Medical eligibility criteria for contraceptive use, World Health Organization.

WHO (2012). Use of Efavirenz During Pregnancy: A Public Health Perspective: Technical Update on Treatment Optimization, World Health Organization.

WHO (2013). Consolidated guidelines on the use of antiretroviral drugs for treating and preventing HIV infection. Geneva: World Health Organization; 2013.

WHO (2016). Consolidated guidelines on the use of antiretroviral drugs for treating and preventing HIV infection: recommendations for a public health approach.

Williams, B. G. and R. Granich (2017). "Ending AIDS: myth or reality?" The Lancet **390**(10092): 357.

Wilson, J. F., et al. (2001). "Population genetic structure of variable drug response." Nature genetics **29**(3): 265-269.

Woodward, C. L., et al. (2009). "Tenofovir‐associated renal and bone toxicity." HIV medicine **10**(8): 482-487.

Wyatt, C. M., et al. (2007). "Chronic kidney disease in HIV infection: an urban epidemic." Aids **21**(15): 2101-2103.

Wyen, C., et al. (2011). "Cytochrome P450 2B6 (CYP2B6) and constitutive androstane receptor (CAR) polymorphisms are associated with early discontinuation of efavirenz-containing regimens." Journal of antimicrobial chemotherapy: dkr272.

Wyen, C., et al. (2008). "Impact of CYP2B6 983T> C polymorphism on non-nucleoside reverse transcriptase inhibitor plasma concentrations in HIV-infected patients." Journal of antimicrobial chemotherapy **61**(4): 914-918.

Yen-Revollo, J., et al. (2009). "Influence of ethnicity on pharmacogenetic variation in the Ghanaian population." The pharmacogenomics journal **9**(6): 373-379.

Yin, W., et al. (2005). "Investigations of the effect of DNA size in transient transfection assay using dual luciferase system." Analytical biochemistry **346**(2): 289-294.

Yombi, J. C., et al. (2014). "Antiretrovirals and the kidney in current clinical practice: renal pharmacokinetics, alterations of renal function and renal toxicity." Aids **28**(5): 621-632.

Zanger, U. M. and K. Klein (2013). "Pharmacogenetics of cytochrome P450 2B6 (CYP2B6): advances on polymorphisms, mechanisms, and clinical relevance." Frontiers in genetics **4**: 24.

Zhang, J., et al. (2001). "The human pregnane X receptor: genomic structure and identification and functional characterization of natural allelic variants." Pharmacogenetics and genomics **11**(7): 555-572.

Zhang, L. and A. Sparreboom (2017). "Predicting transporter‐mediated drug interactions: Commentary on:"Pharmacokinetic evaluation of a drug transporter cocktail consisting of digoxin, furosemide, metformin and rosuvastatin" and "Validation of a microdose probe drug cocktail for clinical drug interaction assessments for drug transporters and CYP3A"." Clinical Pharmacology & Therapeutics **101**(4): 447-449.

Zolk, O., et al. (2009). "Structural determinants of inhibitor interaction with the human organic cation transporter OCT2 (SLC22A2)." Naunyn-Schmiedeberg's archives of pharmacology **379**(4): 337-348.